DOCTORAL THESIS

UNCOVERING THE MECHANISMS BY WHICH ORAL THYROID HORMONES INFLUENCE ENERGY BALANCE

Valentina Capelli

PhD program in EXPERIMENTAL MEDICINE, cycle n. XXXII
UNIVERSITY OF PAVIA, ITALY

PhD program in ENDOCRINOLOGY
UNIVERSITY OF SANTIAGO DE COMPOSTELA, SPAIN

SANTIAGO DE COMPOSTELA
Year 2021

USC
UNIVERSIDADE
DE SANTIAGO
DE COMPOSTELA

DECLARATION OF THE TESIS AUTHOR

UNCOVERING THE MECHANISMS BY WHICH ORAL THYROID HORMONES INFLUENCE ENERGY BALANCE

Miss Valentina Capelli

I present my thesis, following the procedures indicated by the Institutions, and I declare that:

1) *The thesis includes the results of my work*
2) *Being that the case, any external collaboration to the work is mentioned in the thesis*
3) *I confirm that this assignment is my own, original work and that I did not plagiarise it in any way*

Santiago de Compostela, 17th March, 2021

Valentina Capelli

AUTHORIZATION OF THE THESIS DIRECTORS/TUTORS

UNCOVERING THE MECHANISMS BY WHICH ORAL THYROID HORMONES INFLUENCE ENERGY BALANCE

D. Luca Chiovato
D. Miguel Antonio López Pérez
D. Carlos Diéguez Gonzalez

DECLARE

That the present thesis represents the work made by Miss Valentina Capelli, under our direction, and we authorize its presentation, considering that it meets the requirements of the Regulations for Doctoral Studies of both institutions (UNIPV and USC)

Santiago de Compostela, 17th March, 2021

Luca Chiovato Miguel Antonio López Pérez. Carlos Diéguez Gonzalez

DECLARATION OF CONFLICT OF INTEREST

UNCOVERING THE MECHANISMS BY WHICH ORAL THYROID HORMONES INFLUENCE ENERGY BALANCE

Miss Valentina Capelli

I declare that I have no conflict of interest in relation with this doctoral thesis.

For certifying this, I sign this letter in Santiago de Compostela on 8th of June, 2021.

Valentina Capelli

Abstract

It has recently been discovered that thyroid hormones (TH) - 3,3',5,5' tetraiodothyroxyne or T4) and triiodothyronine (3,5,3-L-triiodothyronine, or T3) - action on body metabolism is not only mediated by direct tissue effects, but also by their action on the central nervous system (CNS), leading to hypothalamic-driven outputs to the peripheral targets, and those effects are integrated in a complex machinery which overall functioning remains to be clarified. As the majority of the central effects have been studied in models of direct hypothalamic TH treatment, one of the most challenging issues is the estimation of the relative contribution of the central *vs* peripheral component in the more physiologic conditions of peripherally TH release (or administration). In this study we used two different models of peripherally induced hyperthyroidism (i.e. T4 and T3 oral administration) to assess and compare the serum and hypothalamic TH homeostasis and relate them to the observed metabolic effects. TH treatment affected feeding behaviour, overall growth, core body temperature, body composition, brown adipose tissue (BAT) morphology and metabolic activity, white adipose tissue (WAT) browning, and liver lipid metabolism, resulting in an increased overall uncoupling capacity and a shift of the lipid metabolism from WAT accumulation to BAT fueling and liver deposition. In the hypothalamus, both treatment protocols induced significant changes in TH concentrations (not always reflecting the correspondent serum ones), and T3 treatment induced a downregulation of the hypothalamic AMP-activated protein kinase (AMPK) pathway, this supporting the existence of a central contribution to the observed metabolic effects. These results may be relevant to the ongoing discussion in the clinical setting on thyroid hormone replacement therapy with T4, T3 or both combined in.

Abstract (Italian)

E'stato recentemente scoperto che l'effetto degli ormoni tiroidei (OT) sul metabolismo non dipende solo dalla loro diretta azione tissutale, ma anche da quella che esercitano a livello del sistema nervoso centrale. In questa sede attivano circuiti ipotalamici che mettono in moto vie di segnale dirette agli stessi organi bersaglio periferici. Le due modalità di azione – periferica e centrale – si integrano dando origine a un complesso meccanismo il cui funzionamento non è ancora stato del tutto chiarito. Fino ad ora la maggior parte dei dati riguardanti gli effetti centrali degli OT è stata ottenuta in modelli animali che prevedono la somministrazione degli OT direttamente a livello ipotalamico, lasciando aperta la domanda su quale sia il contributo relativo di ciascuna della due componenti (centrale vs periferica) nella più fisiologica condizione di secrezione (o somministrazione) degli OT, quella periferica. In questo studio abbiamo usato due differenti modelli murini di ipertiroidismo indotto per via periferica (i.e. somministrazione di T4 o T3 per via orale) per valutare e comparare i livelli sierici e ipotalamici di OT e correlarli ai corrispettivi effetti metabolici. Il trattamento con OT ha indotto modifiche nel comportamento alimentare, crescita, temperatura corporea. Si sono osservati inoltre cambiamenti nella morfologia e attività metabolica del tessuto adiposo bruno (brown adipose tissue, BAT), "browning" del tessuto adiposo bianco (white adipose tissue, WAT), e metabolismo lipidico nel fegato. Questi effetti hanno portato a un generale aumento della capacità disaccoppiante, e a un cambio delle modalità di utilizzo dei lipidi, con deposizione nel fegato e nel BAT a scopo di supporto energetico, piuttosto che di accumulo nel WAT. A livello centrale ipotalamico entrambi i trattamenti hanno portato a cambiamenti significativi dei livelli di OT (non sempre corrispondenti ai cambiamenti a livello sierico), e il trattamento con T3 ha indotto un'inibizione della cascata dell'AMPK, a supporto del fatto che la componente centrale abbia un ruolo negli effetti metabolici osservati. Questi dati e le successive linee di studio possono contribuire all'attuale dibattito clinico riguardante le modalità di terapia ormonale sostitutiva (T4, T3, o combinazione) in diverse tipologie di pazienti affetti da ipotiroidismo.

Abstract (Spanish)

Se ha descubierto recientemente que la acción de las hormonas tiroideas (HT) -T4 (3,3´,5,5´-tetrayodotironina) y la T3 (3,5,3´-triyodotrionina)- sobre el metabolismo no depende solo de sus efectos directos en los tejidos, sino también de los que ejercen a nivel del sistema nervioso central, modulando circuitos hipotalámicos específicos que a su vez envían señales de activación a los órganos metabólicos periféricos. Los efectos centrales y periféricos se van así integrando en un complejo mecanismo cuyo funcionamiento aún no ha sido clarificado. Como la mayoría de los efectos centrales han sido estudiados a través de modelos de administración de HT directamente en hipotálamo, queda pendiente estimar cual es la importancia de cada vía (central *vs* periférica) en condiciones fisiológicas (secreción) o de administración periférica de HT. En este estudio hemos usado dos modelos diferentes de hipertiroidismo inducidos ambos por vía periférica (i.e. administración de T4 y T3 por vía oral) para estimar y comparar la homeostasis de las HT en suero e hipotálamo, y relacionarlas con los efectos metabólicos periféricos. El tratamiento con HT ha inducido cambios en ingesta, crecimiento, temperatura corporal, composición corporal, morfología y actividad metabólica del tejido adiposo pardo (*brown adipose tissue*, BAT), "browning" del tejido adiposo blanco (*white adipose tissue*, WAT), y metabolismo de los lípidos en hígado, conllevando un incremento de la capacidad desacoplante y un cambio en la forma de utilización de los lípidos, desde acumulación en el WAT a fuente de energía para el BAT y deposición en el hígado. En el hipotálamo, ambos tratamientos han inducido cambios significativos en las concentraciones de HT, no siempre correspondientes a los cambios registrados en el suero, y el tratamiento con T3 ha inducido también una inhibición de la cascada de la proteína quinasa activada por AMP (AMPK, *AMP-activated protein kinase*), corroborando así la hipótesis de la contribución central en determinar los efectos metabólicos observados. Estos datos pueden tener importantes implicaciones clínicas en el actual debate sobre la terapia de sustitución con HT (T4, T3 o los dos en combinación).

Summary (Galician) - Resumen en Lengua Gallega

Introdución

A homeostase enerxética (HE) do organismo depende do balance entre a enerxía inxerida e a enerxía consumida. O proceso de control da HE involucra unha serie de órganos e tecidos periféricos, e está finamente regulado a nivel do sistema nervioso central (SNC). Dentro do SNC, o hipotálamo é o maior centro implicado, exercendo funcións de 1) recepción e integración de sinais sensoriais e nutricionais 2) elaboración da necesaria resposta adaptativa 3) envío dos consecuentes sinais de activación ou desactivación aos órganos metabólicos periféricos, a través do sistema nervioso autónomo (SNA). Entre as diferentes poboacións neuronais que compoñen o hipotálamo, as mais importantes para este proceso son as do nucleos arcuato (ARC, *arcuate nucleus*) ventromedial (VMH, *ventromedial nucleus*), paraventricular (PVH, *paraventricular nucleus*) e as da área hipotalámica lateral (LHA, *lateral hypothalamic area*). O ARC exerce un papel primario na regulación da inxesta, mentres que o VMH (tamén involucrado en control da inxesta), é o centro mais importante para o control do gasto enerxético, modulando a homeostase glucémica e lipídica, o tremor do musculo esquelético, a termoxénese do tecido adiposo pardo (BAT, *brown adipose tissue*) e o " browning" do tecido adiposo branco (WAT, *white adipose tissue*). O funcionamento dos devanditos circuítos metabólicos hipotalámicos depende da actividade local dunha serie de vías moleculares e sensores celulares, e, entre estes, un papel esencial xógao a proteína quinasa activada por AMP (AMPK, *AMP-activated protein kinase*), o principal sensor do estado enerxético celular, expresado de maneira ubicua e conservado entre todas as especies eucariotas.

AMPK é unha serín/treonín quinasa que se presenta en forma de heterotrímero conformado por subunidades catalíticas α (α1 e α2) e subunidades regulatorias β (β1 e β2) e γ (γ1, γ2, γ3), o que resulta en 12 posibles combinacións de complexos de AMPK. A actividade de AMPK increméntase en resposta a estados de estres enerxético celular que se reflicten en alteracións da abundancia relativa dos nucleótidos de adenina: redución do adenosín trifosfato (ATP) e elevación do adenosín monofosfato (AMP) e adenosín difosfato ADP. Trala súa activación, AMPK promove procesos celulares de tipo catabólico (que xeran ATP), e inhibe as vías anabólicas (que consuman ATP), co obxectivo de re-equilibrar o balance enerxético. A actividade de AMPK resulta aumentada en condicións de xaxún en varias rexións hipotalamicas, e reducida tras a inxesta alimentar. Unha vez activada polo xaxún, AMPK induce a expresión de neuropeptidos orexigénicos no ARC que estimulan o apetito e a introdución de alimentos. Doutra banda, trala alimentación, a inhibición de AMPK no VMH produce un incremento do gasto enerxético, a través da activación do BAT mediada polo SNA. A actividade de AMPK en hipotalamo non participa só na resposta ao estado de xaxún/alimentación, senón tamén na determinación dos efectos centrais de diferentes hormonas, péptidos, e moléculas de sinalización, como leptina, estróxenos, hormonas tiroideas e moitos mais. No contexto da integración e regulación hipotalamica do metabolismo, outro papel importante xógao a diana de rapamicina en células de mamífero (mTOR, Mammalian Target of Rapamycin). mTOR é unha serina-treonina quinasa implicada no ciclo e o crecemento celular ao detectar cambios en factores de crecemento, nutrientes ou oxígeno. A vía de mTOR exprésase nos principais núcleos involucrados no control da inxesta, como o ARC, onde se localizan os neuropéptidos orexigénicos e anorexigénicos. A actividade de mTOR cambia de maneira inversa á de AMPK: en resposta a sinales de abundancia de enerxía celular a actividade de mTOR está incrementada e a de AMPK reducida, e *vice versa*.

O gasto enerxético do organismo depende da combinación do metabolismo basal (MB), a termoxénese adaptiva, e a actividade física. O MB representa o "custo mínimo da supervivencia" en estado de repouso, post-prandial, e en condicións de termoneutralidade, dependendo unicamente da produción de ATP necesaria para o mantemento dos procesos vitais básicos. A termoxénese adaptativa refírese á suma dos eventos necesarios para incrementar a produción de calor baixo a exposición ao frío, i.e. a termoxénese mediada por tremor do músculo esquelético e a termoxénese do BAT. O BAT é un tecido metabólicamente activo especializado en producir calor, e caracterizado por unha morfoloxía distinta da graxa branca (adipocitos de forma poligonal con numerosas pingas lipídicas multiloculares, gran número de mitocondrias, forte inervación por fibras de tipo simpático). A termoxénese ten lugar a través do desacoplamiento do ATP producido a partir da respiración mitocondrial, mediado pola proteína desacoplante 1 (UCP1, *uncoupling protein 1*) que se atopa na membrana interna da mitocondria. Recentemente, describiuse a existencia doutro tipo celular, o adipocito beige ou brite (brown in white), que se atopa en lugares anatómicos correspondentes a células brancas e desenvólvese tras recibir estímulos termoxénicos. Deriva de células precursoras diferentes dos adipocitos pardos, máis próximas ás liñaxes de células que dan lugar aos adipocitos brancos, pero expresa a proteína desacoplante UCP1. A presenciade adipocitos beige no contexto da graxa branca indícase como " browning" do WAT. A pesar da expresión de UCP1, a capacidade termoxénica deste tecido in vivo segue sendo significativamente menor que a do BAT. Entre os factores que modulan o gasto enerxético, un papel relevante xógano as hormonas tiroideas (HT). As HT de maior interese son a T4 (3,3´,5,5´- tetrayodotironina) e a T3 (3,5,3´- triyodotrionina), cuxa síntese e secreción por parte da glándula tiroidea está modulada polo eixo hipotálamo-hipófisis-tiroides (HPT, hypothalamous-pituitary-thyroid), mediante un mecanismo de retroalimentación negativa. A tiroides produce maioritariamente T4, unha pro-hormona con baixa actividade biolóxica, e en menor parte T3, a súa forma metabólicamente activa. A conversión de T4 á súa forma activa T3 realízase por un proceso de deiodinación, i.e. a eliminación dun átomo de iodo da molécula de T4, a través dunha reacción catalizada por unha familia de encimas chamadas yodotironina deiodinasa, que inclúe a deiodinasa tipo 1 (DIO1), tipo 2 (DIO2) e tipo 3 (DIO3). Ditas encimas exprésanse de maneira ubicua, e son responsables non só da activación senón tamén da desactivación e consecuente metabolismo das HT. DIO2 é a principal responsable da conversión de T4 a T3 e considérase unha a encima chave para a regulación local da biodisponibilidade de T3 nos tecidos, onde exerce a súa acción tras unirse aos seus específicos receptores nucleares (TRs, *thyroid hormone receptors*), que actúan como factores transcripcionales ligando-dependentes. Debido ao seu carácter hidrófilo, as HT necesitan transportadores específicos para chegar dentro da célula, onde se atopan tanto as DIOs como os TRs. Varias familias de transportadores foron identificadas sobre todo nos últimos anos, entre as cales teñen ten particular relevancia a familia de polipéptidos transportadores de aniones orgánicos (OATPs, *organic anion-transporting polypeptide*) e a familia de proteínas de transporte monocarboxiladas (MCT, *monocarboxylate transporter*), que regulan o transporte das HT a través da barreira hemato-encefalica, e xogan por tanto un papel esencial na regulación da acción das HT a nivel do SNC. As HT regulan numerosísimos procesos fisiolóxicos, entre os cales destacan crecemento, desenvolvemento, e a maioría dos eventos metabólicos, incluídos os cambios no MB. Estes últimos resultan ben exemplificados en pacientes con desordes tiroideos. O exceso de HT (hipertiroidismo) acompáñase dun aumento xeralizado do metabolismo, normalmente asociado con perda de peso a pesar da concomitante hiperfagia. Doutra banda, niveis reducidos de HT (hipotiroidismo) asócianse a unha diminución do gasto enerxético con consecuente aumento de peso corporal a pesar dunha redución na inxesta. Estes efectos metabólicos das HT dependen

da súa modulación tanto do MB como da termoxénese adaptiva, a través da súa acción sobre todos os órganos e tecidos metabólicamente activos (fígado, BAT, WAT, músculo esquelético). Os cambios inducidos por HT na termoxénese adaptiva realízanse maiormente por un incremento da capacidade desacoplante do BAT, e en menor parte polo aumento da termoxénese inducida por tremor no musculo esquelético. Todos devanditos tecidos expresan diferentes niveis de DIOs e de TRs, e nun principio considerábase que esta acción a nivel receptorial fose o único mecanismo de control das HT sobre o metabolismo. Polo contrario, foi recentemente descuberto que os efectos metabólicos das HT non dependen só da activación receptorial a nivel local local, senón tamén da que exercen a nivel do SNC, modulando circuítos hipotalámicos específicos que á súa vez envían sinais de activación aos órganos metabólicos periféricos. En específico, cando son administradas por vía central en rodedores, as HT inducen activación do BAT con incremento da actividade termoxénica, cambios no metabolismo glucídico e lipídico, "browning" do tecido adiposo branco, e pérdida de peso, a pesar dun concomitante incremento en inxesta. Os efectos termoxénicos son mediados principalmente pola inhibición da vía de AMPK no núcleo VMH y, máis en detalle, nunha poboación neuronal especifica denominada neuronas SF1 (steroidogenic factor 1). De feito, só cando no núcleo VMH (e non noutras rexións hipotalámicas) a inhibición de AMPK inducida por T3 activa a termoxénesis do BAT a través do SNA. A maiores, demostrouse que 1) a inhibición da sinalización das HT no VMH reduce considerablemente os efectos do hipertiroidismo sobre o balance enerxético; 2) o mesmo resultado obtense tras inducir activación constitutiva de AMPK noVMH; 3) a ablación da isoforma AMPKa1 nas neuronas SF1 reproduce os efectos metabólicos da T3 mediados por vía central. Doutra banda, os cambios en inxesta prodúcense a través dá modulación mTOR non ARC, onde mTOR se colocaliza co receptor TRα.

Os efectos centrais e periféricos vanse así integrando nun complexo mecanismo cuxo funcionamento aínda non foi clarificado. Como a maioría dos efectos centrais foron estudados a través de modelos de administración de HT directamente en hipotálamo, queda pendente estimar cal é a importancia de cada vía (central *vs* periférica) en condicións fisiolóxicas secreción) ou de administración periférica de HT.

Hipótesis

Os efectos das HT sobre o metabolismo dependen da combinación das accións directas nos tecidos e das que veñen mediadas por vía central. A administración oral de HT pode representar un modelo adecuado para investigar o funcionamento desta complexa engrenaxe.

Obxectivo

Investigar os mecanismos a través dos cales a administración oral de HT modula o balance enerxético, abordando os seguintes asuntos:

1. Avaliación e comparación dos niveis de HT en soro e hipotálamo de rodedores tratados con HT por vía oral
2. Avaliación dos cambios metabólicos asociados con cada tratamento,
3. Comparación e asociación dos datos obtido en periferia e centralmente

Materiais e métodos

Usáronse dous modelos diferentes de hipertiroidismo inducidos ambos por vía periférica (i.e. administración de T4 e T3 por vía oral) para estimar e comparar a homeostasis das HT en soro e hipotálamo, e relacionalas cos efectos metabólicos periféricos. Empregáronse ratos de xenotipo salvaxe (fondo xenético C57 BL/6) de 8-10 semanas de idade. No ensaio incluíronse tres grupos experimentais, correspondentes a tratamentos con T4, T3,

ou vehículo cunha duración de dúas semanas, con monitoraxe diaria de peso, inxesta, e bebida. Ao final do tratamento, rexistráronse a maiores a temperatura rectal, a da pel a nivel interescapular ao redor do BAT, e a lonxitude corporal (i.e. distancia cola-nariz). As técnicas analíticas empregadas para a seguinte análise dos tecidos obtidos inclúen: radio-immuno-assay (RIA) en soro e homoxenados hipotalámicos para T4 e T3; Western Blot para expresión proteica; PCR en tempo real para expresión xénica; histoloxía, immohistoquímica, e tinción con Oil-Red. Para a análise estatística utilizouse o software GraphPad Prism.

Resultados

Para comprobar a eficacia do tratamento, medíronse os niveis de T4 e T3 totais tanto en soro como no hipotálamo dos ratos dos tres grupos experimentais. Os niveis de ambas as hormonas resultaron significativamente mais elevados nos respectivos grupos de tratamento a nivel periférico, confirmando o estado de hipertiroidismo. Rexistrouse tamén un incremento dos niveis hipotalámicos das dúas hormonas, indicando que a dose periférica administrada é suficiente para alcanzar o SNC. Ambos os tipos de tratamento asociáronse a un incremento progresivo tanto do peso corporal como da inxesta. A lonxitude corporal á fin do tratamento, resultou significativamente máis elevada nos ratos hipertiroideos que nos controis. Cambios significativos rexistráronse tamén na composición corporal, onde o tratamento con hormonas tiroideas resultou asociado cun incremento da masa de tecido adiposo pardo e unha redución da do tecido adiposo branco gonádico. A maiores, o hipertiroidismo resultou asociado cunha elevación da temperatura rectal, pero non se rexistraron cambios na correspondente temperatura do BAT. A análise do tecido adiposo pardo evidenciou cambios significativos en tema de morfoloxía (incremento de deposición de lípidos) e actividade metabólica (incremento da expresión de UCP1 e outros marcadores de activación). O tecido adiposo branco presentaba unha redución do tamaño dos adipocitos e un incremento da expresión de UCP1, datos compatibles co proceso de " browning". Un incremento do depósito dos lípidos rexistrouse tamén a nivel hepático. Para investigar a hipótese dunha contribución central e determinar os efectos metabólicos observados, analizouse o estado da vía metabólica de AMPK no hipotálamo medio-basal (MBH, *medio basal hipothalamus*), que inclúe os núcleos VMH e ARC, involucrados na actividade termoxénica do BAT, browning do WAT, e control da inxesta. A vía de AMPK resultou inhibida baixo tratamento con T3, corroborando así dita hipótese.

Discusión

As HT exercen acción sobre o comportamento alimentario, o crecemento, a temperatura corporal, a morfoloxía e a actividade metabólica do BAT, o " browning" do WAT, o metabolismo dos lípidos no fígado, a actividade do SNC, e moitas mais. Algúns destes efectos – cambios en inxesta, termorregulación e termoxénese – estiveron amplamente descritos e estudados ao longo dos anos. Con todo, hai outros que se descubriron só recentemente, entre os cales a modulación do metabolismo lipídico e o " browning" do WAT. A pesar dos moitos anos de investigación neste campo, segue habendo novos avances, e os mecanismos exactos da base destes procesos aínda non se clarificaron. Mentres os primeiros coñecementos baseábanse sobre a visión "clásica" de que os efectos das HT sobre o metabolismo exércense unicamente a nivel local nos tecidos, datos mais recentes puxeron en evidencia a importancia da acción das HT sobre os sensores enerxético do SNC, que á súa vez van desencadear as respostas hipotalámicas dirixidas aos órganos metabólicos periféricos. Este fundamental descubrimento baseouse, entre outros, sobre o modelo animal de hipertiroidismo "central" en rodedores, que consta na inxección directa dentro do SNC de HT, sexa esa intracerebroventricularmente

(ICV) ou en áreas hipotalámicas específicas, segundo o deseño experimental. Este modelo representou a clave para explorar en detalle as vías hipotalámicas implicada nos efectos metabólicos das HT mediados por vía central. Con todo, na condición mais "fisiolóxica" de secreción periférica das HT, estes efectos centrais súmanse e integran cos eventos mediados directamente a nivel dos tecidos, nunha complexa engrenaxe cuxo exacto funcionamento queda por ser clarificado. Un dos aspectos máis cuestionado é a estimación das respectivas contribucións das accións centrais e periféricas das HT nos órganos involucrados, en diferentes condicións de homeostasis tiroidea. De feito, antes de alcanzar o SNC e os núcleos hipotalámicos, as HT secretas na periferia están sometidas a deiodinacion e metabolismo na circulación, transporte activo a través da barreira hemato-encefalica, e ulteriores procesos de deiodinacion e metabolismo nas neuronas e nos astrocitos. Ademais, cada un destes eventos está suxeito a modulación, segundo as condicións homeostáticas das HT (eutiroidismo, hipertiroidismo, hipotiroidismo) e o concomitante balance enerxético (positivo, negativo, neutral). Neste estudo usamos dous modelos diferentes de hipertiroidismo inducido por vía periférica (administración oral de T4 e T3) co obxectivo de analizar a homeostase das HT circulantes e hipotalámicas, e relacionala cos efectos metabólicos observados. A nivel periférico, o tratamento con HT conlevou un incremento da inxesta, do peso e da lonxitude corporal, sen que isto se asociase a un aumento da porcentaxe da masa de graxa branca, que contrariamente resultou reducida. Os animais hipertiroideos exhibiron tamén un incremento da temperatura corporal, pero non da do BAT, que resultou invariable nas imaxes termográficas. A pesar da falta de variación de temperatura, os depósitos de tecido adiposo pardo resultaron incrementados nos animais tratados, e presentaban unha incrementada acumulación de lípidos e actividade metabólica. O incremento desta acumulación de lípidos rexistrouse tamén a nivel hepático, mentres que resultou reducido o tamaño dos adipocitos nos depósitos de graxa branca, asociado a un proceso de " browning". Ambos os tratamentos induciron cambios significativos nas concentracións hipotalámicas das HT. Os niveis hormonais hipotalámicos alcanzados baixo tratamento con T3 resultaron suficientes para inhibir a ruta de AMPK, un dos sensores enerxéticos celulares mais importantes en mediar a acción central das HT sobre o metabolismo. Ditas observacións representan un primeiro paso para chegar a comprender a complexa relación entre os efectos producidos polas HT directamente nos tecidos e os orixinados a nivel central. Os modelos de hipertiroidismo "central" e "periférico" descritos na literatura asócianse a fenotipos metabólicos dalgunha maneira diferentes, sobre todo polo que ten que ver cos efectos sobre o peso corporal. Esa aparente contradición pode ser resolvida tendo en conta as diferenzas nos protocolos experimentais empregados. Por unha banda, a administración intra-hipotalámica aguda e a curto prazo do T3 resulta nunha resposta metabólica inmediata, que inclúe un incremento da actividade lipolítica no BAT e un incremento da termoxénese, cun efecto neto de balance enerxético negativo e perda de peso. Polo outro lado, a administración crónica de HT por vía periférica induce unha complexa engrenaxe de cambios metabólicos progresivos, co resultado final dunha incrementada capacidade desacoplante (recrutamento do BAT e "browning" do WAT) e un cambio do metabolismo lipídico desde a acumulación no WAT ao depósito no fígado e no BAT, posiblemente como fonte de enerxía para soster o incremento da actividade metabólica. Estes dous fenotipos parecen asemellarse respectivamente á resposta que se produce ao estrés térmico agudo (frío) e á adaptación crónica ás baixas temperaturas. Para profundar esta hipótese, serán necesarios estudos especifico sobre a homeostase central e periférica das HT en diferentes condicións de temperatura ambiental. Este asunto será obxecto de investigacións futuras.

Conclusións

- O tratamento con T4 e T3 induciu cambios significativos nas concentracións hipotalámicas das HT
- O tratamento con T4 e T3 induciu cambios no comportamento alimentario, o crecemento, a temperatura e composición corporal, a morfoloxía e actividade metabólica do BAT, "browning" do WAT, e cambios no metabolismo lipídico hepático.
- O tratamento oral con T3 induciu unha inhibición da ruta de AMPK no MBH, corroborando a hipótese dunha contribución central para os efectos metabólicos observados.
- En xeral, estes resultados indican que a administración oral de T3 e T4 é un modelo adecuado para o estudo das accións das HT sobre o balance enerxético e o metabolismo.

INDEX

USC
UNIVERSIDADE
DE SANTIAGO
DE COMPOSTELA

ABBREVIATIONS

(18)F-FDG PET/CT: positron emission tomography with 2-deoxy-2-[fluorine-18]fluoro- D-glucose integrated with computed tomography
ACC: adenylate cyclase
ADP: adenosine diphosphate
AgRP: agouti-related peptide
AHDS: Allan-Herndon-Dudley syndrome
AMP: adenosine monophosphate
AMPK: AMP-activated protein kinase
ANOVA: analysis of variance
ANS: autonomic nervous system
ARC: arcuate nucleus of the hypotalamus
ATGL: adipose triglyceride lipase
BAT: brown adipose tissue
BBB: blood brain barrier.
BMR: basal metabolic rate
BSA: albumin, from bovine serum
CaMKKs: calmodulin-dependent kinase kinases
cAMP: cyclic adenosinmonophophate
ChREBP: carbohydrate-responsive element-binding protein
CIDEA: cell death–inducing DNA fragmentation factor-α-like effector A
CKK: cholescistokinin
CNS: central nervous system
DIO(s): iodo-thyronine deiodinases
DMH: dorsomedial nucleus of the hypothalamus.
EE: energy expenditure
ER: endoplasmic reticulum
FA: fatty acids
FAS: fatty acid synthase
FFA, fatty free acids
FT3: free T3
FT4: free T4
GH: growth hormone
GHS-R: growth-hormone secretagogues receptor
GI: gastrointestinal tract
GLP-1: glucagon-like peptide 1
GLP-2: glucagon like peptide 2
Gs: excitatory G-protein
gWAT: gonadal white adipose tissue
H&E: Haematoxylin and Eosin
HPT: hypothalamic-pituitary-thyroid axis
HSL: hormone-sensitive lipase
iBAT: interscapular brown adipose tissue
ICH: immunohistochemistry
ICV: intracerebroventricular
IL6: interleukin 6
IRD: inner ring deiodination
JNK: c-Jun N-terminal kinase

LAT(s): L-type amino acid transporters
LHA: lateral hypothalamic area
LKB1: liver kinase B1
LPL: lipoprotein lipase.
LXR(s): liver X receptors
M/O dko: MCT8 and OATP1C1 double knock-out
MAPK: mitogen-activated protein kinase.
MBH: medio-basal hypothalamus
MCP1: monocyte chemoattractant protein 1
MCT(s): monocarboxylate transporters
MGL: monoacylglycerol lipase
mTOR: mechanistic target of rapamycin
NE: norepinephrine
NPY: neuropeptide Y
NTS: nucleus of the solitary tract
OATP(s): organic anion transporters
ORD: outer ring deiodination.
OXM: oxyntomodulin
PAI1: plasminogen activator inhibitor 1
PGC1α: peroxisome-proliferator-activated receptor-gamma co-activator 1 alpha.
PI3K: phosphatidylinositol 3-kinase
PKA: protein kinase A
POMC pro-opiomelanocortin
PP: pancreatic polipeptide
PP2Cα: protein phosphatase 2C alpha
PPARγ: peroxisome proliferator-activated receptor gamma
PRDM16: PR domain containing 16
PSNS: parasympathetic nervous system
PVH: paraventricular nucleus of the hypothalamus.
PYY: peptide YY
RIA: radioimmunoassay
ROS: reactive oxygen species
rT3: reverse T3
SD: standard chow diet
SEM: standard error of the mean
SF1: steroidogenic factor 1
SNS: sympathetic nervous system
SREBP1C: sterol regulatory element-binding protein 1C
sWAT: subcutaneous white adipose tissue
T2: 3,3'-diiodothyronine
T3: triiodothyronine (3,5,30-L-triiodothyronine)
T4: thyroxine (3,3',5,5' tetraiodothyroxyne)
TGs, triglycerides
TH: thyroid hormones
TNFα: tumor necrosis factor alpha
TR(s): thyroid hormone receptors
TRE(s): T3-response elements
TRH: thyrotropin-releasing hormone

TSH: thyroid stimulating hormone
UCP1: uncoupling protein 1
UCP2: uncoupling protein 2
UCP3 uncoupling protein 3
VMH: ventromedial nucleus of the hypothalamus
WAT: white adipose tissue
β3-AR: β3 adrenoreceptor

USC
UNIVERSIDADE
DE SANTIAGO
DE COMPOSTELA

USC
UNIVERSIDADE
DE SANTIAGO
DE COMPOSTELA

INTRODUCTION

USC
UNIVERSIDADE
DE SANTIAGO
DE COMPOSTELA

1 BODY ENERGY HOMEOSTASIS

1.1 PHYSIOLOGICAL CONTROL OF BODY ENERGY HOMEOSTASIS: AN OVERVIEW

Body energy homeostasis consists in the balance between energy intake (i.e. food consumed) and expenditure (burnt calories). The maintenance of this balance depends on the complex coordination of sensory inputs, central integrative circuits, and motor outputs allowing for a feedback regulation of specific functions. [2-4]. In the central nervous system (CNS), peripheral signals of body energy status are received and integrated by different neuronal populations located in the hypothalamus, brainstem, hindbrain and forebrain. Upon elaboration of those signals, proper outputs are sent to the periphery to modulate not only feeding behavior, but also the overall body metabolism, including energy production, storage, mobilization, conversion, and utilization. All this process involves the coordinated actions of the gastrointestinal tract, liver, pancreas, muscle, white adipose tissue (WAT), and brown adipose tissue (BAT) [4].

1.2 PERIPHERAL SIGNALS OF ENERGY STATUS

1.2.1 The white adipose tissue

Adipose tissue has been increasingly recognized as a crucial player in the whole-body metabolic regulation, not only exerting the role of passive fuel reservoir, but also displaying several metabolic and/or endocrine functions [5]. To date, three major types of adipose tissue have been identified, i.e. the WAT, the BAT and the beige/brite (brown-like-in-white) adipose tissue, which differ in origin, morphology, mitochondrial content and thermogenic capacity [5]. Moreover, the body of evidence in the field of adipocytes lineage and plasticity keeps growing, giving rise to a much more complex lineage map than originally appreciated [6]. The WAT is the main responsible for energy storage in the form of lipid depots and for the release of adiposity signals [7], whether the BAT and beige adipose tissue are more directly involved in thermogenesis and therefore, energy expenditure (EE), harboring specific metabolic processes that will be fully addressed later on. The WAT is characterized by large white adipocytes and few mitochondria with a low oxidative rate. In mice, the majority of WAT depots are found around the gonads (gonadal WAT, gWAT) and subcutaneously (subcutaneous WAT, scWAT), while in humans they are located predominantly in the subcutaneous, associated with the digestive tract (visceral WAT), and in lower amounts attached to the walls of internal organs and arteries [8]. The major functions of WAT are 1) to store the energy in the form of triglycerides (TGs) during the fed state and 2) to subsequently mobilize those storages in situations of increased demand, such as cold stress, fasting or disease. The storage process is mediated by the lipogenic pathway, which promotes the conversion of carbohydrates into fatty acids (FA), the biosynthesis of TGs, and the adipocyte lipid droplet expansion. On the other hand, the energy-releasing process depends on the lipolytic pathway, which breaks down the TGs into free fatty acids (FFA) and glycerol that can be either oxidized or released. Both processes may be activated and/or inhibited by nutritional signals, hormonal inputs, and the autonomic nervous system (ANS) activity [5]. Interestingly, depot-specific differences in WAT sensitivity to lipolysis have been described both in humans and in rodents [9]. In addition to the energy storage and mobilization processes, the WAT also exerts an essential endocrine function, producing and releasing a variety of metabolically active peptides, as well as lipids, enzymes, and, more importantly, a specific

family of cytokines, called adipokines [10]. Adipokines not only contribute to the local regulation of adipogenesis, immune cell migration, adipocyte metabolism and TGs storage, but also operate systemically in the control of appetite and satiety, energy expenditure and metabolism, insulin sensitivity, inflammation, blood pressure, hemostasis, endothelial function, and many more [10]. Leptin, the firstly discovered adipokine [11], represents the main WAT anorexigenic protein. At molecular level, it is a 16-kDa peptide encoded by the obese (*ob*) gene and acts via the leptin receptor on target cells. Leptin secretion and circulating levels are proportional to fat mass and caloric intake, and its satiety effect is achieved by targeting the hypothalamus, where it increases the expression of anorexigenic and decreases the expression orexigenic neuropeptides to reduce appetite and food intake [12,13]. Besides regulating the feeding behavior at central level, leptin also promotes several peripheral effects, including insulin-sensitivity in metabolically active organs, as well as fertility, inflammation, immunity, and many others [10]. Another abundantly secreted and metabolically active adipokine is adiponectin, shortly discovered after the cloning of leptin [14]. Adiponectin is essential for the crosstalk between the WAT and the peripheral metabolic organs, being able to suppress hepatic gluconeogenesis and enhancing FA oxidation in skeletal muscle, leading to an overall enhancement of the whole-body insulin sensitivity [15]. In addition to those peripheral actions, other centrally-mediated adiponectin effects have been described, including body weight loss and increase in energy expenditure, furtherly underlying the pivotal role of this adipokine in the control on energy homeostasis [16]. In the last two decades several other adipokines have been discovered and described, including resistin, chemerin, apelin, visfatin, plasminogen activator inhibitor 1 (PAI1), monocyte chemoattractant protein 1 (MCP1), tumor necrosis factor alpha (TNFα), interleukin 6 (IL6), and many more [10], and the body of evidence in this field still keeps growing.

1.2.2 Short-term signals of energy intake: the role of the gastrointestinal tract

Whether the adiposity signals modulate the energy intake and expenditure in a long-term manner, the contemporary short-term control is mediated by the gastrointestinal tract (GI) signaling molecules [7]. The GI is referred to as the largest endocrine organ in the body, expressing more than 30 gut hormone genes and producing more than 100 bioactive peptides [7,17], which are released upon mechanical and chemical stimuli, i.e. anticipation of a meal and/or distension of the stomach and small intestine [7]. These molecules include a panel of orexigenic and anorexigenic peptides, which are responsible for the meal-by-meal modulation of the feeding behavior. To date, the only known orexigenic gut hormone is ghrelin, an endogenous ligand for the growth-hormone secretagogues receptor (GHS-R) which was firstly identified in the rat stomach [18]. Ghrelin main functions are exerted in the CNS, where the GHS-Rs is extensively expressed not only the in anterior pituitary, but also the hypothalamic arcuate nucleus (ARC), this latter being specifically involved in the control of feeding behavior, as extensively discussed in the next section [19]. Ghrelin is secreted by the oxyntic glands of the gastric fundus during fasting (or negative energy balance) to rapidly enhance hunger and food intake [19,20], while its circulating levels rapidly decrease when the energy supply is sufficient, i.e. after consumption of a meal [21]. Even if most of the circulating plasma ghrelin come from the stomach, smaller amounts of this hormone may also be produced by the small intestine, CNS, pancreas, kidney, lymphocytes, lung, and reproductive organs among others. Consistently, in addition to increasing appetite and stimulating GH secretions, ghrelin also contributes to the control of fertility, tumor development, glucose metabolism and the immune response [19,22,23]. On the other hand, the panel of the known GI anorexigenic peptides is much wider, including cholecystokinin (CCK), glucagon like peptide 1 (GLP-1), glucagon like

peptide 2 (GLP-2), peptide YY (PYY) and oxyntomodulin (OXM) produced by the intestine, gastrin by the stomach, and insulin and polipeptide pancreatic (PP) by the pancreas [20]. Those peptides are secreted in response to food consumption, synergistically with the fall in the plasma levels of ghrelin. The amount and proportion of their release may vary depending on the grade of distension of the stomach and/or the nutrient composition (mainly protein or fat) of the meal reaching in the small intestine [20].

1.2.3 Circulating nutrients

Circulating glucose and lipids may derive both from exogenous (food intake and absorption) and endogenous (hepatic production) sources. Besides modulating the synthesis and release of the WAT and GI orexigenic/anorexigenic signals, both these nutrients are also directly involved in activating specific hypothalamic neural sensing pathways to promote a negative feedback on feeding behavior and glucose production [24]. In fact, the hypothalamus houses several distinct sub-populations of glucose-sensing neurons utilizing glucose as a signaling molecule in addition to its fueling role. Those sub-populations harbor distinct mechanisms of glucose level detection, express different panels of neurotransmitters/neuropeptides, and are individually specialized in distinct physiological functions [25]. Moreover, both the hypothalamus and several other brain regions express the enzymes responsible for the transport, utilization and storage of lipids. Recent evidence suggest that neuronal FA can also modulate the hypothalamic activity and regulate energy balance [26,27]. This in a complex "lipid sensing" process involves the control of insulin secretion, hepatic glucose production, adipose storage and food intake, but its precise underlying molecular mechanisms are still matter of controversy [26,27].

1.3 CENTRAL INTEGRATION OF THE PERIPHERAL ENERGY SIGNALS

1.3.1 Anatomo-physiology of the hypothalamus: sensing neurons, nuclei, and neuropeptides

The peripheral signals of energy status are received and integrated in the hypothalamus to produce appropriate homeostatic responses. The hypothalamus is organized in neuronal clusters, called nuclei, which control a variety of basic biological functions, such as feeding, body temperature, energy homeostasis, reproduction, stress responses, and circadian rhythm. Besides being individually specialized to target specific physiological processes, the nuclei are tightly connected to each other by neuronal circuits and axonal projections, indicating neurobiological interactions between their different functions [28,29]. Several nuclei – such as the arcuate nucleus (ARC), the dorsomedial nucleus (DMH), the ventromedial nucleus (VMH) and the paraventricular nucleus (PVH) – together with the lateral hypothalamic area (LHA) are directly involved in the regulation of energy balance [29,30]. For example, the ARC is considered as the primary nutrient-sensing center of the hypothalamus, containing the pro-opiomelanocortin (POMC) and neuropeptide Y /agouti-related peptide (NPY/AgRP) neurons which represent the starting point of the melanocortin system, to date the best-characterized hypothalamic circuit for appetite control [31]. On the other hand, the VMH, which also participates in the control of feeding behavior, exerts a much more decisive role in modulating the body EE [29,32]. To modulate the body EE, the hypothalamic outputs are sent to the periphery through the ANS to target different metabolic pathways, such as hepatic glucose and lipid homeostasis, shivering response in skeletal muscle, BAT thermogenesis and WAT browning

(Figure 1) [28,33,34]. Those processes, as well as other nucleus-specific functions in the control of energy balance will, be furtherly addressed in the following sections.

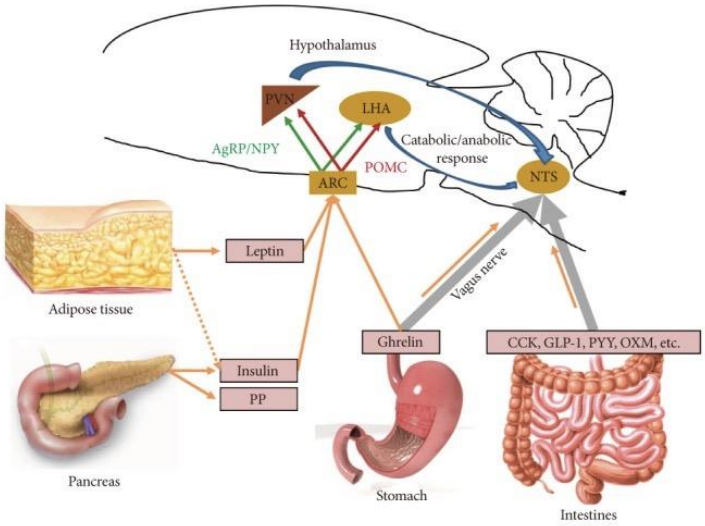

Figure 1. Simplified representation of the body energy-sensing machine. Reproduced from [34]. Creative common license CC BY-NC 3.0.

1.3.2 Hypothalamic cell sensors: AMPK

The above-mentioned metabolically-active hypothalamic circuits involve a variety of molecular pathways and cell sensors, among which a crucial role is played by the AMP-activated protein kinase (AMPK) [29]. AMPK represents the main sensor of cellular energy status, being expressed ubiquitously and highly conserved across all eukaryotic species [35]. AMPK is a serine/threonine kinase, composed by a heterotrimer complex of a catalytic α (α1, α2) subunit, a serine/threonine protein kinase domain, and two regulatory subunits, β (β1, β2) and γ (γ1, γ2, γ3), encoded by different genes [29,36]. In general, it is activated in response to energy stress by sensing increases in AMP:ATP and ADP:ATP ratios and restores energy balance by inhibiting anabolic processes that consume ATP, while promoting catabolic processes that generate ATP [35]. AMPK activation consists in the phosphorylation on Thr-172 of the α subunit, upon allosteric induction by AMP (but not ADP) and catalyzation by several upstream kinases [37], such as liver kinase B1complex (LKB1) [38], and calmodulin-dependent kinase kinases (CaMKKs), especially CaMKK2 [39]. AMPK is highly expressed in almost all hypothalamic nuclei and plays a pivotal role in the process of integration of peripheral hormonal signals to modulate energy intake and expenditure [29]. AMPK activity is increased under fasting in numerous hypothalamic regions and inhibited when submitted to refeeding [40-43]. Following this fasting-induced activation, AMPK modulates mitochondrial FA oxidation, ceramide synthesis in the endoplasmic reticulum (ER), and intracellular levels of reactive oxygen species (ROS), this in turn stimulating the expression of orexigenic neuropeptides in the ARC, leading to increased appetite [29,41]. Conversely, in the fed state, inhibition of AMPK in the VMH induces energy expenditure by boosting sympathetic tone and activating the BAT [44-46] – the molecular details of this process that will be addressed later. Hypothalamic AMPK activity not only participates in the response to fasting and/or feeding, but also mediates the central effects of different circulating hormones, peptides, and signaling molecules, including leptin, estrogens, TH and many more [32,45-47]. Finally, mice with chronic genetic AMPK activation are protected against diet-induced obesity due to an overall increase in EE, both in the case of global or adipose

tissue-specific models [48]. All those data support the potential clinical application of AMPK-targeting drugs in the treatment of metabolic diseases.

1.3.3 Hypothalamic cell sensors: mTOR

Another crucial player in the hypothalamic integratory machinery is the mechanistic target of rapamycin (mTOR) [49,50]. mTOR is a conserved serine-threonine kinase that modulates cell-cycle progression and cell growth by sensing changes in energy balance, growth factors, nutrients and oxygen, and is involved in both the hypothalamic energy-sensing process and modulation of feeding behaviour [50-52]. mTOR is highly expressed in key hypothalamic nuclei modulating feeding, such as the ARC, PVH and VMH [49], and its activity changes inversely with that of AMPK, as when intracellular energy is abundant, mTOR activity is increased and AMPK activity is decreased, and *vice versa* [32,53].

1.4 Closing the loop to the periphery: the metabolic-energy expenditure machinery

Body EE is constituted by three basic components: basal metabolic rate (BMR), adaptive thermogenesis, and physical activity. The BMR represents the "minimal cost of living" at rest, postprandially, and at thermoneutrality, i.e. when the body is in thermal equilibrium with the environment [54]. BMR depends on the ATP production required to maintain these basic physiologic functions (Brand et al. 1999), and the heat generated by BMR is called "obligatory thermogenesis" as it represents the minimal amount necessary for being alive [54,55]. On the other hand, the term "adaptive thermogenesis" (also called "facultative thermogenesis") refers to the sum of the processes which increase the heat production upon cold exposure [54,55], i.e. the shivering and non-shivering thermogenesis, both leading to a consistent raise in energy expenditure [4,55]. Shivering, which takes place in the skeletal muscle, is defined as the repetitive process of muscular fiber contraction and is the first heat-producing mechanism activated during acute cold exposure [55,56]. However, due to its high energy consumption and interference with muscle activity, it is rapidly replaced by the more cost-effective mechanism of non-shivering thermogenesis, which in mammals mainly takes place in BAT [54,55]. All the organs and tissues involved in the metabolic response to energy sensing are innervated by the ANS, which is the main carrier of hypothalamic descending information [57]. The ANS consists of two parts, i.e. the sympathetic and parasympathetic nervous systems (SNS and PSNS), among which the former generally mediates the catabolic responses and the latter the anabolic ones [57]. By consequence, when the SNS is activated the PSNS is inhibited and *vice versa*, except for a restricted number of specific physiological circumstances when both the SNS and PSNS can be activated or inhibited at the same time [3,57]. The SNS regulates BAT thermogenesis upon hypothalamic inputs from the VMH, DMH, and ARC. The VMH is also responsible for the SNS modulation of muscle glucose uptake and WAT lipid metabolism, this latter being additionally controlled by the ARC and LHA too. On the other hand, the hepatic glucose production and pancreatic insulin secretion are regulated by both SNS and PSNS inputs, moving from the VMH, LHA, and ARC in the case of SNS and the dorsal vagal complex in the case of the PSNS [3].

1.4.1 The brown adipose tissue

The BAT is a metabolically active tissue proper of euthermic animals with a highly specialized thermogenic function. Brown adipocytes are characterized by multilocular

morphology, small lipid droplets and a high number of mitochondria [5], expressing the BAT-specific inner mitochondrial membrane uncoupling protein 1 (UCP1), the main responsible for the heat generation process [55], albeit some UCP1 non-dependent mechanisms are also involved [58]. Both brown adipocytes and white adipocytes present lipid accumulation capacity, but whether the WAT storage only represents a body energy reservoir, BAT lipid accumulation is locally employed as energy fuel to support the thermogenic reaction [4,59]. Another feature differentiating BAT from WAT is the origin of their precursor cells. In fact, brown adipocytes precursors share the same lineage as skeletal muscle and are positive for Myf5, while WAT cells originate from a non-myogenic line [8]. In terms of anatomical localization, mice BAT can be found in the interscapular region (iBAT) and to a lesser extent as perirenal and axillary BAT. In humans, BAT is present in the neck region of newborn infants and it had classically be considered to disappear in the early postnatal life [30]. However, recent evidence highlighted that residual areas of functionally active BAT may also be encountered in adults, with these regions possibly being identified and quantified noninvasively with the use of (18)F-FDG PET-CT [60,61]. BAT thermogenic program is activated upon adrenergic stimulation, through the binding of norepinephrine (NE) to the β3 adrenoreceptor (β3-AR) which is located on the brown adipocyte membrane and are coupled to excitatory G-protein (Gs). The Gs activate the adenilate cyclase (AC) with subsequent conversion of ATP in cyclic adenosinmonophophate (cAMP) that activates protein kinase A (PKA). PKA activation promotes both the acute and the chronic thermogenic programs, with these two mechanisms occurring contemporarily and in independent manners. The acute thermogenic process consists in the immediate heat-generation upon the activation of UCP1, which is able to short-circuit the proton gradient generated by the ATP synthase processes [55]. In basal conditions, the energy resulting from the electron movement through the respiratory chain generates a proton gradient across the inner mitochondrial membrane, and this force is used to produce ATP from ADP. UCP1 provides an alternative pathway for the protons to be transported back into the mitochondrial matrix, circumventing ATP synthase and releasing the potential energy of the gradient as heat [54,55]. The thermogenic reaction requires to be supported by energy fuel in the form of FFAs, which are commonly derived by the mobilization of the local TGs storage. In fact, the adrenergic stimulus, as well as the PKA activation, do also increase the lipolytic activity through the activation of adipose triglyceride lipase (ATGL), hormone-sensitive lipase (HSL), and monoacylglycerol lipase (MGL) [30]. However, the thermogenic process can also occur in absence of lipolysis, supported by alternative ways of fueling, such as circulating nutrients [62], FFAs derived from BAT surrounding lipid droplets, and increased BAT glucose uptake with generation of glycolytic metabolites involved in FFAs lipogenesis [30]. In the case of prolonged sympathetic stimulations, sustained PKA activation triggers the chronic thermogenic program. This latter is a long-term process which involves the activation of p38-mitogen-activated protein kinase (MAPK), promoting in mitogenic effects, gene transcription, and protein synthesis, thus stimulating UCP1 expression and brown adipocytes proliferation and differentiation [55]. As mentioned above, the hypothalamic control of BAT thermogenesis depends on the activity of the VMH, DMH, and ARC through SNS-mediated adrenergic stimulation to brown adipocytes [30]. Among those, a crucial role is played by the VMH, which was the first to be recognized to activate the BAT in a feeding-independent manner [63]. Subsequently, both mechanistic and genetic studies have confirmed the link between VMH activation and BAT thermogenesis [30], highlighting that 1) the VMH is involved in the thermogenic response to multiple hormonal and pharmacological signals (TH, estrogens, bone morphogenetic protein 8B, GLP-1 analogues) 2) this function depends on local targeting of the AMPK downstream [32,45,47,64]. In addition to the VMH, other hypothalamic nuclei and areas have been shown to play a role in the BAT

activation, such as the ARC (possibly mediating the thermogenic actions of leptin, but this actions seems controversial [65]), the LHA (*via* the orexin signaling), the DMH (by the local NPY expression), and many more [30,40,66] (Figure 3).

1.4.2 The beige adipose tissue and the "browning" of WAT

In addition to brown and white adipocytes, a third fat cell type was identified the last few years in rodents and termed beige or brite fat, as it shares some specific features of BAT despite being localized in the classical WAT depots [6,67]. Brite/beige adipocytes arise in the anatomical sites characteristic of WAT and derive from the same non-myogenic precursor, but display an increased mitochondrial biogenesis, a multilocular morphology with smaller lipid droplets and express UCP1, all those features making beige adipose tissue more similar to BAT than to WAT [68]. However, despite sharing some features with either WAT or BAT, beige adipocytes display a distinct and unique gene expression profile, this representing the main reason for being defined and accepted as a distinct class of fat cell (see figure 2 for further details) [6,67,69].

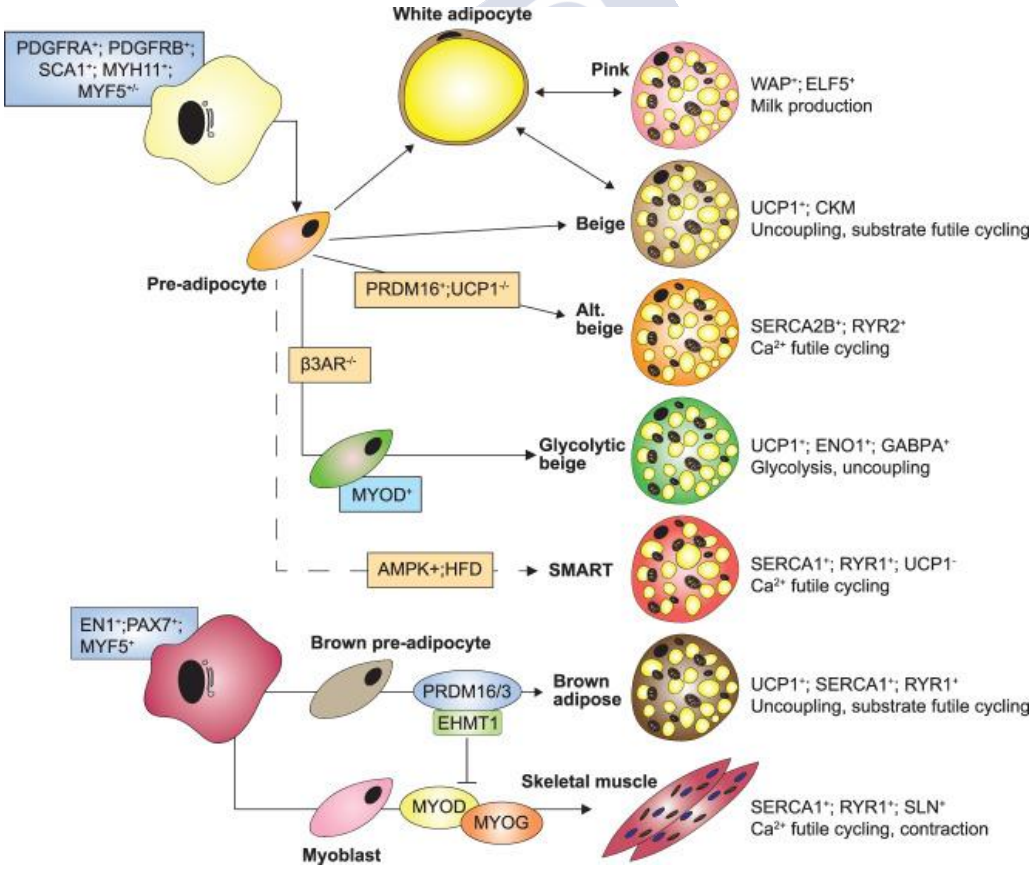

Figure 2. Schematic representation of the adipocyte lineages, including known lineage markers, specialization, and key regulators. From [6]. Creative common license CC BY 4.0

The arising of beige adipocytes in the into the WAT depots – the so-called "browning" of WAT – is usually triggered by thermogenic stimuli and occurs upon CNS-induced SNS output (Figure 3) [1,69]. In addition, other local mechanisms have been shown to participate in the

browning process, including WAT immune cells recruitment, or direct action on white adipocytes and/or beige precursor cells [8]. Through the principal CNS leading areas, a pivotal role is played by the ARC hypothalamic nucleus, projecting different signaling from the POMC and AgRP neurons to promote or inhibit browning respectively [8]. However, recent evidence highlighted that other nuclei, such the VMH, give an important contribution to the hypothalamic-mediated induction of browning [46,70].

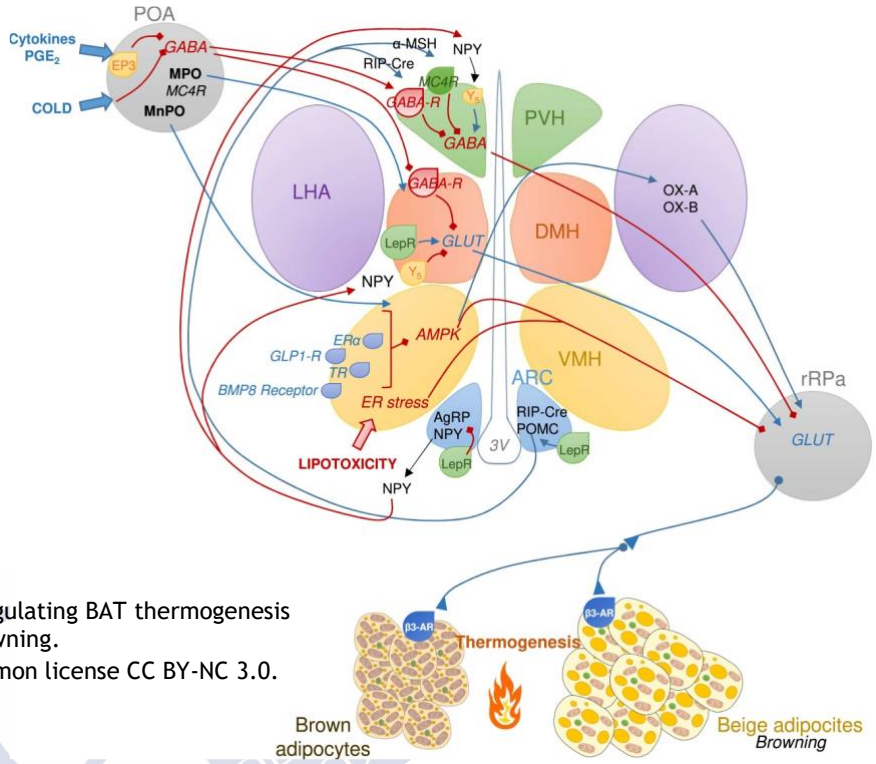

Figure 3. Hypothalamic circuits regulating BAT thermogenesis and WAT browning.
Reproduced from [1]. Creative common license CC BY-NC 3.0.

2 THYROID HORMONES PHYSIOLOGY

2.1 HORMONAL PRODUCTION AND RELEASE: THE HYPOTHALAMIC-PITUITARY-THYROID AXIS

Thyroid hormones (THs), i.e. thyroxine (3,3',5,5' tetraiodothyroxyne or T4) and triiodothyronine (3,5,3-L-triiodothyronine, or T3) are tyrosine-based hormones produced by the thyroid gland and secreted into the general circulation [71]. T4 is a pro-hormone with reduced biological activity, while T3 represents the physiologically active hormone with about a hundred fold greater affinity for the thyroid hormone receptors (TRs) [72]. TH synthesis occurs via iodination of tyrosine residues contained within a large protein called thyroglobulin, coupling of iodinated tyrosines residue to form thyronines, and enzymatic cleavage of thyroglobulin [71]. This process requires iodide uptake by active transport, thyroglobulin biosynthesis and oxidation, iodide binding to thyroglobulin, and - within the matrix of this protein- oxidative coupling of two iodotyrosines into iodothyronines [71]. TH synthesis and secretion is modulated by the hypothalamic-pituitary-thyroid axis (HPT), which involves thyrotropin-releasing hormone (TRH) in the PVH, the pituitary, and the thyroid, in order to

maintain the circulating TH concentrations in euthyroid range [73]. TRH stimulates the release of thyroid stimulating hormone (TSH) from the anterior pituitary gland, which in turn stimulates thyroid follicular cellular cells growth and hormonal release. On the other hand, TH inhibit TRH and TSH synthesis and secretion in the hypothalamus and pituitary to complete the negative feedback loop [74,75].

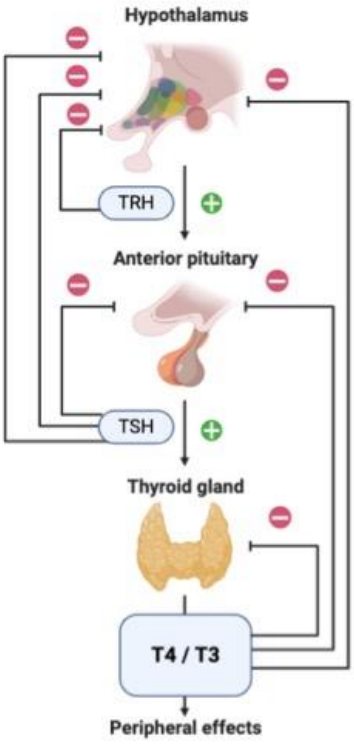

Figure 4. Schematic representation of the negative feedback loop regulation of the HPT axis. Original image, created with BioRender.

TH action, however, does not only depend on their secretion rate and circulating levels, but also on a variety of subsequent pathways which govern both their serum and tissue-specific bioavailability, including binding to serum proteins, circulating and tissue metabolization (i.e. activation and inactivation), cell membrane transporters activity, tissue expression of TR isoforms, and the activity of transcriptional corepressors and coactivators [74,75].

2.2 EXTRA-THYROIDAL HORMONAL METABOLISM

After being synthesized, TH are subjected to further metabolism by a family of enzymes called deiodinases [73]. Deiodination is a stereospecific removal of one iodine atom from T4, T3, and/or their metabolites, catalyzed by three different specific iodo-thyronine deiodinases (DIOs), including two activating enzymes, DIO1 and DIO2, and one inactivating enzyme, DIO3, which are ubiquitously and differentially expressed in all the developing and adult tissues [74]. The thyroid gland predominantly secretes T4 and only small amounts of T3, which is mainly produced by peripheral outer-ring deiodination (ORD) from T4 by the DIO2 enzyme [74]. T3 may than be inactivated by DIO3-catalyzed inner ring deiodination (IRD) leading to the formation of 3,3'-diiodothyronine (T2). IRD of T4 results instead in the formation of reverse T3 (rT3), a different TH metabolite which is unable to bind the TRs [72] (Figure 5).

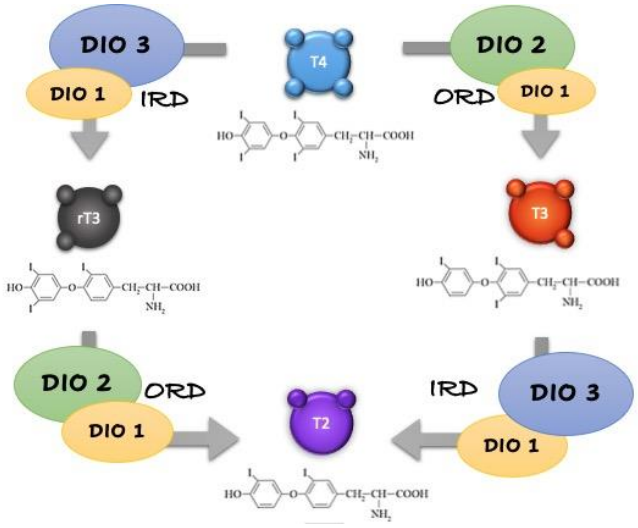

Figure 5. Deiodination of thyroid hormone isoforms. Original image.

DIO2 activity in the TH target tissues represents one of the principal determinants of the tissue-specific response to TH action, being able to rapidly increase the levels of intracellular T3 available for receptor binding [76]. In key thyroid-responsive tissues such as brain, skeletal muscle, and brown fat, DIO2 expression and activity are modulated by developmental, metabolic or environmental stimuli triggering a complex machinery of transcriptional, post-transcriptional, and post-transcriptional mechanisms [77]. DIO2 gene transcription is promoted by the adrenergic/cAMP signaling pathway [78,79], whereas in the post-translational phase, the enzymatic activity is modulated by ubiquitination/deubiquitination and proteasome degradation [73,80,81]. Even if the DIO2 activity modulation is aimed to fulfill T3 requirement, T3 itself only triggers a weak transcriptional gene downregulation, whether T4 interaction with the enzyme leads to a much stronger ubiquitin-dependent activity reduction, shortening DIO2 half-life to approximately 20 minutes [80]. This allows the production of T3 to be regulated according to the availability of T4 [82].

2.3 SERUM CIRCULATION AND CELL MEMBRANE TRANSPORT

Most of T4 and T3 circulate in the form of bound moieties attached to serum proteins (i.e. thyroxine binding globulin, transthyretin, and albumin), and are in equilibrium with their respective free fractions (i.e. FT4 and FT3) which represent the only biologically active ones [73]. Despite the early conception that TH that could passively diffuse through cell membranes, from the 1970s onward growing evidence highlighted that they need instead to be carried by specific transport proteins which govern the cellular uptake and/or efflux, and that the role of passive diffusion, if any, is limited [83,84]. Since then, accumulating evidence came from tissue profiling, experimental models of global and tissue-specific transporter KO, as well as the identification of human diseases associated with TH transporters mutations, but the number of the identified TH transporter proteins is continuously growing and the full knowledge of their respective specific function remains an open challenge [84]. To date, about 16 transporters have been identified, belonging to 5 different protein families, which include the organic anion transporters (OATPs, SLC10, and SLC17), L-type amino acid transporters (LATs), and monocarboxylate transporters (SLC16 also known as MCTs) [84]. Genetic mutations in MCT8 and OATP1C1 have been associated with different clinical syndromes, with complexes multi-organ involvement. Specific attention has been given to the genetic MCT8 deficiency, which

may lead to a severe clinical phenotype including a marked neurocognitive impairment [84-86]. This may not be surprising as the brain, together with the whole CNS, is an early target of TH, which are essential for its correct development since the very first stages of the embryogenesis [87-90]. To reach the brain, circulating molecules need to cross the blood-brain-barrier (BBB), which is composed by the tight epithelium of the microvasculature and by the astrocytic end-feet wrapping the microcapillaries to restrict the paracellular diffusion of low-molecular-weight molecules [84]. In the mouse brain, MCT8 is localized predominantly in the BBB, in the choroid plexus and in neurons, while OATP1C1 in the BBB, in the choroid plexus and in astrocytes [91]. On the other hand, in humans, OATP1C1 is not expressed in the BBB and seems instead to be primarily involved in T4 uptake by astrocytes [92]. Both transporters have been demonstrated to be important for the local TH activity in the CNS [84]. MCT8 has preference for T3, whereas T4 and rT3 are preferentially transported by OATPC1. MCT8-KO mice do not suffer from a defective brain development, as the lack of the MCT8-dependent T3 passage is counterbalanced by a higher rate of T4 transport by a compensatory OATP1C1 over-activation [84,93]. Once in the astrocyte, T4 is deiodinated, and the active T3 may be taken up by neurons or oligodendrocytes to bind the nuclear TRs in neuronal cells [94] (Figure 6). Conversely, the human BBB does not express OATP1C1 neither MCT10, the latter capable of partially compensating MCT8 deficiency in tissues with overlapping expression of the transporters (i.e, liver, kidney, and thyroid), and human MCT8 mutation leads to a much greater TH deprivation in the developing brain, with defective neurodevelopment and locomotor impairment (Allan-Herndon-Dudley syndrome, AHDS) [84]. A useful mice model to get insights into this human disease, is the MCT8 and OATP1C1 double knock-out (M/O dko), currently being used to study the cardiac pathology in AHDS patients [95]. Finally, all the above-mentioned transporters, as well as several others (i.e LAT transporters) are not only expressed in the BBB, but also in a variety of other CNS cells, including neurons, astrocytes, tanycytes, microglia, and more [84,96].

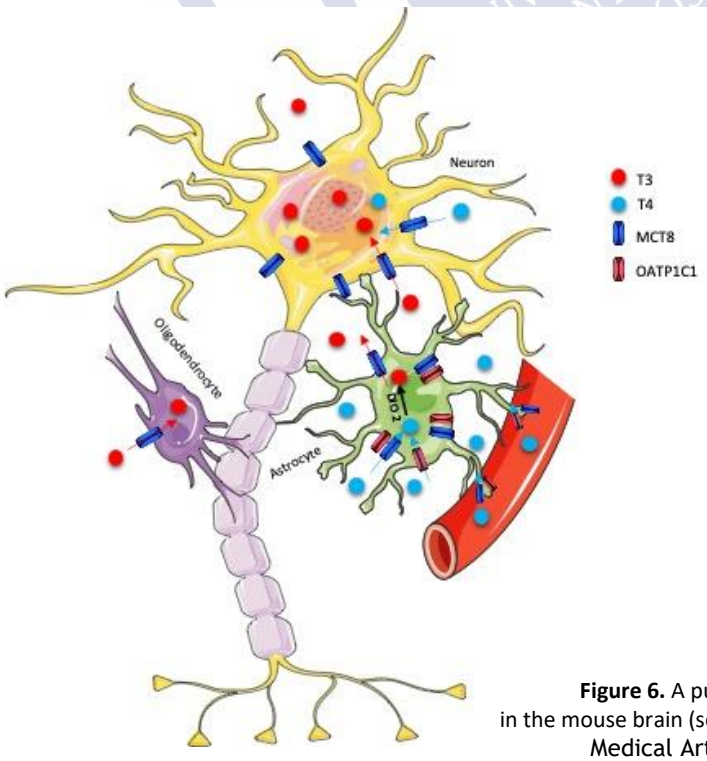

Figure 6. A putative model of TH transport and metabolism in the mouse brain (schematic overview). Modified from Servier Medical Art, Creative common license 3.0.

2.4 RECEPTOR BINDING AND GENOMIC *VS* NON-GENOMIC EFFECTS

Once in the cell, TH exert their genomic effects through binding of T3 to the nuclear TRs, which are bound to T3-response elements (TREs) in the regulatory regions of T3 target genes and can act as transcription factors [84]. TRs, i.e. TRα and TRβ belong to the nuclear hormone receptor superfamily, and are expressed almost ubiquitously in both embryonic and adult tissues [97,98]. TRα and TRβ are encoded by two separate genes, and several protein variants originate by alternative processing of gene transcripts. The transcripts from the TRβ gene produce three (TRβ1-3) ligand-binding proteins with a conserved C-terminal region including DNA and ligand-binding domains but with different N-terminal portions. Regarding the TRα gene, only one of its two major products, TRα1, gives rise to a ligand-receptor, whereas the other three main isoforms, namely TRα2, TRα3 and TRα4, do not bind to the ligand but sustain DNA-binding capabilities, although their function *in vivo* is unclear [75,99]. TRα1 is expressed almost ubiquitously since the earlier stages of development, its expression being higher in neural tissues and lower in hepatocytes [100,101]. TRβ1 is predominantly expressed in the heart, liver, inner ear, retina, hypothalamus and other several brain areas, whether TRβ2 distribution is restricted to the pituitary, retina, inner ear and hypothalamus [100,101]. Most of the well-known effects of THs are mediated at the transcriptional level, with regulation of targets genes by nuclear TRs [75,99]. According to the classic view of the positively regulated TR targets, gene expression is controlled at genomic level by the TRs either in the presence or absence of T3, as unliganded TRs act as aporeceptors that produce the opposing transcriptional effect, an effect that may be exerted via pre-existing protein complexes interacting with the transcriptional machinery [102]. In the absence of T3, the TRs would recruit a multiprotein complex of nuclear corepressors (NCoR1 and SMRT, which in turn recruit HDAC3 and others) mediating transcriptional blockage [103,104]. T3 binding to TRs would lead to release of the corepressor complex and recruitment of coactivators that lead to gene transcription [105]. However, recent findings have challenged this model and the exact mechanisms underlying TRs-mediated gene transcription remain not fully clarified. [73]. Moreover, besides this TRs-mediated modulation of gene transcription, TH action also display a wide range of nongenomic actions, including interaction between TH and membrane integrin receptors, as well as TR-mediated modulation of signal transduction pathways in the cytoplasm [99]. Some of the identified nongenomic mechanisms are: 1) activation of phosphatidylinositol 3-kinase (PI3K) via a liganded TR resulting in downstream phosphorylation and activation of PKB/Akt, mTOR and p70S6K [106]; 2) interaction with the plasma membrane protein, integrin αvβ3, which has been identified as a TH receptor that activates both the PI3K and ERK1/2 pathways [107]. The αvβ3 can bind both T3 and T4 at two possible binding sites, with different metabolic consequences, including proliferation of cancer cell lines, TRβ accumulation in the nucleus, and increased angiogenesis [74,107,108].

3 THYROID HORMONE ACTION ON ENERGY BALANCE

3.1 THYROID HORMONES AND METABOLISM: AN OVERVIEW

TH regulate a vastness of physiological processes, such as growth, development and metabolic rate [47,74,75]. The relationship between thyroid hormone status and EE has been largely known and is well exemplified in patients with thyroid dysfunction [109-111]. On one hand,

hyperthyroidism, i.e. an excess of TH, induces a hypermetabolic state with raising BMR, weight loss, hypocholesterolaemia, increased lipolysis, and gluconeogenesis [112,113]. Remarkably, up to 85% of patients with thyrotoxicosis show weight loss, despite the fact that many of them have elevated food consumption [110,114,115]. On the other hand, a reduction in TH levels is associated with reduced BMR, weight gain, hypercholesterolemia, reduced lipolysis, and reduced gluconeogenesis, with most of the patients gaining weight despite reduced food intake [111,116]. Notably, regarding the lipid metabolism, TH have been reported to induce both lipolysis and lipogenesis [117,118], but in the context of human and rodent hyperthyroidism the net effect is fat loss [44,46,119]. Conventionally, most of the above-mentioned effects have been connected to direct actions of TH on metabolically active organs and/or by enhancing tissue responsiveness to catecholamines [114,115,120,121]. However, more recent data suggest that TH control of metabolism is not only mediated by direct tissue effects, but also by TH action on the CNS, leading to centrally-driven outputs to the peripheral targets. All those mechanisms will be addressed in the next sections.

3.2 PERIPHERAL METABOLIC EFFECTS

3.2.1 Basal metabolic rate and facultative thermogenesis

TH are key modulators of both BMR and facultative thermogenesis in homeotherm (*"warm-blooded"*) species [47,114], being able to act on almost all metabolically active tissues, including liver, WAT, BAT, skeletal muscle and heart [114,120,121]. To maintain BMR, TH act by uncoupling oxidative phosphorylation in the mitochondria, or reducing the activity of shuttle molecules that transfer reducing equivalents into the mitochondria [122]. In addition, TH can increase BMR by increasing ATP production for metabolic processes and by generating and maintaining ion gradients [123]. TH also stimulate metabolic cycles involving fat, glucose, and protein catabolism and anabolism, but these latter pathways only give a minor contribution to BMR [55]. On the other hand, TH promote the adaptive thermogenesis mainly by enhancement of the BAT mitochondrial uncoupling process [55], and, to a lesser extent, by enabling the shivering thermogenesis by modulation of the skeletal muscle contractile properties [124]. Regarding BAT thermogenesis, TH act both by increasing the stimulatory action of NE and enhancing the cAMP-mediated rise in UCP1 gene expression [100,115]. Brown adipocytes express a high amount both TRα and TRβ, as well as all the DIOs enzymes isoforms [125]. UCP1 gene overexpression depends on TRβ, whether the TRα1 is essential to maintain the BAT responsiveness to adrenergic stimuli [100,126,127]. Evidence about the requirement of TH for the NE-induced BAT activation is provided by the phenotype of mice with global TRα1 deficiency, TR-α1/β deficiency, and/or deletion of all isoforms of TRα (Thra-0/0). All those mice display a normal BAT morphology, development, and recruitment with a functional obligatory thermogenesis, but are intolerant to cold due to impaired facultative thermogenesis, as all the BAT responses to NE are blunted [128,129]. Of note, Thra-0/0 mice with disruption of BAT thermogenesis display an alternative facultative thermogenesis, probably originating in skeletal muscle. However, this other pathway is less effective and more energy demanding, being consequently associated with leanness, increased capacity to oxidize fat, and relative resistance to diet-induced obesity [128,130]. Several other studies using different TR knockout mice and/or treatment with isoform-selective TR agonists confirmed that TRα is essential for thermogenesis and pointed out an additional role for TRβ in controlling cholesterol metabolism [127,128,131]. In addition to the TRs, the DIOs enzymes activity also plays critical role in modulating BAT response to TH. Among them, the most extensively studied is DIO2, representing the main local source of T3 by intracellular conversion from T4, thus being essential for a full thermogenic

response of BAT to adrenergic stimulation [79,132]. Early *in vitro* evidences showed that upon cold exposure there is an acute 50-fold increase in BAT DIO2 activity, leading to an accelerated T4 to T3 conversion [79]. This was confirmed by studies in thyroidectomized and hypothyroid rats, which revealed that BAT itself could represent a major source of T3 under acute or chronic thermic stimuli [133]. The increase in T3 concentration in brown adipocytes consequently leads to TR saturation which in turn increases the adrenergic responsiveness in a feed-forward mechanism, allowing the BAT to produce heat in a sustainable manner [134]. A deeper understanding of this process came from the mouse model of DIO2-deficiency (DIO2−/−), characterized by impaired adaptive thermogenesis and hypothermia in response to cold exposure which can be rescued by administration of T3 [134]. In these animals, the non-stimulated brown adipocytes display normal amounts of mitochondria and UCP1, but their cAMP generation capacity in response to adrenergic stimulation is reduced [135]. Contrary to expectation, the reduced BAT adrenergic responsiveness is not the preponderant mechanism underlying the impairment of cold-induced adaptive thermogenesis in in DIO2−/− mice. In fact, when exposed to cold, those animals develop a compensatory increase in BAT SNS-stimulation (up to nine-fold) that bypasses the relative adrenergic insensitivity. However, this SNS overstimulation leads to a hyper-activation of the lipolytic pathway in brown adipocytes with concomitant suppression of the usual cold-induced lipogenic surge, resulting a in a rapid depletion of the FA source. This depletion of the energy fuel for heat production is the main determinant of their impaired adaptive thermogenesis [134,135]. Finally, in addition to these well described pathways, recent in vitro evidence also pointed out a cell autonomous T3 effect on BAT mitochondria. According to these data, T3 would directly act on the brown adipocyte by inducing 1) autophagy-dependent FA oxidation; 2) autophagy-dependent mitochondrial respiration; 3) increase in mitochondrial biogenesis, mitophagy, and mitochondrial turnover [136]. In mice, it has recently been demonstrated that TH do not only contribute to heat production, but also to excess heat dissipation over the tail, this being a crucial mechanism of body defense from hyperthermia [137-139]. The evidence came from mice carrying a mutant TRα1 gene with impaired TH signaling. Those mice displayed an unexpected sympathetic overactivation with increased BAT thermogenesis, which, even more surprisingly, did not lead to a correspondent increase in body temperature [137]. This phenotype was demonstrated to depend on an impaired in the tail artery vasoconstriction, resulting in consistent heat loss and body temperature reduction which in turn activate the compensatory BAT thermogenesis [137]. The increased heat loss in this hypothyroid-like condition may contribute to explain the reduced cold tolerance of hypothyroid patients [95].

3.2.2 Glucose and lipid metabolism

In the hyperthyroidism-induced hypermetabolic state there is an increased demand for glucose, leading to an enhanced rate of its endogenous production which does not respond to the suppressive effects of insulin [140]. The TH-induced change in the body glucose metabolism is complex and involves several pathways in different metabolically active organs. In the liver, TH induce hepatic gluconeogenesis and glycogenolysis both directly, through activation of the hepatic TRs, and indirectly, by increasing the pancreatic and adrenal secretion of glucagon and adrenaline respectively, which do also contribute to increase glucose production in hepatocytes [140]. Then, to provide substrates for the gluconeogenic process, TH also stimulate 1) muscle and adipose tissue Cori cycle to increase lactate formation; 2) adipose tissue lipolysis to liberate plasma FFA; 3) skeletal muscle proteolysis to secrete amino acids and glycerol [140]. In addition to glucose production, TH also regulate hepatic lipid metabolism, and those two processes are

tightly interconnected. For example, in the context of hyperthyroidism there is an increase in liver FFAs uptake, as well as de novo lipogenesis, which in the fed state requires diet-derived carbohydrate or glucose to be shuttled to FFA generation [46,117]. Even if the more expressed hepatic TR isoform is TRβ, TH modulation of lipid metabolism relies on the differentiated and coordinated action of both TRα and TRβ [117]. In fact, mice with a dominant negative mutation in TRβ display an accelerated liver lipid accumulation with early hepatic steatosis, due to an increased peroxisome proliferator-activated receptor-γ (PPARγ) signaling and a reduced TH-dependent fatty acid β-oxidation [141]. Conversely, mice with suppressed TRα signaling are characterized by reduced liver weights and lipid accumulation due reduced lipogenesis [141]. In hyperthyroid rats the net effect is an increased hepatic lipid accumulation, with display an enhanced liver Oil Red O staining and TG content [46]. At cellular level, TH action include 1) increase of the transcription of several key lipogenic genes, such as ACC1 and FAS; 2) modulation of the activity of other transcription factors, such as sterol regulatory element-binding protein 1C (SREBP1C), liver X receptors (LXRs) and carbohydrate-responsive element-binding protein (ChREBP) 3) reduction of AMPK and Acetyl-CoA carboxylase (ACC) phosphorylation and simultaneous increase of fatty acid synthase (FAS) activity [117] [46]. Of note, the pro-lipogenic effect is restricted to the liver, not being reported in muscle, WAT, or BAT [46]. Finally, in addition to inducing lipogenesis, TH modulate several others lipid-related hepatic metabolic pathways, including cholesterol synthesis, reverse cholesterol transport, and ketogenesis [117].

3.2.3 Browning of white adipose tissue

The role of TH in promoting WAT browning is a relatively recent discovery, and its possible contribution to the TH-induced thermogenesis still represents a matter of debate. The first evidence came from a rodent study in which low-dose treatment with triiodothyracetic acid (TRIAC), a T3 metabolite with a higher affinity for TRβ was associated with increased UCP1 expression in abdominal WAT [142]. Subsequent *in vitro* experiments demonstrated that physiological doses of T3 in 3T3-L1 adipocytes can decrease TRα and increases TRβ expression, and enhance the expression of the thermogenic genes, those actions possibly involving the activation of AMPK [143]. Accordingly, the use of synthetic TRβ-selective agonist GC-1 in *ob/ob* mice induced browning of subcutaneous WAT together with accelerated metabolism, fat loss, and increased cold tolerance. GC-1 treatment contemporarily decreased BAT thermogenic function, suggesting the metabolic effects of GC-1 to be entirely mediated by WAT browning, and this hypothesis was further supported by the full recapitulation of the results after BAT denervation [144,145]. The browning effect of TH was subsequently confirmed in a rat model of peripherally-induced T4 hyperthyroidism, as well in a cohort of hyperthyroid humans in which the expression of browning genes was found to correlate with serum T4 [70]. Finally, further recent evidence came from a study in mice which were rendered systemically hyperthyroid by oral administration of either T4 or T3. This study confirmed that 1) systemic hyperthyroidism strongly induces browning in the inguinal WAT; 2) this process required an intact TRβ signaling, being absent in hyperthyroid TRβ KO mice; 3) the effect does not entirely depend on the SNS activity, being still observed after adipose tissue functional denervation – i.e. at thermoneutrality [146]. Moreover, upon calorimetric and metabolic assays this beige fat did not result to be metabolically active neither thermogenically efficient, and the hyperthyroid metabolic phenotype was reproduced in UCP1 knockout mice [146], and all those data account for a minor if any role for browning in the metabolic and thermogenic manifestations of systemic hyperthyroidism. However, the browning of WAT is not an exclusive feature of

hyperthyroidism, but it has also been described in the context of hypothyroidism [145]. This process, together with the report of increased circulating NE levels, could represent a compensatory mechanism for the contemporary hypothyroidism-related BAT inactivity [145].

3.3 CENTRALLY-DRIVEN METABOLIC EFFECTS

3.3.1 Brown adipose tissue

As mentioned before, recent data account for a pivotal role for the CNS in TH regulation of metabolism, which in the case of BAT thermogenesis involves a central control of the sympathetic tone to brown adipocytes [127,147,148]. The first evidence came from a study in mice with a heterozygous mutation of TRα1 with low affinity for T3 which, contrary to expectation, leaded to a hypermetabolic phenotype, with increased O2 consumption, lower amount of fat mass, increased feeding behaviour and resistance to diet-induced obesity [149]. As all the metabolic alterations were blunted after functional BAT denervation, the hypermetabolic phenotype was attributed to an increase in brown adipocytes activity induced by enhanced CNS signalling, highlighting the capability of the hypothalamic outputs to overrule peripheral effects [149]. The origin of this CNS overactivation comes from the embryonic brain development, where the defective TR signalling interferes with the proper establishment of the hypothalamic thermostat [150]. Moreover, in the adult mice, the mutant unliganded receptor was proven to exert a central action, further increasing the sympathetic outflow [149]. Since then, several sophisticated studies have been conducted to distinguish the central T3 actions from its well-known peripheral ones. Intracerebroventricular (ICV) administration of T3 in rodents was proven to BAT activation and thermogenesis as well as different other peripheral gluco-metabolic processes, leading to increased energy expenditure and weight loss, despite the contemporary marked hyperphagia [44,151-153], all those actions being mediated by the SNS and recapitulated in hypothyroid rats [152]. As mentioned before, to centrally activate the BAT thermogenic program, TH act in the hypothalamic VMH by inhibiting the AMPK signalling, and this occurs in a specific VMH neuronal population, namely steroidogenic factor 1(SF1) neurons [44,152]. In details, in the VMH, but not in other brain regions, T3-induced inhibition of hypothalamic AMPK and its lipogenic downstream targets, i.e. ACC, FAS, and carnitine palmitoyltransferase 1 (CPT1), increases local de novo lipogenesis, including the levels of malonyl–CoA and complex lipid species, leading in turn to the activation of the SNS and induction of BAT thermogenesis [44]. As a proof of this: 1) the VMH-specific targeted inhibition of TH signalling totally blunts the effects of hyperthyroidism on energy balance; 2) the same effect is obtained after treatment with injections of adenoviruses harbouring constitutive active isoforms of AMPK (AMPK-CA) in the VMH [44]; 3) SF1 neuron-specific ablation of the AMPKa1 isoform entirely recapitulates the central effects of T3 [152,154]. As expected, central T3 administration in UCP1 KO mice fails to induce BAT activation, despite correct inhibition of hypothalamic AMPK. However, in the same model all the other above-mentioned metabolic effects were also blunted, demonstrating the essential role of UCP1 in mediating the central actions of TH on energy balance [153].

3.3.2 Browning of white adipose tissue

Shortly after the confirmation that TH induce browning of WAT, the contribution of the central TH actions in this process was also investigated, revealing that centrally-administered T3 in rats promotes a similar pattern of WAT browning as observed in the peripherally-induced hyperthyroid model [70]. Once again, this process was demonstrated to occur in VMH by local

downregulation of the AMPK pathway. In fact, the VMH-specific (but not ARC-specific) T3 administration recapitulates the browning effect, and the genetic constitutional AMPK activation in the VMH reverses the central effect of T3 on browning [70,145,155].

3.3.3 Thyroid thermogenesis: beyond UCP1

In addition to mediating the energy-wasting effect of hyperthyroidism, UCP1 activity was also considered a key component of the so-called "thyroid thermogenesis". However, this concept has recently been challenged by the demonstration that nor BAT thermogenesis neither WAT browning significantly contribute to the raise of body temperature in hyperthyroid animals [146,156]. As this thermal elevation is observed in a wide range of environmental temperatures, it has been hypothesized that the TH effect may be the elevation of the hypothalamic thermal set-point (i.e. a fever-like or pyretic state), triggering all the peripheral heat-preserving (vasoconstriction) and thermogenic mechanisms (shivering or BAT activation) to raise the core temperature up to the new set-point. [156]. This hypothesis is supported by the results of a recent study in M/O dko mice, lacking both MCT8 and OATP1C1 transporters. Because of the lack of TH BBB crossing, those mice display a profound hypothyroid state in the CNS, despite a contemporary elevation of peripheral TH (this latter due to the negative feedback loop of the HPT), thus representing an interesting model to dissect the peripheral *vs* central TH contributions to body temperature regulation. The M/O dko mice displayed normal skin and fur insulation, with no signs of impairment in the body temperature regulation, and normal cardiac function. On the other hand, T3-treated wild-type (WT) mice developed mild daytime hyperthermia and cardiac hypertrophy, suggesting that these hyperthyroid phenotypes depend on central actions of TH [95]. However, as several other factors may influence the thermoregulatory process in the M/O dko mice (e.g. contemporary peripheral TH transport, developmental brain defect, etc…), additional future studies will be needed to further address this issue.

3.3.4 Liver glucose and lipid metabolism

It has recently been shown that TH can modulate hepatic glucose production and insulin sensitivity from the PVH to the liver via SNS, independent from the circulating glucoregulatory hormones [151,157,158]. Hyperthyroid rats display an increased glucose production in the liver, which was attenuated by sympathectomy but not by parasympathectomy, this latter decreasing instead the hepatic insulin sensitivity [151,157]. Moreover, specific administration of T3 into the PVH stimulates hepatic glucose production, this effect also being blunted by hepatic sympathectomy [157]. Another potential player in this hypothalamic-liver axis is the ARC, which also expresses TRs, is connected to sympathetic outflow neurons, and has an established role in the central modulation of hepatic glucose production [27,159-162]. Finally, hepatic lipid metabolism has also been demonstrated to be targeted by hypothalamic-dependent TH action, as emerged by the observation that central T3 administration stimulates the same expression of liver pro-lipogenic enzymes that is found in systemic hyperthyroidism [46]. The underlying molecular mechanism is analogous to the one described for BAT thermogenesis, i.e. targeting the AMPK activity in the VMH SF-1 neurons. This leads in turn to the activation of the c-Jun N-terminal kinase 1 (JNK1) signaling, which controls hepatic lipid metabolism [46]. Of note, while the hypothalamic outputs to BAT are carried by the SNS, the descending information reaches the liver through the PSNS, as vagotomy totally reversed the central T3 hepatic effects without altering the ones on either body weight or BAT [46]

3.3.5 Feeding behaviour

Alterations in TH status are associated with changes in feeding behaviour in both humans and rodents, being hyperthyroidism usually characterized by hyperphagia and hypothyroidism by overall reduced appetite and food intake [163-165]. Hyperphagia in hyperthyroidism was previously considered to only represent a compensatory response to the negative energy balance, but more recent evidence suggest that TH also exert a direct central orexigenic action independent from the peripheral energy waste [49,166]. In this line, interesting data came from a study in which *ad libitum* fed rats were treated with low-dose T3, i.e. a dose leading to a slight increase of plasma fT3 levels without exceeding the normal range and not exerting TSH-suppressive effects [166]. This treatment increased the rats feeding behaviour without altering locomotor activity, energy expenditure, or plasma leptin levels, being instead associated with a trend toward increased weight gain [166]. TH direct orexigenic effect has been shown to depend on T3 action on the hypothalamus, with specific regard to the ARC, where it induces an upregulation of the orexigenic neuropeptides AgRP and NPY and a downregulation of the anorectic POMC [49,167]. Those changes in the ARC neuropeptide expression are mediated by a complex molecular mechanism involving several TH molecular targets, such as DIO2 [168], uncoupling protein 2 (UCP2) [169,170], and mTOR [49,50]. In vitro data showed that T3 is able to activate mTOR signalling [106], and in vivo studies revealed that hyperthyroid rats do not only display a marked down-regulation of hypothalamic AMPK phosphorylation [44], but also a marked up-regulation of the mTOR downstream [49]. Specifically in the ARC, mTOR expression highly colocalizes with the one of TRα, and the administration of T3 in this nucleus - but not in the VMH -, leads to the local activation of mTOR signalling and promotes food intake. The same result is obtained upon the constitutive activation of TRs in the ARC using adenoviral therapy, both in euthyroid and hyperthyroid rats [49]. Finally, central treatment with the specific mTOR inhibitor rapamycin, totally reverses the hyperthyroidism-induced hyperphagia and normalized the AgRP and NPY expression in the ARC [49], all those data pointing out the pivotal role of mTOR in mediating central TH action on feeding.

HIPOTHESIS

USC
UNIVERSIDADE
DE SANTIAGO
DE COMPOSTELA

The effects of TH on metabolism depend on the combination of their direct tissue effects and the centrally-driven ones. The oral administration of TH may represent a suitable experimental model to investigate the functioning of this complex machinery.

USC
UNIVERSIDADE
DE SANTIAGO
DE COMPOSTELA

OBJECTIVE

To uncover the mechanisms by which oral administration of T4 or T3 influence energy balance. To this end we specifically addressed the following issues:

1. To assess and compare the serum and hypothalamic concentrations of thyroid hormones in a murine model of peripherally (oral thyroid hormones administration) induced hyperthyroidism.
2. To assess the whole-body metabolic changes induced by the above-mentioned treatment, with particular regard to the brown and white adipose tissue
3. To compare and relate the data obtained at central level with the corresponding peripheral metabolic profile

MATERIALS AND METHODS

1 ANIMAL EXPERIMENTATION

Animal care, handling, and experimental procedures were performed in agreement with the International Law on Animal Experimentation and were approved by the USC Ethical Committee, under the responsibility of Miguel A. López Pérez with the proceeding numbers: ID 15005AE/10/FUN/FISIO2/MLP2 and ID 15010/14/006 according to the current regulations:

- Directive 2010/63/EU of the European Parliament and of the Council of September 22th on the protection of the animals used for scientific purposes.
- State law 32/2007 of November 7th, for the care of animals in their exploitation, transportation, experimentation and sacrifice.
- Decree 296/2008 of December 30th, on the protection of animals used for experimentation and other scientific purposes, including teaching, and by which the Register of breeding centers, suppliers and users, and the Galician Commision of Animal Welfare of Experimentation is created.
- Royal decree 53/2013 of February 1st, which establishes the basic rules applicable for the protection of animals used in experimentation and other scientific purposes, including teaching.
- Order of September 15th, 2006 by which is created the "Comité de Bioética da Consellería Rural".

The experimental designs were made according to the Royal decree 53/2013, with particular regard to the Article 4 (Principle of replacement, reduction and refinement). The experimental procedures involved the minimum number of animals to achieve the objectives and reduce as much as possible their stress or suffering.

2 EXPERIMENTAL DESIGN

2.1 ANIMAL MODELS

Adult male wild-type mice (C57BL/6 background; 8-10 weeks old, Animalario General University of Santiago de Compostela, Santiago de Compostela, Spain) were housed in groups (4 mice/cage) with an artificial 12 hours light (8:00 to 20:00)/12 hours dark cycle, under controlled temperature and humidity conditions. Before starting the experimental procedure, the animals underwent a 7 days period of acclimatation to the facility and to the handling procedure under non-stressful conditions. During all this time, free access to standard laboratory chow diet (*STD, SAFE A04: 3,1% fat, 59,9% carbohydrates, 16,1% proteins, 2.791 kcal/g*; Scientific Animal Food & Engineering; Nantes, Francia) and tap water was granted. To comprobate the animals' well-being, they were monitored daily by performing a physical examination. Body weight and food intake were measured daily with precision scale, as well as water intake with a graduated cylinder, both during acclimatation and for the whole course of the experiment.

2.2 INDUCTION OF HYPERTHYROIDISM

Mice were treated with TH in drinking water at the following concentrations: 1 mg/L L-Thyroxine (T2501, Sigma Aldrich) in 0.01% BSA (BSA, *Albumin, from bovine serum*, Sigma-Aldrich) or 0.5 mg/L 3,3',5-Triiodo-L-thyronine (T32877, Sigma-Aldrich,) in 0.01% BSA for 14 days. These treatment doses had previously been proven to be sufficient to induce

hyperthyroidism but low enough to avoid cachexia [116,146]. Control mice received 0.01% BSA (vehicle treatment).

2.3 EXPERIMENTAL DESIGN

After the acclimatation phase, the mice were divided in three experimental groups, i.e. T4 treatment, T3 treatment, or vehicle treatment (control group). Mice were kept housed in groups (n. 4 per cage). Each experimental group included 3 cages, for a total of 12 mice. The mice were treated for a total of 14 days by ad libitum access to drinking water containing either T4, T3, or vehicle as previously detailed. Free access to standard chow diet was also provided for all the duration of the treatment. The whole experiment was repeated 3 times.

2.4 ANIMALS MONITORING

During the whole treatment, body weight and food intake were measured daily at the same hour with precision scale, and water intake with a graduated cylinder. Core body temperature was measured at the end of the treatment using a rectal probe connected to digital thermometer (BAT-12 Microprobe-Thermometer; Physitemp, Clifton, NJ). Skin temperature surrounding BAT was recorded at the end of the treatment with an infrared camera (B335: Compact-Infrared-Thermal-Imaging-Camera; FLIR; West Malling, Kent, UK) and analyzed with a specific software package (FLIR-Tools-Software, FLIR; West Malling, Kent, UK). For each image, the area surrounding BAT was delimited and the average temperature of the skin area was calculated as the average of 2 pictures/animal. Body length, i.e. nose to tail distance, was measured at the end of the treatment with a ruler.

2.5 SACRIFICE AND DISSECTION

Animals were killed at day 14 by cervical dislocation. From each animal, the whole the hypothalamus (for RIA), or the MBH (dissected from the whole hypothalamus, for WB) were extracted, as well as the liver, the BAT, the gWAT and the scWAT. The tissues were weighted freshly with a precision scale and subsequently harvested and homogenized on ice. The blood of the animals was collected in specific tubes and centrifuged during 15 min at 2000 rpm to separate the serum. Samples were stored at -80°C until further processing.

3 ANALYTICAL METHODOLOGY

3.1 RADIOIMMUNOASSAY

High specific activity ^{125}I-T3 and ^{125}I-T4 (3000 μCi/μg) were labeled with ^{125}I (Perkin Elmer, NEZ033A) using as substrates T2 (Sigma–Aldrich; D0629) and T3 (Sigma–Aldrich; T2877), respectively [171] . The separation of the labeled products was modified using ascending paper chromatography for 16 hours in the presence of butanol:ethanol:ammonia 0.5N (5:1:2) as solvent. The ^{125}I-T3 and ^{125}I-T4 were eluted and kept in ethanol at 4°C. T3 and T4 were extracted from individual 80 μL aliquots of plasma with methanol (1:6), evaporated to dryness, and taken up in the radioimmunoassay (RIA) buffer for determinations. In the case of hypothalamus, the extraction was performed from frozen samples in methanol, followed by a second extraction with chloroform-methanol (2:1) and purification using AG 1-X2 resin colums (BIO-RAD 140-1251) with 70% acetic acid as eluent. Samples were evaporated to dryness and resuspended in RIA buffer. The efficacy of the extraction was verified by the adding tracer

amounts of ^{125}I-T3 and ^{125}I-T4 both in serum and tissue initial homogenates. Determinations of T3 and T4 were performed, as previously described [172,173], with the dynamic range being 0.4–100 pg T3/tube and 2.5–320 pg T4/tube.

3.2 WESTERN BLOTTING

3.2.1 Protein extraction

Tissues were preserved at -80°C. The MBH (dissected from the whole hypothalamus), and a small portion of liver and BAT were separated for further processing. The tissues were put in a 2 ml safe tube (*Safe-Lock Tubes 2,0 ml*, Eppendorf, Hamburgo, Alemania) with appropriate amount of lysis buffer (Tables 1 and 2) with freshly added protease inhibitor cocktail tablets (Roche Diagnostics; Indianapolis, IN, USA) and a steel pellet. The tubes were placed in the Tissue Lyser (*TissueLyser II*, Quiagen, Germantown, MD, EEUU). for mechanical homogenization, and subsequently centrifuged at 13200 rpm at 4°C for 30 minutes. The supernatant (i.e. protein extract) was aliquoted to a new tube, discarding the precipitate and the possible top layer. In the case of liver and BAT the process was repeated two and three times, respectively, in order to obtain a clean extract.

Table 1. Lysis buffer amount for each tissue.

Tissue	Volume
MBH	80 µl
BAT	250 µl
Liver	500 µl

Table 2. Lysis buffer components (in 500 ml of distilled water, adjusted to 7.5 pH**).**

Tris-HCL pH 7,5	2,5 ml
EGTA 0,2 M (pH8)	2,5 ml
EDTA 0,2 M (pH8)	2,5 ml
Tritón X-100	5 ml
Sodium orthovanadate 0,1 M	5 ml
Sodium fluoride	1 g
Sodium pyrophosphate	1,1 g
Sucrose	46 g
All reagents from Sigma-Aldrich; St. Louis, MO, USA	

3.2.1 Protein quantification and sample preparation

The protein content of each extract was quantified by colorimetric method with the Bradford solution (Bio-rad Protein Assay Kit, Hercules, CA, USA), using a standard curve of BSA. To perform the quantification, the samples were diluted 1:51 for the liver, 1:26 for the BAT, and 1:10 for the MBH. The spectrophotometer microplate (*Multiskan Go Microplate Spectrophotometer*, Thermo Scientific, Rockford, IL, EEUU) was prepared by pipetting 10 µl of each standard curve point and sample solution into separate wells in duplicate, and subsequently adding 250 µl of Bradford solution (1:4 diluition, *Bio-Rad Protein Assay*, Protein Assay Dye Reagent, Bio-Rad, Hercules, CA, EEUU) previously incubated at 37°C for 7 minutes. Once introduced into the instrument, the microplate was further incubated at 37°C for 7 minutes, followed by measurement of the absorbance at the wavelength of 595 nm, and protein concentrations were determined by extrapolation from the calibration curve. After determining protein concentration, an aliquot of each sample was prepared with the desired total protein amount (10 µg) by dilution in protease inhibitor lysis buffer and addition of 5x loading buffer – the latter containing reducing and denaturing agents, including SDS, mercaptoethanol, and glycerol.

3.2.2 Western blot

Electroforesis

The proteins were separated by electrophoresis on polyacrylamide gels (SDS-PAGE, Sodium Dodecyl Sulfate Polyacrylate Gel Electrophoresis), with a fixed concentrating fraction of 4% acrylamide/bis-acrylamide, and different resolving fractions depending on the target protein molecular weight (Table 3a-d).

Table 3a. Electrophoresis resolving gel 6,5%

Distilled H_2O	2,45 ml
Acrylamide/Bisacrylamide (30%)	2,18 ml
Buffer A	5,06 ml
APS 10 %	56,2 µl
TEMED	28,1 µl

Table 3b. Electrophoresis resolving gel 8% and 10%

	Gel 8%	Gel 10%
Distilled H_2O	4,6 ml	4,0 ml
Acrylamide/Bisacrylamide (30%)	2,7 ml	3,3 ml
1,5M Tris (pH 8,8)	2,5 ml	2,5 ml
SDS 10 %	0,1 ml	0,1 ml
APS 10 %	0,1 l	0,1 ml
TEMED	6 µl	4 µl

Table 3c. Electrophoresis concentrating gels 8% and 10%

For the 6,5% resolving gel		For the 8% and 10% resolving gel	
Distilled H_2O	1,77 ml	Distilled H_2O	3,4 ml

Acrylamide/Bisacrylamide (30%)	0,65 ml	Acrylamide/Bisacrylamide (30%)	0,83 ml
Buffer B	2,5 ml	1M Tris (pH 6,8)	0,63 ml
		SDS 10 %	50 ml
APS 10 %	25 µl	APS 10 %	50 µl
TEMED	12,5 µl	TEMED	4 µl

Table 3d. Buffer A and B composition

Buffer A		Buffer B	
Tris-HCL	90,1 g	Tris-HCL	30,2 g
SDS	2 g	SDS	2 g
In 1 l of distilled H_2O at pH a 8,8		In 1 l of distilled H2O at pH a 6,8	

The samples were shaked and heated to 95 °C for 10 minutes and loaded into the lanes (the first lane was loaded with 3 µL of a molecular weight marker, *Precision Plus Protein Standard- Dual Color*, Bio-Rad, Hercules, CA, USA) and subjected to an electric field (voltage of 100V-120V; amperage of 180 mA), connecting the electrophoresis kit filled with running buffer (Table 4) to a power source (PowerPac HC High Current Power Supply, Bio-Rad, Hercules, CA, USA).

Table 4. Running buffer composition

Glicine	72 g
Tris-HCl	15 g
SDS	5 g
In 1 l of distilled H_2O	

Semidry Transfer

The proteins were then transferred to a polyvinylidene polyfluoride (PVDF, Immobilon-P, Millipore) using a semi-dry transfer cell (Trans-Blot® SD) where membrane and gel were sandwiched between two stacks of absorbent paper soaked in transfer buffer (Table 5a-b), at constant amperage (0,25A) for 2 h.

Table 5a. Transfer buffer 25x composition

Glicine	36,5 g
Tris-HCl	72,5 g
SDS	4,5 g
In 500 ml of distilled H_2O	

Table 5b. Transfer buffer 1x composition

Transfer buffer 25x	40 ml
Methanol	200 ml

Distilled H_2O	760 ml

Protein immunodetection

Each membrane was blocked in BSA 3% (3 g of BSA in 100ml of TBS-TWEEN (Table 6a-b) at room temperature and subsequently incubated with the primary antibody (Table 7a) diluted in BSA-TWEEN for 1 h at room temperature or overnight at 4ºC according to the protein of interest. The membranes were than washed 3 times for 5 minutes each with TBS-T, and incubated with the corresponding secondary antibody (Table 7b) for one hour at room temperature, followed by another cycle of washing prior to detection.

Table 6a. Buffer TBS 10X composition

Tris-HCl	24,2 g
NaCl	80 g
In 1 l of distilled H2O at pH a 7,6	

Table 6b. TBS-TWEEN

TBS 10X	100 ml
TWEEN-20	1 ml
Distilled H_2O	760 ml

Table 7a. List of the primary antibodies

Antibody	Dilution	Provider	Reference
Mouse monoclonal Anti-α-tubulin	1:5000	Sigma	T5168
Mouse monoclonal Anti ß-actin	1:5000	Sigma	A5316
Mouse monoclonal Anti-GAPDH	1:5000	Sigma-Aldrich/MERK	CB1001
Rabbit monoclonal Anti-phospho-AMPK α (Trh172)	1:2000	Cell Signaling Technology	#2535S
Rabbit polyclonal Anti-AMPKα1	1:1000	Merck Millipore	07-350
Rabbit polyclonal Anti-AMPKα2	1:1000	Merck Millipore	07-363
Rabbit polyclonal Anti-AMPK alpha	1:1000	Cell Signaling Technology	#2532S
Rabbit polyclonal Anti-Phospho-AcetylCoA Carboxylase (Ser79)	1:1000	Cell Signaling Technology	#3661S
Purified mouse Anti-Fatty Acid Syntase (FAS)	1:1000	BD BIOSCIENCES	610963
Rabbit polyclonal Anti-UCP1	1:5000	Abcam	ab10983

Rabbit polyclonal Anti-UCP3	1:1000	Abcam	ab3477
Rabbit monoclonal Anti-PGC-1α	1:1000	Santa Cruz Biotechnology	sc-517380
Rabbit polyclonal Anti-DIO2	1:2000	Abcam	ab77779
Rabbit polyclonal Anti-Phospho-HSL (Ser660)	1:1000	Cell Signaling Technology	#4126

Table 7b. List of the secondary antibodies

Antibody	Dilution	Provider	Reference
Goat polyclonal Anti-rabbit	1:5000	DAKO	#P0448
Rabbit polyclonal Anti-mouse	1:5000	DAKO	#P0260

Protein detection was performed by chemiluminescence, using the horseradish peroxidase substrate in a ratio of 1:1 (Pierce ECL Western Blotting Substrate, Cultek, Thermo Fisher, Waltham, USA) and a developing cassette (Hypercassette, Amersham Biosciences, Little Chalfont, UK) in a dark room appropriate for X-ray film exposure. The membranes were exposed to an X-ray film (Fujifilm; Tokyo, Japan) and developed using developer (Developer G150; AGFA HealthCare: Mortsel, Belgium) and Fixator (Manual Fixing G354; AGFA Health- Care: Mortsel, Belgium).

Protein quantification

The developing sheets were digitalized by using a high-resolution scanner (800 ppp resolution, Canon Scan 9900F, Canon, Tokio, Japan), and the bands signal was quantified by densitometry using ImageJ-1.33 software (NIH; Bethesda, MD, USA). Values were expressed in relation to the respective internal control and the final value was normalized. In all the figures showing images of gels, all the bands for each picture come always from the same gel, although they may be spliced for clarity.

3.3 Real-time quantitative PCR

RNA extraction and quantification

Total RNA content was isolated using Trizol (*TRIZOL Reagent*; Invitrogen, Carlsbad, CA, EEUU), and phenol-chloroform. Tissues were cut and mechanically homogenized in th tissue lyser with appropriate amounts of Trizol (1 mL) in a 2 mL safe tube with a steel ball. After centrifugation, addition of 250 µL of chloroform, and further centrifugation, the aqueous phase (RNA) was isolated and 3 more volumes of isopropanol were added to allow RNA precipitation. The precipitate was washed with 1 mL of 70% ethanol (dissolved with H_2O DEPC), purified with repeated centrifugations, and finally resuspended in H_2O DEPC (20 to 30 µl according to the pellet size) by heating it at 60 °C for 15 minutes. The purity and the RNA amount of each sample were determined with a spectrophotometer. A ratio of RNA absorbance/proteins absorbance (260/280) of 1.8 to 2 was considered acceptable purity, and the absorbance value of 260 nm was used to quantify the RNA content. Aliquots of each sample

were prepared for the retrotranscription at the concentration of 500 ng/µl for the BAT and 1 µg/µl for the WAT.

Reverse transcription (RT)

Retrotranscription - i.e. amplification of RNA extracted as complementary DNA (cDNA) - RT was performed in a mixture of a final volume of 30 µL with the following proportions:

- 5X first strand buffer (250 nM Tris-HCl, pH 8,3, 375nM KCl, 15mM MgCl, 50nM DDT) (*Invitrogen, Carlsbad*, CA, EEUU): 6 µL
- Mixture of dNTPs (dTTp, dCTp, dGTp. dATp at 10 mM each) (*Invitrogen, Carlsbad*, CA, EEUU): 6 µL
- 50 mM MgCl2: 1.5 µL
- Random primers (*Random primers*, Invitrogen, Carlsbad, CA, EEUU): 0.17 µL
- RNAse inhibitor (*RNaseOUT*, 40 U/µl Invitrogen, Carlsbad, CA, EEUU): 0.25 µL
- Reverse Transcriptase (*M-MLV*, 200 U/µl, Invitrogen, Carlsbad, CA, EEUU).): 1 µL
- Sample: 10 µL
- DEPC H_2O to reach the final volume of 30 µL

The mixture was incubated in a thermocycler with a program of consecutive steps of 5 minutes at 37 °C, 15 minutes at 42 °C and 5 minutes at 95 °C. At the end of the samples are stored at 4 °C.

Real time-PCR (RT-PCR)

From the cDNA, the mRNA levels of the genes of interest were determined by real-time PCR (*7500 Real Time PCR System*, Applied Biosystems, Foster City, CA, EEUU) specific primers and probes (Table 8) and the results were expressed by comparing the gene of interest with the control gene. Amplification protocol (whole sequence repeated for 40 cycles):

- 2 min 50 ºC
- 10 min 95ºC
- 15 seg 95ºC
- 1 min 65ºC

Table 8. RT-PCR primers and probes

mRNA	GenBank		Sequence
UCP1	NM_009463.3	Assay ID	ThermoFisher TaqMan® Gene Expression Assays Assay ID Mm01244861_m1
CIDEA	NM_007702.2	Assay ID	ThermoFisher TaqMan® Gene Expression Assays Assay ID Mm00432554_m1
Pparg	NM_011146.3	Assay ID	ThermoFisher TaqMan® Gene Expression Assays Assay ID Mm01184322_m1
Ppargc1a	NM_008904.2 NR_027710.1	Assay ID	ThermoFisher TaqMan® Gene Expression Assays Assay ID Mm01208835_m1
Prdm16	NM_001177995.1 NM_001291026.1 NM_001291029.1 NM_027504.3	Assay ID	ThermoFisher TaqMan® Gene Expression Assays Assay ID Mm01266512_m1

Dio2	NM_010050.2	Assay ID	ThermoFisher TaqMan® Gene Expression Assays Assay ID Mm00515664_m1
Dio3	NM_172119.2	Assay ID	ThermoFisher TaqMan® Gene Expression Assays Assay ID Mm0051548953_s1
Hr	NM_021877.3	Assay ID	ThermoFisher TaqMan® Gene Expression Assays Assay ID Mm00498963_m1
Klf9	NM_010638.4	Assay ID	ThermoFisher TaqMan® Gene Expression Assays Assay ID Mm00495172_m1
Aldh1a1	NM_013467.3	Assay ID	ThermoFisher TaqMan® Gene Expression Assays Assay ID Mm00657317_m1
TRα	NM_178060.3	Assay ID	ThermoFisher TaqMan® Gene Expression Assays Assay ID Mm00617505_m1
TRβ	NM_001113417.1 NM_009380.3	Assay ID	ThermoFisher TaqMan® Gene Expression Assays Assay ID Mm00437044_m1
Hprt	NM_012583	Sense Antisense Probe	5'-AGCCGACCGGTTCTGTCAT-3' 5'-GGTCATAACCTGGTTCATCATCAC-3' FAM-5'-CGACCCTCAGTCCCAGCGTCGTGAT-3'-TAMRA

3.4 HISTOLOGICAL ANALYSIS

Hematoxylin/eosin staining and immunohistochemistry

The tissues were fixed in 10% formalin and maintained in 70% ethanol prior to paraffin embedding. Subsequently, they were included in paraffin, cut with a microtome, placed in slides, and stained with Haematoxylin and Eosin (H&E) or incubated with UCP1 antibody *UCP1*, Abcam, Cambridge, UK), followed by DAB staining (*ENVISION*, DAKO; Glostrup, Denmark). Images were taken with a digital camera Olympus XC50 (Olympus Corporation; Tokyo, Japan) at 20x.

Oil-red O staining

Hepatic frozen sections were cut (8 mm) and fixed in 10% buffered formaldehyde. The sections were subsequently stained in filtered Oil Red O (Sigma-Aldrich; St. Louis, MO, USA), washed in distilled H_2O, counterstained with Harris hematoxylin (Bio-Optica; Milan, Italy) and washed distilled H_2O. Sections were mounted in aqueous mounting medium (Bio-Optica; Milan, Italy). Images were taken with a digital camera Olympus XC50 (Olympus Corporation; Tokyo, Japan) at 40x, and quantified with ImageJ-1.33 (NIH; Bethesda, MD, USA).

4 STATISTICAL ANALYSIS

Statistical analysis was conducted using GraphPad Prism 6 Software (GraphPad Software; La Jolla, CA, USA). Data are expressed as AVERAGE ± SEM as percentage of the controls (vehicle-treated mice). Error bars represent SEM. Statistical significance was determined by t-Student (when two groups were compared) or ANOVA (for the comparison among all the three groups) followed of post hoc two-tailed Bonferroni test. $P < 0.05$ was considered significant.

USC
UNIVERSIDADE
DE SANTIAGO
DE COMPOSTELA

RESULTS

1. THE ORAL T4 AND T3 ADMINISTRATIONS LEAD TO A SIGNIFICANT INCREASE IN BOTH SERUM AND HYPOTHALAMIC THYROID HORMONE LEVELS

To verify the effectiveness of the treatment, we assessed (by RIA) the tT4 and tT3 serum levels in the mice of the three experimental groups. Treatment with T4 induced a significant raise in the circulating levels of both tT4 (4.3-fold increase vs control) and tT3 (3-fold increase vs control) while T3-trated mice displayed a 3-fold increase of tT3 and a 75% decrease in tT4, in line with the negative feedback loop of the HPT axis (Figures 7A-B). Therefore, our treatment achieved a clear hyperthyroid status. We then assessed the correspondent intra-hypothalamic concentration of tT4 and tT3 in each experimental group. In T4-treated mice, the hypothalamic levels of both TH resulted to be increased when compared with controls (2.5-fold and 3.5-fold for tT4 and tT3, respectively) in line with the corresponding changes in their serum values. On the other hand, in the T3-treated group there was a 4.5-fold increase in hypothalamic tT3 but only a slight non-significant decrease in tT4 levels, despite the reported fall in serum T4 (Figures 7C-D).

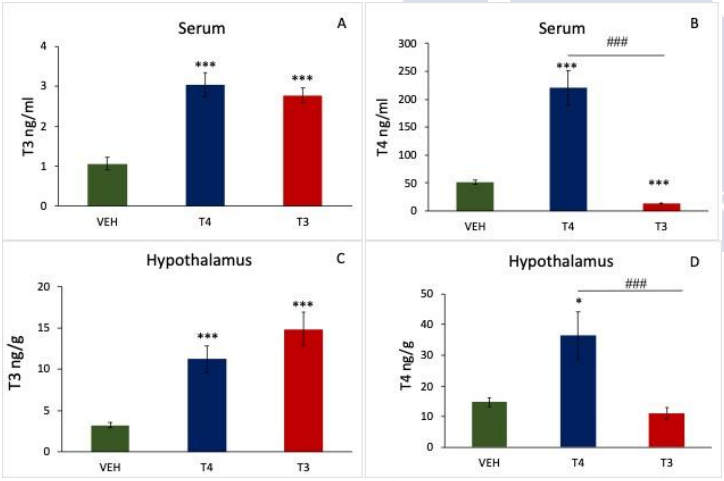

Figure 7. Serum and hypothalamic levels of total T4 and T3 in the different treatment groups. Values represented ad AVERAGE ± SEM. * p < 0,05 vs vehicle; ** p < 0,01 vs vehicle; *** p < 0,001 vs vehicle; ### p < 0,001 T4 vs T3

The calculated tT4/tT3 serum ratio was 70:1 in control mice, resulting almost unchanged upon T4 treatment (85:1, p=0,51), and significantly decreased in T3-treated mice (5:1 p<0,001 vs CT). Conversely, the hypothalamic tT4/tT3 ratio resulted to be 5:1 in control mice and significantly decreased upon both T4 (3:1, p=0,011 vs CT), and T3-treated mice (0,8:1, p<0,0001 vs CT) (Figure 8A-B).

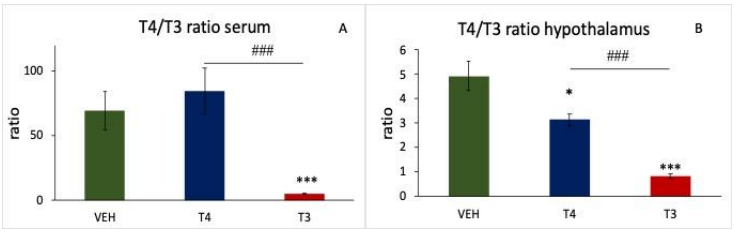

Figure 8. T4/T3 ratio in serum and hypothalamus of the different treatment groups. * p < 0,05 vs vehicle; *** p < 0,001 vs vehicle; ### p < 0,001

2. HYPERTHYROIDISM INDUCES HYPERPHAGIA, BODY GROWTH, AND CHANGES IN THE FAT MASS COMPOSITION

TH treatment induced significant changes in body weight, body composition, and food intake in both experimental groups. Among the two-weeks of treatment, we reported a progressive body weight gain in both T3 and T4-treated mice when compared with controls, which became significant since day 4 for the T3-treated group and since day 9 for the T4-treated group (Figure 9).

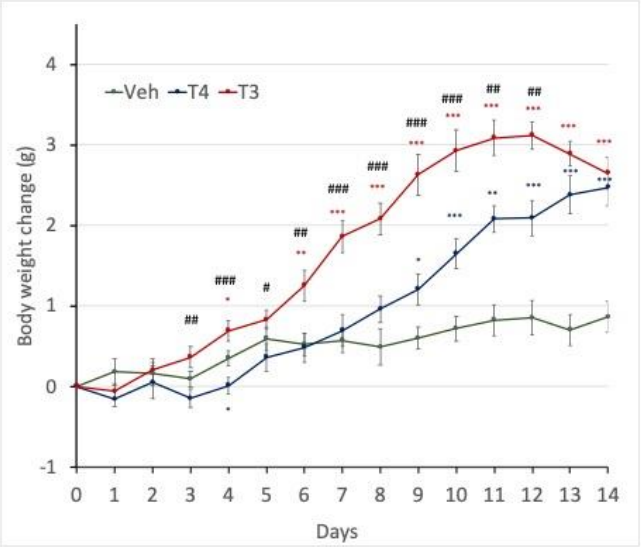

Figure 9. Body weight change in the three experimental groups among the 14 days of treatment. Values represented as AVERAGE ± SEM. * p < 0,05 vs vehicle; ** p < 0,01 vs vehicle; *** p < 0,001 vs vehicle; # p < 0,05 T4 vs T3; ## p < 0,01 T4 vs T3 ### p < 0,001 T4 vs T3

Treated mice were also characterized by hyperphagia. A gradual rise in daily food intake was reported in both T4 and T3-treated groups during the first week of treatment with respect to controls, this difference reaching significance since day 6 and subsequently becoming stable up to the end of the treatment (Figure 9A-B).

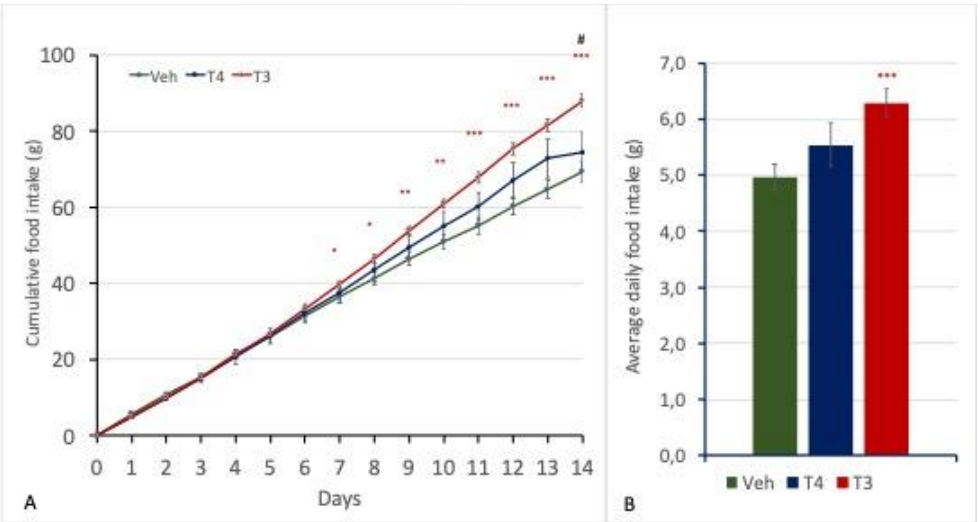

Figure 9. Cumulative (A) and average daily (B) food intake in the three experimental groups. Values represented as AVERAGE ± SEM. * p < 0,05 vs vehicle; ** p < 0,01 vs vehicle; *** p < 0,001 vs vehicle; # p < 0,05 T4 vs T3

The body length (i.e. nose to base of tail distance) measured at the end of the experiment resulted to be significantly higher in hyperthyroid mice than in controls (9,96 ± 0,07 cm in T3-treated group; 9,63 ± 0,16 in T4 treated group; 9,12 ± 0,09 cm in controls p <0,0001 and p=0,013 T3 and T4 respectively, vs control) (Figure 10A). At sacrifice, iBAT, gWAT and scWAT were extracted and weighted freshly, and values were normalized for BW for inter-group comparison. The amount of iBAT resulted to be significantly higher in hyperthyroid mice than in controls, as well as in T3-treated when compared with T4-treated mice. T3-treated mice also displayed a significant reduction in the gWAT depots, whether no changes were reported in the scWAT mass (Figure 10B).

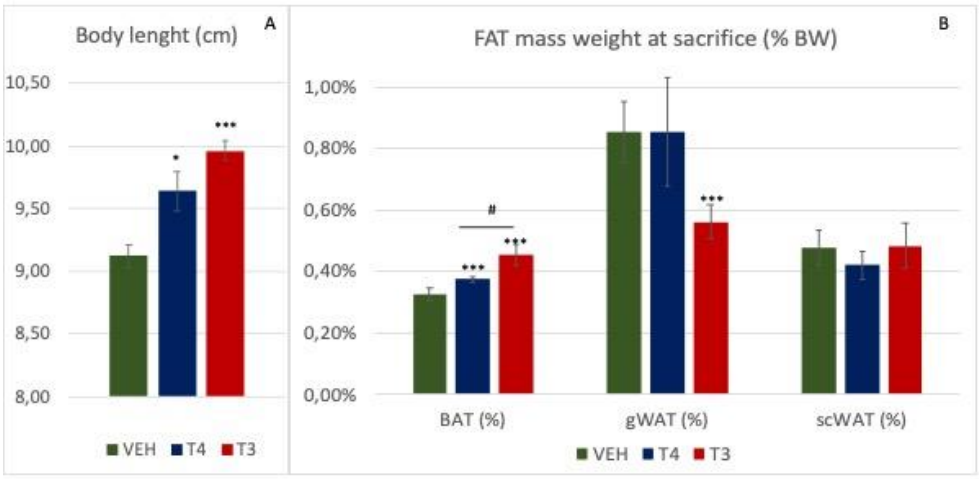

Figure 10. (A) Body length (nose-to-tail distance) at the end of treatment. (B) BAT, gWAT and scWAT weights measured freshly at dissection, and normalized for body weight. All values represented as AVERAGE ± SEM. * p < 0,05 vs vehicle; ** p < 0,01 vs vehicle; *** p < 0,001 vs vehicle; # p < 0,05 T4 vs T3

3. HYPERTHYROIDISM INCREASED THE ACCUMULATION OF LIPIDS IN THE LIVER

Hepatic Oil Red O staining was increased in hyperthyroid mice, indicating lipid accumulation in the liver, which reached significant differences in T3-treated mice (Figure 15A-D).

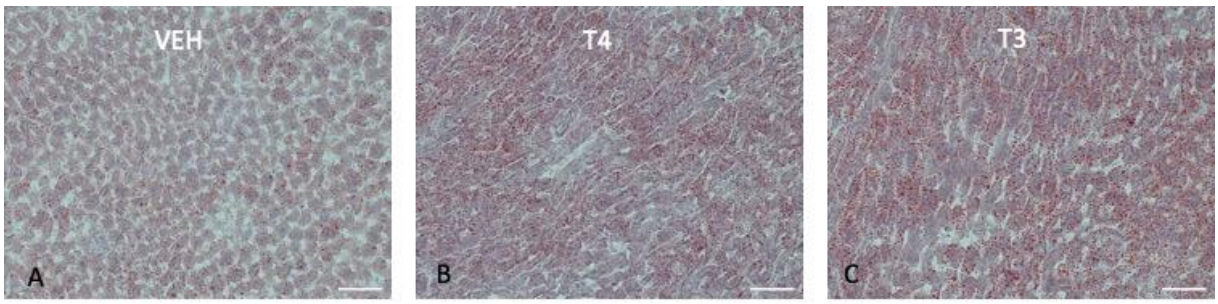

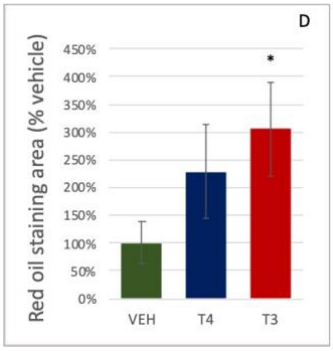

Figure 15. Representative liver Oil Red O staining of (A) vehicle treated, (B) T4-treated and (C) T3-treated mice. Scale bar 10 μm. (D) Oil Red O staining analysis. Data expresses as % of controls, in AVERAGE ± SEM. * p < 0,005 vs vehicle

Protein expression analysis revealed an increased expression of FAS, consistent with enhanced de novo lipogenesis, whereas the levels of the pAMPKα and acetyl-CoA carboxylase (pACCα) did not differ among the three groups. However, total ACC, total AMPK and the AMPKα1 subunit were found to be increased in the T3-treated group (Figure 16).

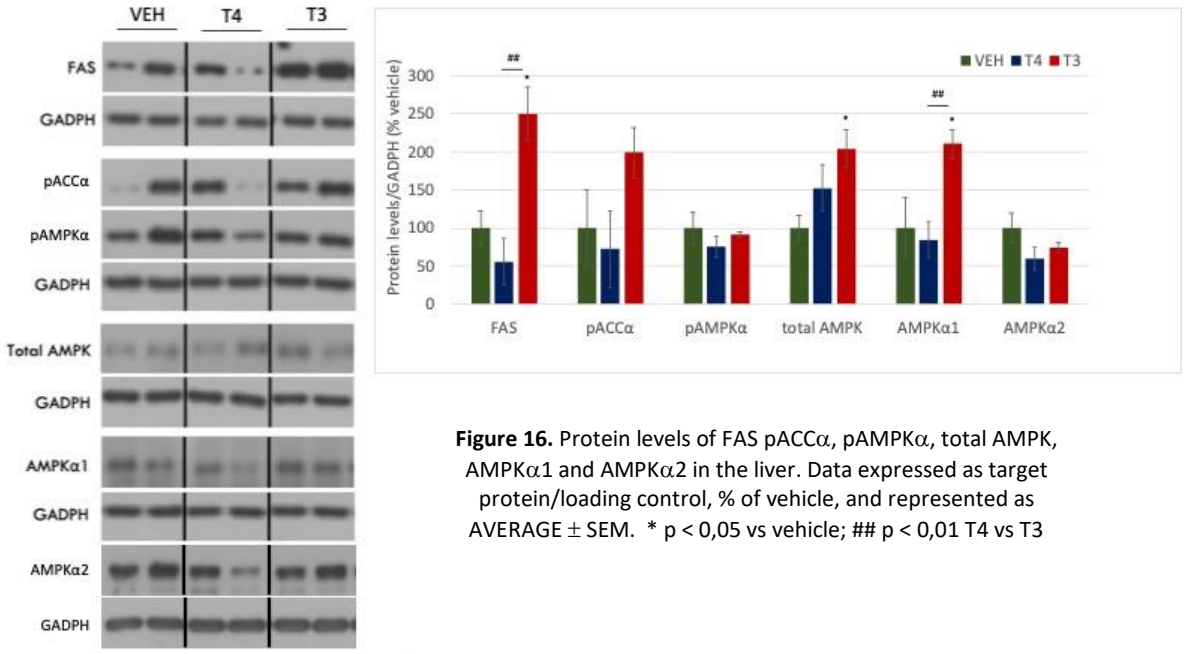

Figure 16. Protein levels of FAS pACCα, pAMPKα, total AMPK, AMPKα1 and AMPKα2 in the liver. Data expressed as target protein/loading control, % of vehicle, and represented as AVERAGE ± SEM. * p < 0,05 vs vehicle; ## p < 0,01 T4 vs T3

4. CORE BODY TEMPERATURE BUT NOT BAT TEMPERATURE WAS SIGNIFICANTLY MODIFIED BY THYROID HORMONE TREATMENT

At the end of treatment, core body temperature resulted to be significantly increased in hyperthyroid mice (37,6 ± 0,1 °C in T3-treated group; 37,7 ± 0,1 °C in T4 treated group; 36,6 ± 0,2 °C in controls p <0,0001; Figure 11A), but no significant differences were reported when analyzing the thermographic data of BAT (Figure 11B-E).

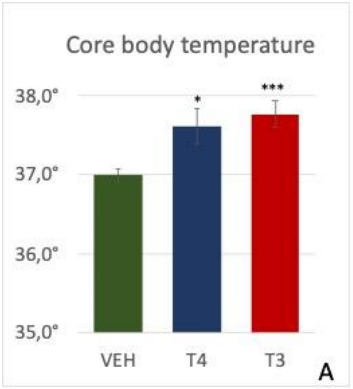

Figure 11. (A) Core body temperature. (B-D) Representative infrared pictures of iBAT of (B) vehicle, (C) T4, and (D) T3 treated mice. (E) iBAT temperature measured by infrared thermography. Values of the graphs in °C, represented as AVERAGE ± SEM. * $p < 0,05$ vs vehicle; *** $p < 0,001$ vs vehicle.

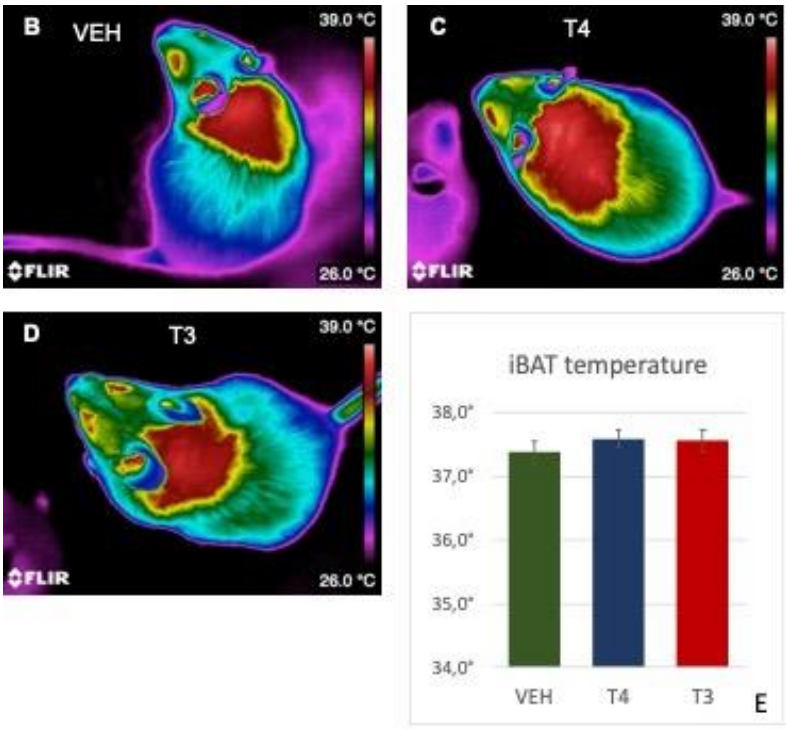

5. HYPERTHYROIDISM INCREASED THE LIPID DROPLETS SIZE AND THERMOGENIC CAPACITY IN BAT

The iBAT depots were significantly larger in hyperthyroid mice, with lager lipid droplets conferring a "whitened" appearance (Figure 12A-D).

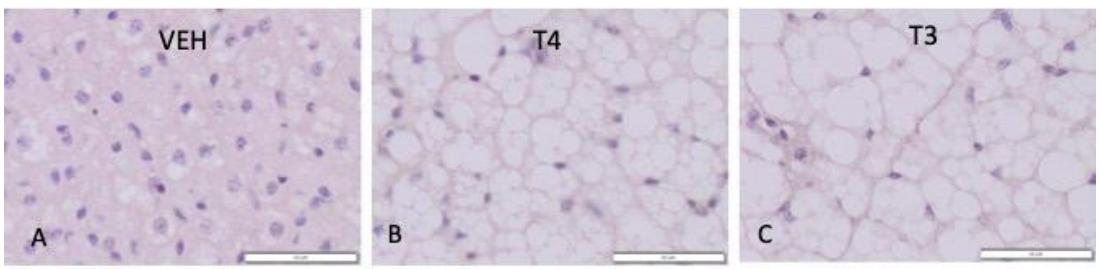

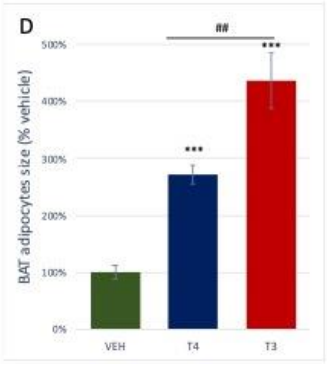

Figure 12. Representative H&E stainings iBAT of (A) vehicle treated, (B) T4-treated and (C) T3-treated mice. Scale bar 50 μm. (D) Calculated average BAT adipocytes area in the three treatment groups. Data expressed as % of controls, in AVERAGE ± SEM. *** p < 0,001 vs vehicle; ## p < 0,01 T4 vs T3

At gene expression analysis, UCP1 resulted to be unchanged upon T3 treatment, and slightly reduced in the T4-treated group. The analysis of the other thermogenic markers revealed a decrease in CIDEA, DIO2, and FGF21 in both experimental groups, as well as a reduction of PRDM16 in the T4-treated one (Figure 13).

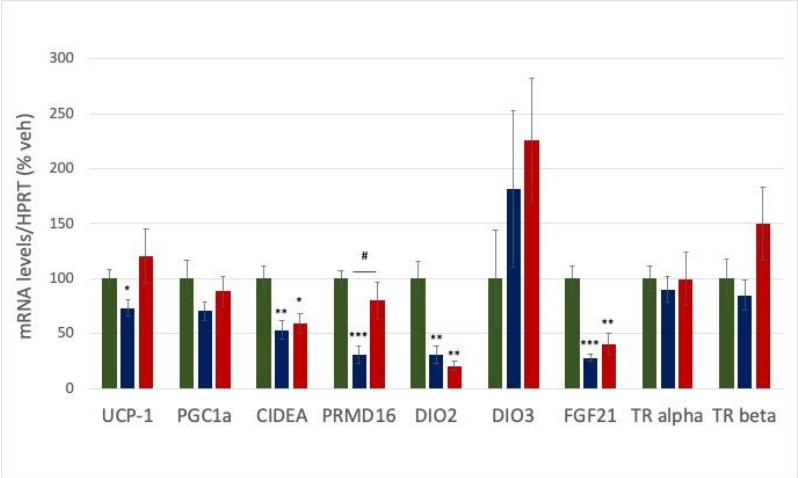

Figure 13. Gene expression analysis of browning markers and TRs in BAT. Data expressed as target gene mRNA/HPRT, % of vehicle, and represented as AVERAGE ± SEM. * p < 0,05 vs vehicle; ** p < 0,01 vs vehicle; *** p < 0,001 vs vehicle; # p < 0,05 T4 vs T3

However, western blot analysis showed a significant increase in the UCP1 protein expression in the T3-treated group, as well as an elevation of UCP3 protein levels in both groups of hyperthyroid mice, consistent with increased thermogenic capacity. FAS protein levels resulted to be significantly lower in both T3 and T4 treated groups, indicating that the increased lipid deposition did not depend on enhanced de novo lipogenesis. The phosphorylated form of AMPK (pAMPK) levels were also decreased in both treated groups, whether no changes were reported in the levels of pACC (Figure 14).

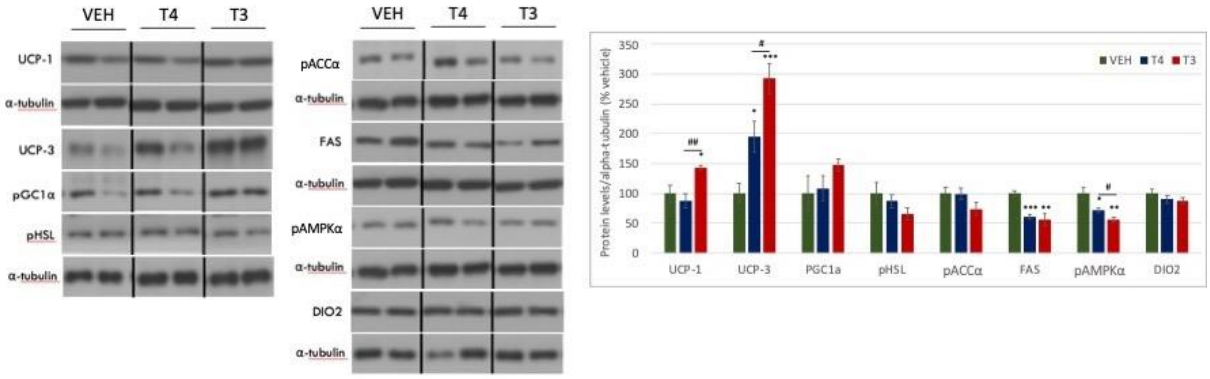

Figure 14. Protein levels of UCP1, UCP3, PGC1α, pHSL, pACCα, FAS, pAMPKα, and DIO2 in the BAT. Data expressed as target protein/loading control, % of vehicle, and represented as AVERAGE ± SEM. * $p < 0,05$ vs vehicle; ** $p < 0,01$ vs vehicle; *** $p < 0,001$ vs vehicle; # $p < 0,05$ T4 vs T3; ## $p < 0,01$ T4 vs T3

6. THYROID HORMONE TREATMENT INDUCED BROWNING OF GONADAL AND SUBCUTANEOUS WAT

Upon H&E staining, both gWAT and scWAT of hyperthyroid mice displayed a multilocular, "brown-like" pattern and a significant reduction in the calculated average adipocyte area. Subsequent IHC analysis revealed a significant increase in UCP1 staining in both subtypes of white fat of the two treated groups (Figure 17-18).

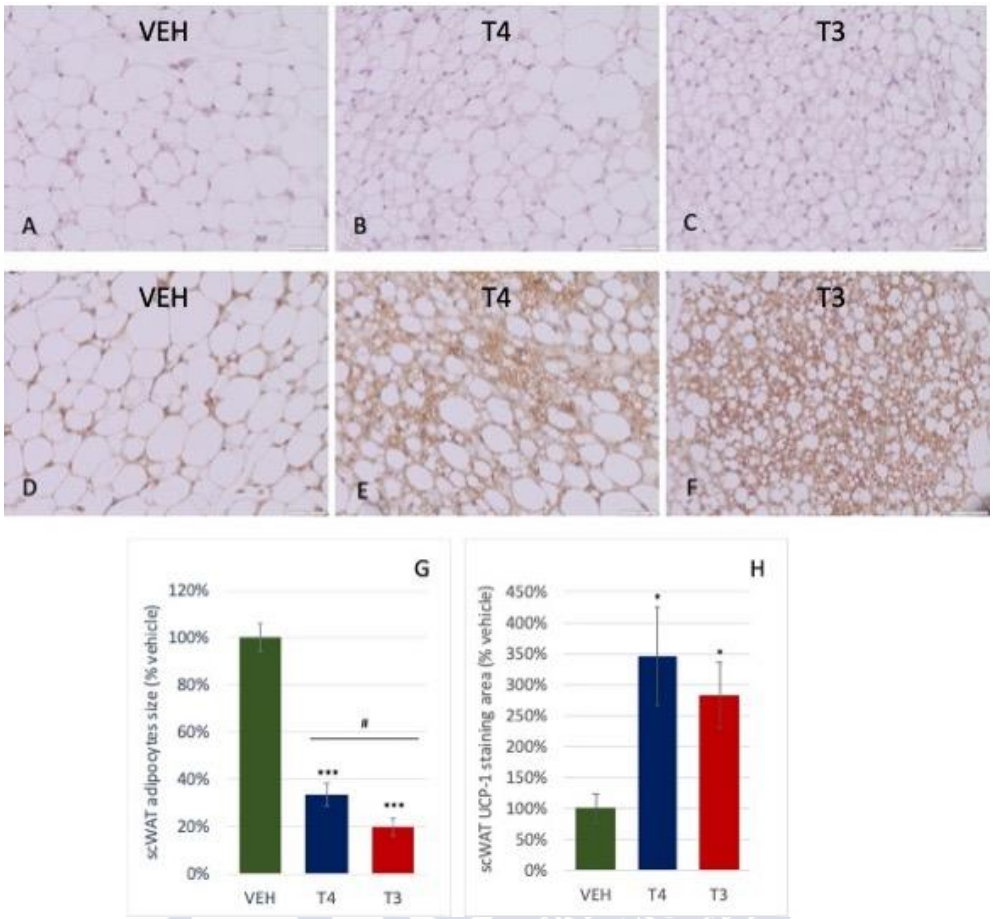

Figure 17. Representative scWAT H&E stainings of (A) vehicle treated, (B) T4-treated and (C) T3-treated mice, and representative scWAT UCP1 stainings of (D) vehicle treated, € T4-treated and (F) T3-treated mice. Scale bar 50 μm. Calculated average scWAT adipocytes area (G) and UCP1 staining analysis (H) in the three treatment groups. Data expressed as % of controls, in AVERAGE ± SEM. * $p < 0,05$ vs vehicle; *** $p < 0,001$ vs vehicle; # $p < 0,05$ T4 vs T3

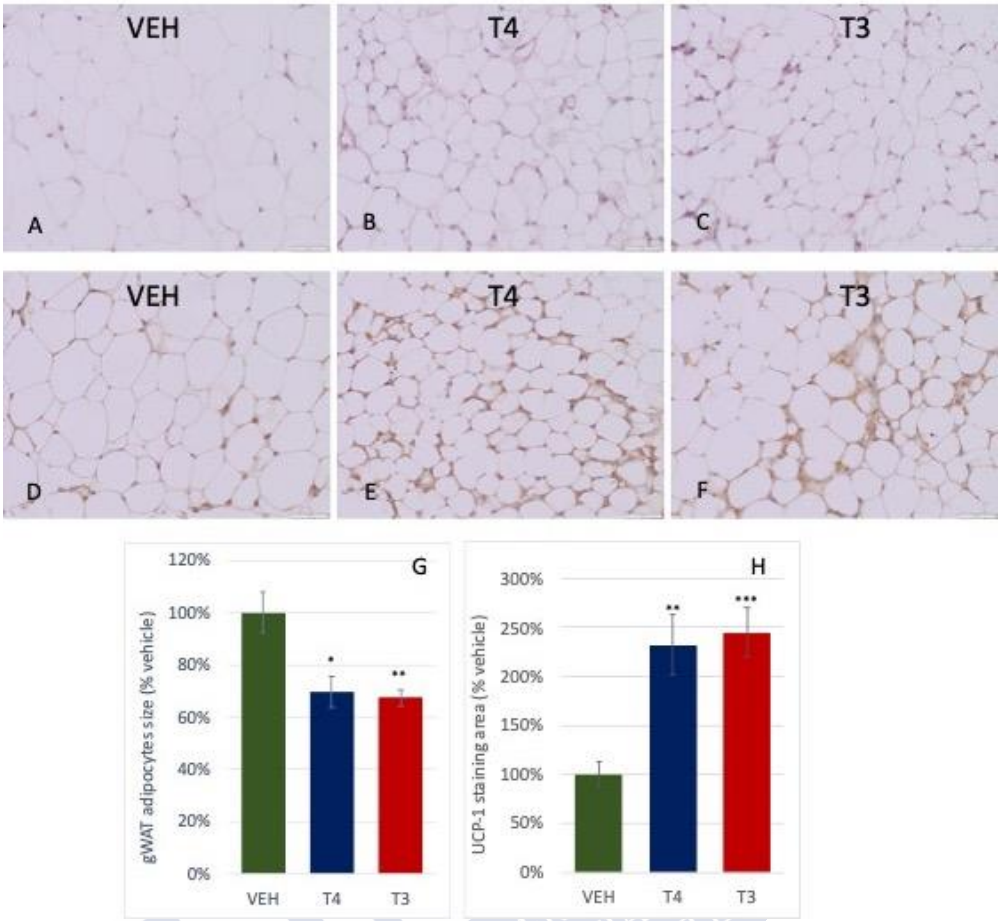

Figure 18. Representative gWAT H&E stainings of (A) vehicle treated, (B) T4-treated and (C) T3-treated mice, and representative gWAT UCP1 stainings of (D) vehicle treated, € T4-treated and (F) T3-treated mice. Scale bar 50 μm. Calculated average scWAT adipocytes area (G) and UCP1 staining analysis (H) in the three treatment groups. Data expressed as % of controls, in AVERAGE ± SEM. * $p < 0,05$ vs vehicle; ** $p < 0,01$ vs vehicle ; *** $p < 0,001$ vs vehicle

This latter data was confirmed by UCP1 mRNA expression assay which led to an equivalent result in the same tissues and groups of treatment. Among the other tested thermogenic markers, DIO2 gene was also increased in both subtypes of white fat and treated groups. In addition, scWAT, but not gWAT, displayed an enhanced expression of CIDEA in both T3 and T4 treated animals and of PRDM16 and PPARγ in the T3-treated group (Figure 19).

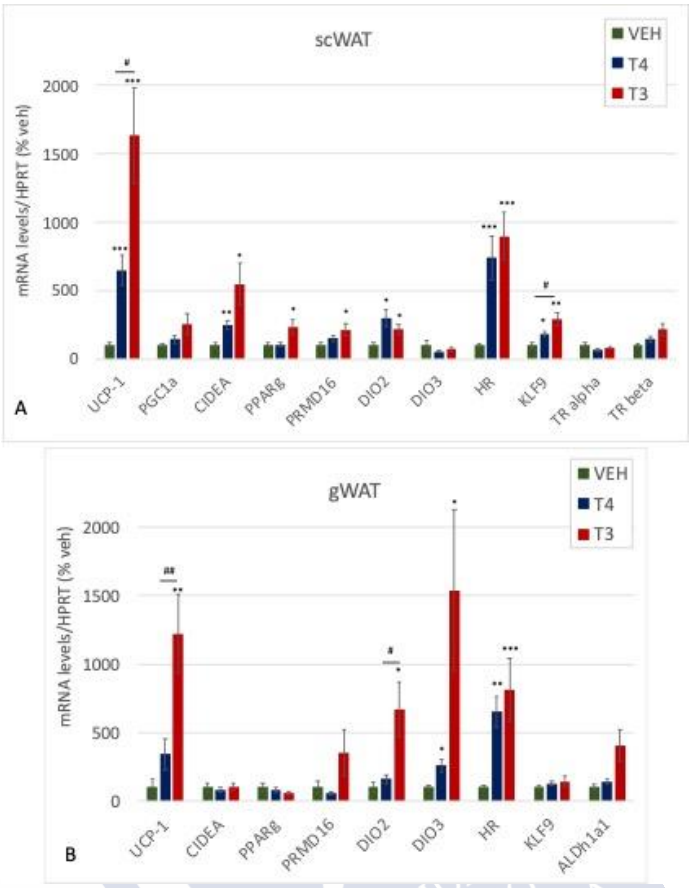

Figure 19. Gene expression analysis of browning markers and TRs scWAT (A) and gWAT (B) of the three treatment groups. Data expressed as target gene mRNA/HPRT, % of vehicle, and represented as AVERAGE ± SEM. * p < 0,05 vs vehicle; ** p < 0,01 vs vehicle; *** p < 0,001 vs vehicle; # p < 0,05 T4 vs T3

7. ORALLY-INDUCED HYPERTHYROIDISM INDUCED DOWNREGULATION OF THE AMPK SIGNALING IN THE MEDIO-BASAL HYPOTHALAMUS

It was previously demonstrated that TH effects on BAT thermogenesis, WAT browning, and feeding, do not only rely on the direct targeting of peripheral organs, but also on the induction of specific centrally-driven outputs. Following the demonstration that our employed oral treatment significantly raised the hypothalamic levels of both T4 and T3 (see section 1), we tested whether those TH concentrations were able to trigger the above-described pathways. We decided to analyze the medio-basal portion of the hypothalamus (MBH) which includes both the VMH and the ARC nuclei (involved in BAT thermogenesis, WAT browning, and appetite control), and perform a WB analysis of the AMPK downstream signalling pathway. T3-treated hyperthyroid mice showed a marked decrease in pAMPKα and pACCα. T4-treated mice also displayed a non-significant tendency towards the reduction of pAMPKα and pACCα, whether FAS protein concentration did not result to be affected by any of the experimental treatments (Figure 20).

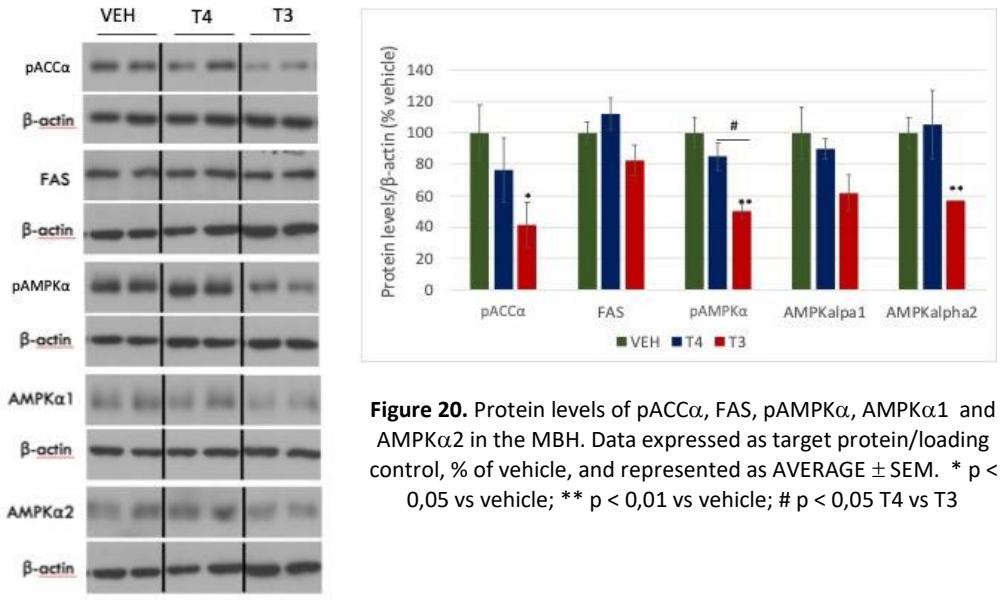

Figure 20. Protein levels of pACCα, FAS, pAMPKα, AMPKα1 and AMPKα2 in the MBH. Data expressed as target protein/loading control, % of vehicle, and represented as AVERAGE ± SEM. * p < 0,05 vs vehicle; ** p < 0,01 vs vehicle; # p < 0,05 T4 vs T3

DISCUSSION

THs affect feeding behaviour, overall growth, core body temperature, body composition, BAT morphology and metabolic activity, WAT browning, liver lipid metabolism, and hypothalamic function, among other actions. Some of those effects, such as feeding [49,166] and thermogenesis [44,47,123,147,174,175] have largely been known, while some others represent a relative recent discovery, through which the modulation of liver lipid metabolism [151,157,158] and WAT browning [46,70,146]. Despite years of literature, new and challenging evidence keep emerging, leaving the exact mechanisms underlying each of those processes to be clarified. While most of the past knowledge relied on the "classical" view of the direct TH effect on peripheral metabolic tissues, more recent data highlighted the importance of TH action on the CNS global energy sensors, leading to hypothalamic-driven outputs to the peripheral targets [44,46,47]. This milestone discovery relied, through others, on the experimental murine model of "central" hyperthyroidism (i.e. ICV and/or nucleus-specific hypothalamic TH administration) [46,47,49], which allowed a detailed exploration of the hypothalamic TH-induced outputs to the peripheral targets. However, in the "more physiological" condition of peripherally released TH, these centrally driven effects interact and integrate with the direct tissue TH action, in a complex machinery which overall functioning remains to be clarified. One of the most challenging issues is represented by the estimation of the relative contribution and/or integration of central *vs.* peripheral TH action on target organs at different serum concentrations. In fact, before reaching and targeting the hypothalamic nuclei, peripherally released TH undergo serum deiodination and metabolism, subsequent active transport through the BBB, and further site-specific neuronal and astrocyte deiodination/metabolism, each passage being differentially regulated depending on TH status (euthyroidism, hypo- or hyperthyroidism) and energy homeostasis (positive, negative or neutral energy balance) [73,82,84,94,176]. On the other hand, the same variables also modify the peripheral tissue specific response to TH, by exerting a local modulation of receptor activity and ligand availability [73,176]. As a first step to address this issue, we determined and compared the serum and hypothalamic TH levels of our mice at the end of the two weeks of oral treatment, which in addition to preserve a more physiological setting, meaning that TH need to cross the BBB, will also have the added value that in the clinical setting TH replacement is mostly based in the use of the oral route. The duration of the treatment, two weeks, is somewhat equivalent to 8 months TH replacement in humans which is considered an adequate time-schedule to achieve stable thyroid hormone concentrations [177]. Another issue when assessing TH effects is whether to use hypothyroid or euthyroid animals. We decided against the former as it is quite difficult to reach firm conclusions in hypothyroid animals since it elicits a wide heterogeneity on the degree of hypothyroidism as defined by TH concentrations in different tissues and a large mismatch with TH serum concentrations [177,178]. By contrast, the response to exogenous (s.c.) TH administration in euthyroid animals is similar in all tissues, as previously assessed by tissue TH levels measurement by mass spectrometry [178].

Upon oral treatment, T4 and T3 levels significantly increased both in the serum, thus confirming the hyperthyroid status, and hypothalamus of the corresponding treatment groups, and the T3 concentrations did also increase in both serum and hypothalamus of the T4-treated mice, consistent with effective BBB crossing of the exogenous hormones and proper serum and hypothalamic cellular deiodination. Interestingly, in the T3-treated group, the expected deep fall in serum T4 levels was not accompanied by a contemporary decrease in the T4 hypothalamic concentration, which remained unchanged with respect to controls, even in presence of much higher levels of hypothalamic T3. The molecular basis, as well as the physiological significance of this T4 "preservation" in the hypothalamus remains to be clarified, but it is in line with previous data reported following exogenous TH administration and assessment of total TH levels in total brain [179,180]. This may possibly be explained by the fact

that in the euthyroid state only 20% of T3 levels are derived directly from the circulation while the rest is produced locally by deiodination [179]. Therefore, it could be postulated the need for a preservation of the brain T4 levels as main local source of T3, and because access of TH to the CNS is confronted by the presence of the BBB and the need of specific transport availability.

It has been demonstrated that TH central modulation of body metabolism depends on targeting the majors CNS energy sensors such as AMPK and mTOR in specific groups of hypothalamic neurons [44,46,47,175]. Then, to asses if the reported hypothalamic TH concentrations were high enough to trigger those pathways, we determined the state of the AMPK downstream in the MBH, which allocates the principal neuronal populations involved in the control of energy homeostasis. In the T3-treated group, the AMPK phosphorylation resulted to be inhibited, as it happens upon direct central T3 administration [46,49] and in line with previous reports on hyperthyroid rats [44,49]. Interestingly, this inhibition was not observed in the T4-treated mice, despite reaching similar hypothalamic T3 concentrations to the ones of the T3-treated group. This data, together with the observed "preservation" of hypothalamic T4, suggest that the TH-dependent modulation of AMPK may not entirely rely on the T3 binding to TRs, but could involve a more complex mechanism of hormonal/receptor interplay, in which a role for intact T4 cannot be excluded.

Human hyperthyroidism has classically been associated with body weight loss despite hyperphagia due to excess energy waist [112,113]. In mice, the overall effect on body weight is more variable, due to the different thermal physiology and the lifelong body growth pattern [181]. In the present study, treated mice increased their food intake accordingly, but did not experience body weight loss, displaying instead an early and progressive gain along the two weeks of treatment, significantly more pronounced than the one of the control group. The increase in body weight did not seem to depend on fat mass deposition, being instead accompanied by an overall body growth (i.e. increased body length), with no change in scWAT depots and only with a reduction in the gWAT ones. The same effect on body weight and composition has recently been reported in other studies in T4-treated mice at thermoneutrality, in which the authors also described an increased percentage of lean mass at MRI [146,156]. It has been demonstrated that the orexigenic effect of TH does not only occur as compensatory reaction in response to energy waste, but also represent an independent early event, capable of being induced by low-doses of T3 which do not affect energy expenditure [166]. This could lead to postulate that in the euthyroid-to-hyperthyroid transition the early rise in food intake may cause an initial weight gain, before shifting to the negative energy balance status of the more advanced stages of overt hyperthyroidism. This hypothesis is partially supported by the flattening of the growth curve of the T3-treated (but not T4-treated) mice in the very last days of our experiment. However, overfeeding alone would have led to an overweight/obese phenotype and fat mass hypertrophy, rather than body lengthen, reduction in WAT depots, or the elsewhere reported increased lean mass [156]. Moreover, WAT depots not only resulted to be reduced in size, with particular regard to gWAT, but also acquired the features of browning, a phenomenon which had already been described both in the peripherally and centrally-induced models of hyperthyroidism [46,70,146]. On the other hand, the iBAT depots resulted to be increased in size with larger lipid droplets despite reduced expression of local lipogenic enzymes, suggesting the implemented lipid deposition to mostly depend on enhanced peripheral uptake, in line with what previously described upon central T3 administration [46]. Of note, even if this could resemble the obesity-related BAT "whitening" process [182], there was no evidence of the "whitening"-associated cellular dysfunction, emerging instead a massive increase in both UCP1 and UCP3 protein expression, consistent with effective BAT recruitment [156]. An increase in lipid accumulation was also reported in the liver, another key metabolic organ, but contrarily to

what happens in BAT it was associated with enhanced hepatic de novo lipogenesis. Interestingly, this process can be induced by direct TRα activation on hepatocytes [141], but also by targeting AMPK and JNK1 activity in the SF-1 neurons of the VMH [46], and the relative contribution of each pathway will be object of further studies, for example by the generation conditional SF1 null mice. Finally, our data also confirmed that both T4 and T3 treatment led to a significant increase in core body temperature [114,123,174]. Despite being well assessed that TH regulate both obligatory and facultative thermogenesis, the molecular nature of the so-called "thyroid thermogenesis", i.e. the body temperature elevation in the context of hyperthyroidism, remains to been clarified. In the past, the most trusted hypothesis was that this could depend on an increased BAT metabolic activity, as TH are able to stimulate brown adipocytes both directly [54,77] and indirectly, through acute induction of hypothalamic-driven SNS stimulation, which in turn requires adequate BAT TH levels for an appropriate response [46,47]. However, recent evidences have challenged this view, demonstrating that thyroid thermogenesis is a UCP1-independent process [156], and that both BAT recruitment and WAT browning give a very minor contribution to core temperature elevation of the chronic hyperthyroid state [146,156]. In line, in our model we did not find any change in the temperature of the interscapular skin above BAT in either of the treated groups, further supporting the idea that the molecular basis of thyroid thermogenesis relies on different pathways than adipocytes uncoupling.

In summary, in this study we used two different models of peripherally induced hyperthyroidism (i.e. T4 and T3 oral administration) to analyze the serum and hypothalamic TH homeostasis and relate them to the observed metabolic effects. Both treatment protocols induced significant changes in the hypothalamic concentrations of TH, which did not always reflect the corresponding changes in the serum TH levels. The hypothalamic TH status reached upon T3 treatment was able to target the downstream pathway of AMPK, one of the most important energy sensors mediating the TH-induced hypothalamic outputs to the metabolic organs. Those observation represent a first step towards the understanding of the complex interplay between the centrally-mediated and the direct local metabolic effect of TH in the context of hyperthyroidism. Even if the previously described "central" model [44,46,47,175] and the present "peripheral" model of experimental hyperthyroidism led to somehow distinct phenotypes, this does not necessarily represent a contradiction if we consider the different experimental treatment protocols. On one hand, the short-term acute intrahypothalamic T3 injection induces an acute metabolic response, including enhanced BAT lipolysis and increased thermogenesis, with the net effect of negative energy balance and body weight loss. On the other hand, the chronic peripheral TH administration gradually mediates a machinery of progressive metabolic changes, finally resulting in an increased overall uncoupling capacity (i.e. BAT recruitment and WAT browning) and a shift of the lipid metabolism from WAT accumulation to BAT and liver deposition, possibly to provide adequate fueling to face the increased metabolic activity. These two phenotypes mimic the acute cold response and chronic cold adaptation, respectively. To address this issue, a deeper investigation of the central *vs.* peripheral TH homeostasis in different thermal stress conditions would be needed and will be object of future research.

CONCLUSIONS

T3 and T4 treatment induced significant changes in the hypothalamic TH concentrations which did not always reflect the correspondent serum levels.

T3 and T4 treatment affected feeding, growth, core body temperature, body composition, BAT morphology, WAT browning, and hepatic lipid metabolism.

Oral T3 (but not T4) treatment induced a downregulation of the hypothalamic AMPK pathway, supporting the central contribution to the observed metabolic effects.

Overall, these data indicate that oral administration of T3 and T4 in a suitable model for the study of TH actions on energy balance and metabolism

REFERENCES

1 Contreras, C., Nogueiras, R., Dieguez, C., Rahmouni, K. & Lopez, M. Traveling from the hypothalamus to the adipose tissue: The thermogenic pathway. *Redox Biol* **12**, 854-863, doi:10.1016/j.redox.2017.04.019 (2017).
2 Rohner-Jeanrenaud, F. & Nogueiras, R. Endocrine control of energy homeostasis. *Mol Cell Endocrinol* **418 Pt 1**, 1-2, doi:10.1016/j.mce.2015.11.003 (2015).
3 Seoane-Collazo, P. *et al.* Hypothalamic-autonomic control of energy homeostasis. *Endocrine* **50**, 276-291, doi:10.1007/s12020-015-0658-y (2015).
4 Munzberg, H., Qualls-Creekmore, E., Berthoud, H. R., Morrison, C. D. & Yu, S. Neural Control of Energy Expenditure. *Handb Exp Pharmacol* **233**, 173-194, doi:10.1007/164_2015_33 (2016).
5 Luo, L. & Liu, M. Adipose tissue in control of metabolism. *J Endocrinol* **231**, R77-r99, doi:10.1530/joe-16-0211 (2016).
6 Pollard, A. E. & Carling, D. Thermogenic adipocytes: lineage, function and therapeutic potential. *Biochem J* **477**, 2071-2093, doi:10.1042/bcj20200298 (2020).
7 Suzuki, K., Simpson, K. A., Minnion, J. S., Shillito, J. C. & Bloom, S. R. The role of gut hormones and the hypothalamus in appetite regulation. *Endocr J* **57**, 359-372, doi:10.1507/endocrj.k10e-077 (2010).
8 Warner, A. & Mittag, J. Breaking BAT: can browning create a better white? *J Endocrinol* **228**, R19-29, doi:10.1530/joe-15-0408 (2016).
9 Wajchenberg, B. L. Subcutaneous and visceral adipose tissue: their relation to the metabolic syndrome. *Endocr Rev* **21**, 697-738, doi:10.1210/edrv.21.6.0415 (2000).
10 Fasshauer, M. & Bluher, M. Adipokines in health and disease. *Trends Pharmacol Sci* **36**, 461-470, doi:10.1016/j.tips.2015.04.014 (2015).
11 Zhang, Y. *et al.* Positional cloning of the mouse obese gene and its human homologue. *Nature* **372**, 425-432, doi:10.1038/372425a0 (1994).
12 Brunner, L. *et al.* Leptin is a physiologically important regulator of food intake. *Int J Obes Relat Metab Disord* **21**, 1152-1160, doi:10.1038/sj.ijo.0800529 (1997).
13 Considine, R. V. *et al.* Serum immunoreactive-leptin concentrations in normal-weight and obese humans. *N Engl J Med* **334**, 292-295, doi:10.1056/nejm199602013340503 (1996).
14 Scherer, P. E., Williams, S., Fogliano, M., Baldini, G. & Lodish, H. F. A novel serum protein similar to C1q, produced exclusively in adipocytes. *J Biol Chem* **270**, 26746-26749, doi:10.1074/jbc.270.45.26746 (1995).
15 Wang, Z. V. & Scherer, P. E. Adiponectin, the past two decades. *J Mol Cell Biol* **8**, 93-100, doi:10.1093/jmcb/mjw011 (2016).
16 Qi, Y. *et al.* Adiponectin acts in the brain to decrease body weight. *Nat Med* **10**, 524-529, doi:10.1038/nm1029 (2004).
17 Rehfeld, J. F. The new biology of gastrointestinal hormones. *Physiol Rev* **78**, 1087-1108, doi:10.1152/physrev.1998.78.4.1087 (1998).
18 Kojima, M. *et al.* Ghrelin is a growth-hormone-releasing acylated peptide from stomach. *Nature* **402**, 656-660, doi:10.1038/45230 (1999).
19 Muller, T. D. *et al.* Ghrelin. *Mol Metab* **4**, 437-460, doi:10.1016/j.molmet.2015.03.005 (2015).
20 Farias, G., Netto, B. D. M., Bettini, S. C., Damaso, A. R. & de Freitas, A. C. T. Neuroendocrine regulation of energy balance: Implications on the development and surgical treatment of obesity. *Nutr Health* **23**, 131-146, doi:10.1177/0260106017719369 (2017).
21 Al Massadi, O. *et al.* Review of novel aspects of the regulation of ghrelin secretion. *Curr Drug Metab* **15**, 398-413, doi:10.2174/1389200215666140505153723 (2014).
22 Al Massadi, O., Nogueiras, R., Dieguez, C. & Girault, J. A. Ghrelin and food reward. *Neuropharmacology* **148**, 131-138, doi:10.1016/j.neuropharm.2019.01.001 (2019).

23 Nogueiras, R., Williams, L. M. & Dieguez, C. Ghrelin: new molecular pathways modulating appetite and adiposity. *Obes Facts* **3**, 285-292, doi:10.1159/000321265 (2010).
24 Obici, S. & Rossetti, L. Minireview: nutrient sensing and the regulation of insulin action and energy balance. *Endocrinology* **144**, 5172-5178, doi:10.1210/en.2003-0999 (2003).
25 Fioramonti, X., Chretien, C., Leloup, C. & Penicaud, L. Recent Advances in the Cellular and Molecular Mechanisms of Hypothalamic Neuronal Glucose Detection. *Front Physiol* **8**, 875, doi:10.3389/fphys.2017.00875 (2017).
26 Cruciani-Guglielmacci, C., Lopez, M., Campana, M. & le Stunff, H. Brain Ceramide Metabolism in the Control of Energy Balance. *Front Physiol* **8**, 787, doi:10.3389/fphys.2017.00787 (2017).
27 Obici, S. *et al.* Central administration of oleic acid inhibits glucose production and food intake. *Diabetes* **51**, 271-275, doi:10.2337/diabetes.51.2.271 (2002).
28 Contreras, C., Nogueiras, R., Dieguez, C., Medina-Gomez, G. & Lopez, M. Hypothalamus and thermogenesis: Heating the BAT, browning the WAT. *Mol Cell Endocrinol* **438**, 107-115, doi:10.1016/j.mce.2016.08.002 (2016).
29 Lopez, M., Nogueiras, R., Tena-Sempere, M. & Dieguez, C. Hypothalamic AMPK: a canonical regulator of whole-body energy balance. *Nat Rev Endocrinol* **12**, 421-432, doi:10.1038/nrendo.2016.67 (2016).
30 Gonzalez-Garcia, I. *et al.* HYPOTHesizing about central comBAT against obesity. *J Physiol Biochem*, doi:10.1007/s13105-019-00719-y (2019).
31 Blouet, C. & Schwartz, G. J. Hypothalamic nutrient sensing in the control of energy homeostasis. *Behav Brain Res* **209**, 1-12, doi:10.1016/j.bbr.2009.12.024 (2010).
32 Lage, R., Dieguez, C., Vidal-Puig, A. & Lopez, M. AMPK: a metabolic gauge regulating whole-body energy homeostasis. *Trends Mol Med* **14**, 539-549, doi:10.1016/j.molmed.2008.09.007 (2008).
33 Hirschberg, P. R., Sarkar, P., Teegala, S. B. & Routh, V. H. Ventromedial hypothalamus glucose-inhibited neurones: A role in glucose and energy homeostasis? *J Neuroendocrinol* **32**, e12773, doi:10.1111/jne.12773 (2020).
34 Yu, J. H. & Kim, M. S. Molecular Mechanisms of Appetite Regulation. *Diabetes Metab J* **36**, 391-398, doi:10.4093/dmj.2012.36.6.391 (2012).
35 Garcia, D. & Shaw, R. J. AMPK: Mechanisms of Cellular Energy Sensing and Restoration of Metabolic Balance. *Mol Cell* **66**, 789-800, doi:10.1016/j.molcel.2017.05.032 (2017).
36 Carling, D., Mayer, F. V., Sanders, M. J. & Gamblin, S. J. AMP-activated protein kinase: nature's energy sensor. *Nat Chem Biol* **7**, 512-518, doi:10.1038/nchembio.610 (2011).
37 Gowans, G. J., Hawley, S. A., Ross, F. A. & Hardie, D. G. AMP is a true physiological regulator of AMP-activated protein kinase by both allosteric activation and enhancing net phosphorylation. *Cell Metab* **18**, 556-566, doi:10.1016/j.cmet.2013.08.019 (2013).
38 Woods, A. *et al.* LKB1 is the upstream kinase in the AMP-activated protein kinase cascade. *Curr Biol* **13**, 2004-2008, doi:10.1016/j.cub.2003.10.031 (2003).
39 Woods, A. *et al.* Ca2+/calmodulin-dependent protein kinase kinase-beta acts upstream of AMP-activated protein kinase in mammalian cells. *Cell Metab* **2**, 21-33, doi:10.1016/j.cmet.2005.06.005 (2005).
40 Lopez, M. Hypothalamic AMPK and energy balance. *Eur J Clin Invest* **48**, e12996, doi:10.1111/eci.12996 (2018).
41 Lopez, M. *et al.* Hypothalamic fatty acid metabolism mediates the orexigenic action of ghrelin. *Cell Metab* **7**, 389-399, doi:10.1016/j.cmet.2008.03.006 (2008).
42 U, A. *et al.* AMP-activated Protein Kinase Plays a Role in the Control of Food Intake. *The Journal of biological chemistry* **279**, doi:10.1074/jbc.C300557200 (2004).
43 Minokoshi, Y. *et al.* AMP-kinase regulates food intake by responding to hormonal and nutrient signals in the hypothalamus. *Nature* **428**, 569-574, doi:10.1038/nature02440 (2004).

44 Lopez, M. *et al.* Hypothalamic AMPK and fatty acid metabolism mediate thyroid regulation of energy balance. *Nat Med* **16**, 1001-1008, doi:10.1038/nm.2207 (2010).
45 Martinez de Morentin, P. B. *et al.* Estradiol regulates brown adipose tissue thermogenesis via hypothalamic AMPK. *Cell Metab* **20**, 41-53, doi:10.1016/j.cmet.2014.03.031 (2014).
46 Martinez-Sanchez, N. *et al.* Hypothalamic AMPK-ER Stress-JNK1 Axis Mediates the Central Actions of Thyroid Hormones on Energy Balance. *Cell Metab* **26**, 212-229.e212, doi:10.1016/j.cmet.2017.06.014 (2017).
47 Lopez, M., Alvarez, C. V., Nogueiras, R. & Dieguez, C. Energy balance regulation by thyroid hormones at central level. *Trends Mol Med* **19**, 418-427, doi:10.1016/j.molmed.2013.04.004 (2013).
48 Pollard, A. E. *et al.* AMPK activation protects against diet induced obesity through Ucp1-independent thermogenesis in subcutaneous white adipose tissue. *Nat Metab* **1**, 340-349, doi:10.1038/s42255-019-0036-9 (2019).
49 Varela, L. *et al.* Hypothalamic mTOR pathway mediates thyroid hormone-induced hyperphagia in hyperthyroidism. *J Pathol* **227**, 209-222, doi:10.1002/path.3984 (2012).
50 Martinez de Morentin, P. B. *et al.* Hypothalamic mTOR: the rookie energy sensor. *Curr Mol Med* **14**, 3-21, doi:10.2174/1566524013666131118103706 (2014).
51 Catania, C., Binder, E. & Cota, D. mTORC1 signaling in energy balance and metabolic disease. *Int J Obes (Lond)* **35**, 751-761, doi:10.1038/ijo.2010.208 (2011).
52 Cota, D. *et al.* Hypothalamic mTOR signaling regulates food intake. *Science* **312**, 927-930, doi:10.1126/science.1124147 (2006).
53 Dennis, P. B. *et al.* Mammalian TOR: a homeostatic ATP sensor. *Science* **294**, 1102-1105, doi:10.1126/science.1063518 (2001).
54 Silva, J. E. Physiological importance and control of non-shivering facultative thermogenesis. *Front Biosci (Schol Ed)* **3**, 352-371, doi:10.2741/s156 (2011).
55 Cannon, B. & Nedergaard, J. Brown adipose tissue: function and physiological significance. *Physiol Rev* **84**, 277-359, doi:10.1152/physrev.00015.2003 (2004).
56 Rowland, L. A., Bal, N. C. & Periasamy, M. The role of skeletal-muscle-based thermogenic mechanisms in vertebrate endothermy. *Biol Rev Camb Philos Soc* **90**, 1279-1297, doi:10.1111/brv.12157 (2015).
57 Buijs, R. M. The autonomic nervous system: a balancing act. *Handb Clin Neurol* **117**, 1-11, doi:10.1016/b978-0-444-53491-0.00001-8 (2013).
58 Roesler, A. & Kazak, L. UCP1-independent thermogenesis. *Biochem J* **477**, 709-725, doi:10.1042/BCJ20190463 (2020).
59 Bartelt, A. *et al.* Brown adipose tissue activity controls triglyceride clearance. *Nat Med* **17**, 200-205, doi:10.1038/nm.2297 (2011).
60 Cypess, A. M. *et al.* Identification and importance of brown adipose tissue in adult humans. *N Engl J Med* **360**, 1509-1517, doi:10.1056/NEJMoa0810780 (2009).
61 Virtanen, K. A. *et al.* Functional brown adipose tissue in healthy adults. *N Engl J Med* **360**, 1518-1525, doi:10.1056/NEJMoa0808949 (2009).
62 Shin, H. *et al.* Lipolysis in Brown Adipocytes Is Not Essential for Cold-Induced Thermogenesis in Mice. *Cell Metab* **26**, 764-777.e765, doi:10.1016/j.cmet.2017.09.002 (2017).
63 Perkins, M. N., Rothwell, N. J., Stock, M. J. & Stone, T. W. Activation of brown adipose tissue thermogenesis by the ventromedial hypothalamus. *Nature* **289**, 401-402, doi:10.1038/289401a0 (1981).
64 Whittle, A. J. *et al.* BMP8B increases brown adipose tissue thermogenesis through both central and peripheral actions. *Cell* **149**, 871-885, doi:10.1016/j.cell.2012.02.066 (2012).
65 Fischer, A. W., Cannon, B. & Nedergaard, J. Leptin: Is It Thermogenic? *Endocr Rev* **41**, doi:10.1210/endrev/bnz016 (2020).
66 Contreras, C. *et al.* The brain and brown fat. *Ann Med* **47**, 150-168, doi:10.3109/07853890.2014.919727 (2015).

67 Wu, J. *et al.* Beige adipocytes are a distinct type of thermogenic fat cell in mouse and human. *Cell* **150**, 366-376, doi:10.1016/j.cell.2012.05.016 (2012).
68 Keipert, S. & Jastroch, M. Brite/beige fat and UCP1 - is it thermogenesis? *Biochim Biophys Acta* **1837**, 1075-1082, doi:10.1016/j.bbabio.2014.02.008 (2014).
69 Walden, T. B., Hansen, I. R., Timmons, J. A., Cannon, B. & Nedergaard, J. Recruited vs. nonrecruited molecular signatures of brown, "brite," and white adipose tissues. *Am J Physiol Endocrinol Metab* **302**, E19-31, doi:10.1152/ajpendo.00249.2011 (2012).
70 Martinez-Sanchez, N. *et al.* Thyroid hormones induce browning of white fat. *J Endocrinol* **232**, 351-362, doi:10.1530/joe-16-0425 (2017).
71 Jameson, J. L. & De Groot, L. *Endocrinology: Adult and Pediatric*. 7th Edition edn, (Elsevier Saunders, 2015).
72 van der Spek, A. H., Fliers, E. & Boelen, A. The classic pathways of thyroid hormone metabolism. *Mol Cell Endocrinol* **458**, 29-38, doi:10.1016/j.mce.2017.01.025 (2017).
73 Mendoza, A. & Hollenberg, A. N. New insights into thyroid hormone action. *Pharmacol Ther* **173**, 135-145, doi:10.1016/j.pharmthera.2017.02.012 (2017).
74 Mullur, R., Liu, Y. Y. & Brent, G. A. Thyroid hormone regulation of metabolism. *Physiol Rev* **94**, 355-382, doi:10.1152/physrev.00030.2013 (2014).
75 Brent, G. A. Mechanisms of thyroid hormone action. *J Clin Invest* **122**, 3035-3043, doi:10.1172/jci60047 (2012).
76 Maia, A. L., Kim, B. W., Huang, S. A., Harney, J. W. & Larsen, P. R. Type 2 iodothyronine deiodinase is the major source of plasma T3 in euthyroid humans. *J Clin Invest* **115**, 2524-2533, doi:10.1172/jci25083 (2005).
77 Arrojo, E. D. R., Fonseca, T. L., Werneck-de-Castro, J. P. & Bianco, A. C. Role of the type 2 iodothyronine deiodinase (D2) in the control of thyroid hormone signaling. *Biochim Biophys Acta* **1830**, 3956-3964, doi:10.1016/j.bbagen.2012.08.019 (2013).
78 Bartha, T. *et al.* Characterization of the 5'-flanking and 5'-untranslated regions of the cyclic adenosine 3',5'-monophosphate-responsive human type 2 iodothyronine deiodinase gene. *Endocrinology* **141**, 229-237, doi:10.1210/endo.141.1.7282 (2000).
79 Silva, J. E. & Larsen, P. R. Adrenergic activation of triiodothyronine production in brown adipose tissue. *Nature* **305**, 712-713, doi:10.1038/305712a0 (1983).
80 Gereben, B., Goncalves, C., Harney, J. W., Larsen, P. R. & Bianco, A. C. Selective proteolysis of human type 2 deiodinase: a novel ubiquitin-proteasomal mediated mechanism for regulation of hormone activation. *Mol Endocrinol* **14**, 1697-1708, doi:10.1210/mend.14.11.0558 (2000).
81 Arrojo, E. D. R. *et al.* Endoplasmic reticulum stress decreases intracellular thyroid hormone activation via an eIF2a-mediated decrease in type 2 deiodinase synthesis. *Mol Endocrinol* **25**, 2065-2075, doi:10.1210/me.2011-1061 (2011).
82 Bianco, A. C. *et al.* Paradigms of Dynamic Control of Thyroid Hormone Signaling. *Endocr Rev* **40**, 1000-1047, doi:10.1210/er.2018-00275 (2019).
83 Hennemann, G. *et al.* Plasma membrane transport of thyroid hormones and its role in thyroid hormone metabolism and bioavailability. *Endocr Rev* **22**, 451-476, doi:10.1210/edrv.22.4.0435 (2001).
84 Groeneweg, S., van Geest, F. S., Peeters, R. P., Heuer, H. & Visser, W. E. Thyroid Hormone Transporters. *Endocr Rev* **41**, doi:10.1210/endrev/bnz008 (2020).
85 Schwartz, C. E. *et al.* Allan-Herndon-Dudley syndrome and the monocarboxylate transporter 8 (MCT8) gene. *Am J Hum Genet* **77**, 41-53, doi:10.1086/431313 (2005).
86 Choi, J. H. *et al.* Variable Clinical Characteristics and Molecular Spectrum of Patients with Syndromes of Reduced Sensitivity to Thyroid Hormone: Genetic Defects in the THRB and SLC16A2 Genes. *Horm Res Paediatr* **90**, 283-290, doi:10.1159/000493468 (2018).
87 Dumitrescu, A. M., Liao, X. H., Weiss, R. E., Millen, K. & Refetoff, S. Tissue-specific thyroid hormone deprivation and excess in monocarboxylate transporter (mct) 8-deficient mice. *Endocrinology* **147**, 4036-4043, doi:10.1210/en.2006-0390 (2006).

88 Obregon, M. J., Mallol, J., Pastor, R., Morreale de Escobar, G. & Escobar del Rey, F. L-thyroxine and 3,5,3'-triiodo-L-thyronine in rat embryos before onset of fetal thyroid function. *Endocrinology* **114**, 305-307, doi:10.1210/endo-114-1-305 (1984).
89 Morreale de Escobar, G., Obregon, M. J. & Escobar del Rey, F. Fetal and maternal thyroid hormones. *Horm Res* **26**, 12-27, doi:10.1159/000180681 (1987).
90 Morreale de Escobar, G., Obregon, M. J. & Escobar del Rey, F. Role of thyroid hormone during early brain development. *Eur J Endocrinol* **151 Suppl 3**, U25-37, doi:10.1530/eje.0.151u025 (2004).
91 Roberts, L. M. *et al.* Expression of the thyroid hormone transporters monocarboxylate transporter-8 (SLC16A2) and organic ion transporter-14 (SLCO1C1) at the blood-brain barrier. *Endocrinology* **149**, 6251-6261, doi:10.1210/en.2008-0378 (2008).
92 Schnell, C. *et al.* The multispecific thyroid hormone transporter OATP1C1 mediates cell-specific sulforhodamine 101-labeling of hippocampal astrocytes. *Brain Struct Funct* **220**, 193-203, doi:10.1007/s00429-013-0645-0 (2015).
93 Heuer, H. *et al.* The monocarboxylate transporter 8 linked to human psychomotor retardation is highly expressed in thyroid hormone-sensitive neuron populations. *Endocrinology* **146**, 1701-1706, doi:10.1210/en.2004-1179 (2005).
94 Schweizer, U. & Kohrle, J. Function of thyroid hormone transporters in the central nervous system. *Biochim Biophys Acta* **1830**, 3965-3973, doi:10.1016/j.bbagen.2012.07.015 (2013).
95 Herrmann, B. *et al.* Central Hypothyroidism Impairs Heart Rate Stability and Prevents Thyroid Hormone-Induced Cardiac Hypertrophy and Pyrexia. *Thyroid*, doi:10.1089/thy.2019.0705 (2020).
96 Lee, J. Y. *et al.* Overcoming Monocarboxylate Transporter 8 (MCT8)-Deficiency to Promote Human Oligodendrocyte Differentiation and Myelination. *EBioMedicine* **25**, 122-135, doi:10.1016/j.ebiom.2017.10.016 (2017).
97 Williams, G. R. & Bassett, J. H. Deiodinases: the balance of thyroid hormone: local control of thyroid hormone action: role of type 2 deiodinase. *J Endocrinol* **209**, 261-272, doi:10.1530/joe-10-0448 (2011).
98 Dentice, M., Marsili, A., Zavacki, A., Larsen, P. R. & Salvatore, D. The deiodinases and the control of intracellular thyroid hormone signaling during cellular differentiation. *Biochim Biophys Acta* **1830**, 3937-3945, doi:10.1016/j.bbagen.2012.05.007 (2013).
99 Cheng, S. Y., Leonard, J. L. & Davis, P. J. Molecular aspects of thyroid hormone actions. *Endocr Rev* **31**, 139-170, doi:10.1210/er.2009-0007 (2010).
100 Ribeiro, M. O. *et al.* Expression of uncoupling protein 1 in mouse brown adipose tissue is thyroid hormone receptor-beta isoform specific and required for adaptive thermogenesis. *Endocrinology* **151**, 432-440, doi:10.1210/en.2009-0667 (2010).
101 Flamant, F. & Gauthier, K. Thyroid hormone receptors: the challenge of elucidating isotype-specific functions and cell-specific response. *Biochim Biophys Acta* **1830**, 3900-3907, doi:10.1016/j.bbagen.2012.06.003 (2013).
102 Lazar, M. A. Thyroid hormone receptors: multiple forms, multiple possibilities. *Endocr Rev* **14**, 184-193, doi:10.1210/edrv-14-2-184 (1993).
103 Sun, Z. *et al.* Deacetylase-independent function of HDAC3 in transcription and metabolism requires nuclear receptor corepressor. *Mol Cell* **52**, 769-782, doi:10.1016/j.molcel.2013.10.022 (2013).
104 You, S. H. *et al.* Nuclear receptor co-repressors are required for the histone-deacetylase activity of HDAC3 in vivo. *Nat Struct Mol Biol* **20**, 182-187, doi:10.1038/nsmb.2476 (2013).
105 Astapova, I. Role of co-regulators in metabolic and transcriptional actions of thyroid hormone. *J Mol Endocrinol* **56**, 73-97, doi:10.1530/jme-15-0246 (2016).
106 Cao, X., Kambe, F., Moeller, L. C., Refetoff, S. & Seo, H. Thyroid hormone induces rapid activation of Akt/protein kinase B-mammalian target of rapamycin-p70S6K cascade

through phosphatidylinositol 3-kinase in human fibroblasts. *Mol Endocrinol* **19**, 102-112, doi:10.1210/me.2004-0093 (2005).

107 Bergh, J. J. *et al.* Integrin alphaVbeta3 contains a cell surface receptor site for thyroid hormone that is linked to activation of mitogen-activated protein kinase and induction of angiogenesis. *Endocrinology* **146**, 2864-2871, doi:10.1210/en.2005-0102 (2005).

108 Lin, H. Y. *et al.* L-Thyroxine vs. 3,5,3'-triiodo-L-thyronine and cell proliferation: activation of mitogen-activated protein kinase and phosphatidylinositol 3-kinase. *Am J Physiol Cell Physiol* **296**, C980-991, doi:10.1152/ajpcell.00305.2008 (2009).

109 Fox, C. S. *et al.* Relations of thyroid function to body weight: cross-sectional and longitudinal observations in a community-based sample. *Arch Intern Med* **168**, 587-592, doi:10.1001/archinte.168.6.587 (2008).

110 Ross, D. S. *et al.* 2016 American Thyroid Association Guidelines for Diagnosis and Management of Hyperthyroidism and Other Causes of Thyrotoxicosis. *Thyroid* **26**, 1343-1421, doi:10.1089/thy.2016.0229 (2016).

111 Garber, J. R. *et al.* Clinical practice guidelines for hypothyroidism in adults: cosponsored by the American Association of Clinical Endocrinologists and the American Thyroid Association. *Endocr Pract* **18**, 988-1028, doi:10.4158/ep12280.gl (2012).

112 De Leo, S., Lee, S. Y. & Braverman, L. E. Hyperthyroidism. *Lancet* **388**, 906-918, doi:10.1016/s0140-6736(16)00278-6 (2016).

113 Brent, G. A. Clinical practice. Graves' disease. *N Engl J Med* **358**, 2594-2605, doi:10.1056/NEJMcp0801880 (2008).

114 Silva, J. E. The thermogenic effect of thyroid hormone and its clinical implications. *Ann Intern Med* **139**, 205-213 (2003).

115 Silva, J. E. Thermogenic mechanisms and their hormonal regulation. *Physiol Rev* **86**, 435-464, doi:10.1152/physrev.00009.2005 (2006).

116 Jonklaas, J. *et al.* Guidelines for the treatment of hypothyroidism: prepared by the american thyroid association task force on thyroid hormone replacement. *Thyroid* **24**, 1670-1751, doi:10.1089/thy.2014.0028 (2014).

117 Sinha, R. A., Singh, B. K. & Yen, P. M. Direct effects of thyroid hormones on hepatic lipid metabolism. *Nat Rev Endocrinol* **14**, 259-269, doi:10.1038/nrendo.2018.10 (2018).

118 Duntas, L. H. & Brenta, G. A Renewed Focus on the Association Between Thyroid Hormones and Lipid Metabolism. *Front Endocrinol (Lausanne)* **9**, doi:10.3389/fendo.2018.00511 (2018).

119 Oppenheimer, J. H., Schwartz, H. L., Lane, J. T. & Thompson, M. P. Functional relationship of thyroid hormone-induced lipogenesis, lipolysis, and thermogenesis in the rat. *J Clin Invest* **87**, 125-132, doi:10.1172/jci114961 (1991).

120 Warner, A. & Mittag, J. Thyroid hormone and the central control of homeostasis. *J Mol Endocrinol* **49**, R29-35, doi:10.1530/jme-12-0068 (2012).

121 Kim, B. Thyroid hormone as a determinant of energy expenditure and the basal metabolic rate. *Thyroid* **18**, 141-144, doi:10.1089/thy.2007.0266 (2008).

122 Harper, M. E. & Seifert, E. L. Thyroid hormone effects on mitochondrial energetics. *Thyroid* **18**, 145-156, doi:10.1089/thy.2007.0250 (2008).

123 Silva, J. E. Thyroid hormone and the energetic cost of keeping body temperature. *Biosci Rep* **25**, 129-148, doi:10.1007/s10540-005-2882-9 (2005).

124 Bianco, A. C. & McAninch, E. A. The role of thyroid hormone and brown adipose tissue in energy homoeostasis. *Lancet Diabetes Endocrinol* **1**, 250-258, doi:10.1016/s2213-8587(13)70069-x (2013).

125 Hernandez, A. & Obregon, M. J. Presence and mRNA expression of T3 receptors in differentiating rat brown adipocytes. *Mol Cell Endocrinol* **121**, 37-46, doi:10.1016/0303-7207(96)03849-x (1996).

126 Bianco, A. C., Sheng, X. Y. & Silva, J. E. Triiodothyronine amplifies norepinephrine stimulation of uncoupling protein gene transcription by a mechanism not requiring protein synthesis. *J Biol Chem* **263**, 18168-18175 (1988).
127 Ribeiro, M. O. *et al.* Thyroid hormone--sympathetic interaction and adaptive thermogenesis are thyroid hormone receptor isoform--specific. *J Clin Invest* **108**, 97-105, doi:10.1172/JCI12584 (2001).
128 Marrif, H. *et al.* Temperature homeostasis in transgenic mice lacking thyroid hormone receptor-alpha gene products. *Endocrinology* **146**, 2872-2884, doi:10.1210/en.2004-1544 (2005).
129 Golozoubova, V. *et al.* Depressed thermogenesis but competent brown adipose tissue recruitment in mice devoid of all hormone-binding thyroid hormone receptors. *Mol Endocrinol* **18**, 384-401, doi:10.1210/me.2003-0267 (2004).
130 Pelletier, P., Gauthier, K., Sideleva, O., Samarut, J. & Silva, J. E. Mice lacking the thyroid hormone receptor-alpha gene spend more energy in thermogenesis, burn more fat, and are less sensitive to high-fat diet-induced obesity. *Endocrinology* **149**, 6471-6486, doi:10.1210/en.2008-0718 (2008).
131 Wikstrom, L. *et al.* Abnormal heart rate and body temperature in mice lacking thyroid hormone receptor alpha 1. *Embo j* **17**, 455-461, doi:10.1093/emboj/17.2.455 (1998).
132 Bianco, A. C. & Silva, J. E. Intracellular conversion of thyroxine to triiodothyronine is required for the optimal thermogenic function of brown adipose tissue. *J Clin Invest* **79**, 295-300, doi:10.1172/jci112798 (1987).
133 Silva, J. E. & Larsen, P. R. Potential of brown adipose tissue type II thyroxine 5'-deiodinase as a local and systemic source of triiodothyronine in rats. *J Clin Invest* **76**, 2296-2305, doi:10.1172/jci112239 (1985).
134 Christoffolete, M. A. *et al.* Mice with targeted disruption of the Dio2 gene have cold-induced overexpression of the uncoupling protein 1 gene but fail to increase brown adipose tissue lipogenesis and adaptive thermogenesis. *Diabetes* **53**, 577-584, doi:10.2337/diabetes.53.3.577 (2004).
135 de Jesus, L. A. *et al.* The type 2 iodothyronine deiodinase is essential for adaptive thermogenesis in brown adipose tissue. *J Clin Invest* **108**, 1379-1385, doi:10.1172/JCI13803 (2001).
136 Yau, W. W. *et al.* Thyroid hormone (T3) stimulates brown adipose tissue activation via mitochondrial biogenesis and MTOR-mediated mitophagy. *Autophagy* **15**, 131-150, doi:10.1080/15548627.2018.1511263 (2019).
137 Warner, A. *et al.* Inappropriate heat dissipation ignites brown fat thermogenesis in mice with a mutant thyroid hormone receptor alpha1. *Proc Natl Acad Sci U S A* **110**, 16241-16246, doi:10.1073/pnas.1310300110 (2013).
138 Vanhoutte, G., Verhoye, M., Raman, E., Roberts, M. & Van der Linden, A. In-vivo non-invasive study of the thermoregulatory function of the blood vessels in the rat tail using magnetic resonance angiography. *NMR Biomed* **15**, 263-269, doi:10.1002/nbm.768 (2002).
139 Warner, A. & Mittag, J. Brown fat and vascular heat dissipation: The new cautionary tail. *Adipocyte* **3**, 221-223, doi:10.4161/adip.28815 (2014).
140 Mitrou, P., Raptis, S. A. & Dimitriadis, G. Insulin action in hyperthyroidism: a focus on muscle and adipose tissue. *Endocr Rev* **31**, 663-679, doi:10.1210/er.2009-0046 (2010).
141 Araki, O., Ying, H., Zhu, X. G., Willingham, M. C. & Cheng, S. Y. Distinct dysregulation of lipid metabolism by unliganded thyroid hormone receptor isoforms. *Mol Endocrinol* **23**, 308-315, doi:10.1210/me.2008-0311 (2009).
142 Medina-Gomez, G., Calvo, R. M. & Obregon, M. J. Thermogenic effect of triiodothyroacetic acid at low doses in rat adipose tissue without adverse side effects in the thyroid axis. *Am J Physiol Endocrinol Metab* **294**, E688-697, doi:10.1152/ajpendo.00417.2007 (2008).

143 Wang, C. Z., Wei, D., Guan, M. P. & Xue, Y. M. Triiodothyronine regulates distribution of thyroid hormone receptors by activating AMP-activated protein kinase in 3T3-L1 adipocytes and induces uncoupling protein-1 expression. *Mol Cell Biochem* **393**, 247-254, doi:10.1007/s11010-014-2067-6 (2014).
144 Lin, J. Z. *et al.* Pharmacological Activation of Thyroid Hormone Receptors Elicits a Functional Conversion of White to Brown Fat. *Cell Rep* **13**, 1528-1537, doi:10.1016/j.celrep.2015.10.022 (2015).
145 Weiner, J. *et al.* Thyroid hormone status defines brown adipose tissue activity and browning of white adipose tissues in mice. *Sci Rep* **6**, 38124, doi:10.1038/srep38124 (2016).
146 Johann, K. *et al.* Thyroid-Hormone-Induced Browning of White Adipose Tissue Does Not Contribute to Thermogenesis and Glucose Consumption. *Cell Rep* **27**, 3385-3400.e3383, doi:10.1016/j.celrep.2019.05.054 (2019).
147 Nedergaard, J., Dicker, A. & Cannon, B. The interaction between thyroid and brown-fat thermogenesis. Central or peripheral effects? *Ann N Y Acad Sci* **813**, 712-717, doi:10.1111/j.1749-6632.1997.tb51772.x (1997).
148 López, M., Alvarez, C. V., Nogueiras, R. & Diéguez, C. Energy balance regulation by thyroid hormones at central level. *Trends Mol Med* **19**, 418-427, doi:10.1016/j.molmed.2013.04.004 (2013).
149 Sjogren, M. *et al.* Hypermetabolism in mice caused by the central action of an unliganded thyroid hormone receptor alpha1. *Embo j* **26**, 4535-4545, doi:10.1038/sj.emboj.7601882 (2007).
150 Vujovic, M. *et al.* Interference of a mutant thyroid hormone receptor alpha1 with hepatic glucose metabolism. *Endocrinology* **150**, 2940-2947, doi:10.1210/en.2008-1085 (2009).
151 Fliers, E., Klieverik, L. P. & Kalsbeek, A. Novel neural pathways for metabolic effects of thyroid hormone. *Trends Endocrinol Metab* **21**, 230-236, doi:10.1016/j.tem.2009.11.008 (2010).
152 Martínez-Sánchez, N. *et al.* Hypothalamic AMPK-ER Stress-JNK1 Axis Mediates the Central Actions of Thyroid Hormones on Energy Balance. *Cell Metab* **26**, 212-229.e212, doi:10.1016/j.cmet.2017.06.014 (2017).
153 Alvarez-Crespo, M. *et al.* Essential role of UCP1 modulating the central effects of thyroid hormones on energy balance. *Mol Metab* **5**, 271-282, doi:10.1016/j.molmet.2016.01.008 (2016).
154 Seoane-Collazo, P. *et al.* SF1-Specific AMPKα1 Deletion Protects Against Diet-Induced Obesity. *Diabetes* **67**, 2213-2226, doi:10.2337/db17-1538 (2018).
155 J, W., M, H., JT, H., W, F. & K, K. Thyroid Hormones and Browning of Adipose Tissue. *Molecular and cellular endocrinology* **458**, doi:10.1016/j.mce.2017.01.011 (2017).
156 Dittner, C., Lindsund, E., Cannon, B. & Nedergaard, J. At thermoneutrality, acute thyroxine-induced thermogenesis and pyrexia are independent of UCP1. *Mol Metab* **25**, 20-34, doi:10.1016/j.molmet.2019.05.005 (2019).
157 Klieverik, L. P. *et al.* Thyroid hormone modulates glucose production via a sympathetic pathway from the hypothalamic paraventricular nucleus to the liver. *Proc Natl Acad Sci U S A* **106**, 5966-5971, doi:10.1073/pnas.0805355106 (2009).
158 Klieverik, L. P. *et al.* Effects of thyrotoxicosis and selective hepatic autonomic denervation on hepatic glucose metabolism in rats. *Am J Physiol Endocrinol Metab* **294**, E513-520, doi:10.1152/ajpendo.00659.2007 (2008).
159 Cook, C. B., Kakucska, I., Lechan, R. M. & Koenig, R. J. Expression of thyroid hormone receptor beta 2 in rat hypothalamus. *Endocrinology* **130**, 1077-1079, doi:10.1210/endo.130.2.1733708 (1992).
160 Bartness, T. J. & Song, C. K. Brain-adipose tissue neural crosstalk. *Physiol Behav* **91**, 343-351, doi:10.1016/j.physbeh.2007.04.002 (2007).

161 Bartness, T. J., Shrestha, Y. B., Vaughan, C. H., Schwartz, G. J. & Song, C. K. Sensory and sympathetic nervous system control of white adipose tissue lipolysis. *Mol Cell Endocrinol* **318**, 34-43, doi:10.1016/j.mce.2009.08.031 (2010).

162 Obici, S., Zhang, B. B., Karkanias, G. & Rossetti, L. Hypothalamic insulin signaling is required for inhibition of glucose production. *Nat Med* **8**, 1376-1382, doi:10.1038/nm1202-798 (2002).

163 Pijl, H. *et al.* Food choice in hyperthyroidism: potential influence of the autonomic nervous system and brain serotonin precursor availability. *J Clin Endocrinol Metab* **86**, 5848-5853, doi:10.1210/jcem.86.12.8112 (2001).

164 Gonzalez, C. R. *et al.* Hyperthyroidism differentially regulates neuropeptide S system in the rat brain. *Brain Res* **1450**, 40-48, doi:10.1016/j.brainres.2012.02.024 (2012).

165 López, M., Seoane, L., Señarís, R. M. & Diéguez, C. Prepro-orexin mRNA levels in the rat hypothalamus, and orexin receptors mRNA levels in the rat hypothalamus and adrenal gland are not influenced by the thyroid status. *Neurosci Lett* **300**, 171-175, doi:10.1016/s0304-3940(01)01569-5 (2001).

166 Kong, W. M. *et al.* Triiodothyronine stimulates food intake via the hypothalamic ventromedial nucleus independent of changes in energy expenditure. *Endocrinology* **145**, 5252-5258, doi:10.1210/en.2004-0545 (2004).

167 Ishii, S. *et al.* Hypothalamic neuropeptide Y/Y1 receptor pathway activated by a reduction in circulating leptin, but not by an increase in circulating ghrelin, contributes to hyperphagia associated with triiodothyronine-induced thyrotoxicosis. *Neuroendocrinology* **78**, 321-330, doi:10.1159/000074885 (2003).

168 Coppola, A. *et al.* Suppression of hypothalamic deiodinase type II activity blunts TRH mRNA decline during fasting. *FEBS Lett* **579**, 4654-4658, doi:10.1016/j.febslet.2005.07.035 (2005).

169 Diano, S. & Horvath, T. L. Mitochondrial uncoupling protein 2 (UCP2) in glucose and lipid metabolism. *Trends Mol Med* **18**, 52-58, doi:10.1016/j.molmed.2011.08.003 (2012).

170 Andrews, Z. B. *et al.* UCP2 mediates ghrelin's action on NPY/AgRP neurons by lowering free radicals. *Nature* **454**, 846-851, doi:10.1038/nature07181 (2008).

171 Weeke, J. & Orskov, H. Synthesis of 125I monolabelled 3, 5, 3'-triiodothyronine and thyroxine of maximum specific activity for radioimmunoassay. *Scand J Clin Lab Invest* **32**, 357-360, doi:10.3109/00365517309084359 (1973).

172 Morreale de Escobar, G., Pastor, R., Obregon, M. J. & Escobar del Rey, F. Effects of maternal hypothyroidism on the weight and thyroid hormone content of rat embryonic tissues, before and after onset of fetal thyroid function. *Endocrinology* **117**, 1890-1900, doi:10.1210/endo-117-5-1890 (1985).

173 Ruiz de Oña, C., Obregón, M. J., Escobar del Rey, F. & Morreale de Escobar, G. Developmental changes in rat brain 5'-deiodinase and thyroid hormones during the fetal period: the effects of fetal hypothyroidism and maternal thyroid hormones. *Pediatr Res* **24**, 588-594, doi:10.1203/00006450-198811000-00010 (1988).

174 Silva, J. E. The multiple contributions of thyroid hormone to heat production. *J Clin Invest* **108**, 35-37, doi:10.1172/jci13397 (2001).

175 Martinez-Sanchez, N. *et al.* Hypothalamic effects of thyroid hormones on metabolism. *Best Pract Res Clin Endocrinol Metab* **28**, 703-712, doi:10.1016/j.beem.2014.04.004 (2014).

176 Bianco, A. C. & Kim, B. W. Deiodinases: implications of the local control of thyroid hormone action. *J Clin Invest* **116**, 2571-2579, doi:10.1172/JCI29812 (2006).

177 Escobar-Morreale, H. F., Obregón, M. J., Escobar del Rey, F. & Morreale de Escobar, G. Replacement therapy for hypothyroidism with thyroxine alone does not ensure euthyroidism in all tissues, as studied in thyroidectomized rats. *J Clin Invest* **96**, 2828-2838, doi:10.1172/JCI118353 (1995).

178 Donzelli, R. *et al.* Effect of Hypothyroidism and Hyperthyroidism on Tissue Thyroid Hormone Concentrations in Rat. *Eur Thyroid J* **5**, 27-34, doi:10.1159/000443523 (2016).
179 Bárez-López, S. & Guadaño-Ferraz, A. Thyroid Hormone Availability and Action during Brain Development in Rodents. *Front Cell Neurosci* **11**, 240, doi:10.3389/fncel.2017.00240 (2017).
180 Escobar-Morreale, H. F., Obregón, M. J., Escobar del Rey, F. & Morreale de Escobar, G. Tissue-specific patterns of changes in 3,5,3'-triiodo-L-thyronine concentrations in thyroidectomized rats infused with increasing doses of the hormone. Which are the regulatory mechanisms? *Biochimie* **81**, 453-462, doi:10.1016/s0300-9084(99)80095-9 (1999).
181 Ganeshan, K. & Chawla, A. Warming the mouse to model human diseases. *Nat Rev Endocrinol* **13**, 458-465, doi:10.1038/nrendo.2017.48 (2017).
182 Shimizu, I. & Walsh, K. The Whitening of Brown Fat and Its Implications for Weight Management in Obesity. *Curr Obes Rep* **4**, 224-229, doi:10.1007/s13679-015-0157-8 (2015).